Agricultural Drought Assessment using Multiple Indices under Climate Change, over Pakistan
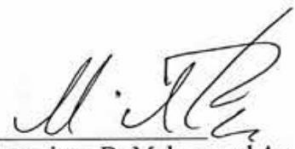
By

Maryam Arif

(2020-NUST-MS-GIS-328397)

A thesis submitted in partial fulfillment of the requirements for the degree of Master of Science in Remote Sensing and Geographical Information Systems
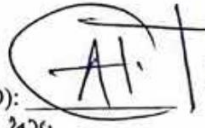
Institute of Geographical Information Systems
School of Civil and Environmental Engineering
National University of Sciences & Technology
Islamabad, Pakistan

August, 20

THESIS ACCEPTANCE CERTIFICATE

Certified that final copy of MS/MPhil thesis written by **Maryam Arif (Registration No. MSRSGIS 00000328397), of Session 2020 (Institute of Geographical Information systems)** has been vetted by undersigned, found complete in all respects as per NUST Statutes/Regulation, is free of plagiarism, errors, and mistakes and is accepted as partial fulfillment for award of MS/MPhil degree. It is further certified that necessary amendments as pointed out by GEC members of the scholar have also been incorporated in the said thesis.

Signature: _____

Name of Supervisor: Dr Muhammad Azmat

Date: 23/08/2024

Signature (HOD): _____

Date: 30-9-2024

Dr. Muhammad Ali Tahir
HoD & Assoc. Prof. SCEE (IGIS)
NUST, H-12, Islamabad.

Signature (Principal & Dean SCEE): _____

Date: 07 OCT 2024

PROF DR MUHAMMAD IRFAN
Principal & Dean
SCEE, NUST

ii

ACADEMIC THESIS: DECLARATION OF AUTHORSHIP

I, **Maryam Arif**, declare that this thesis and the work presented in it is my own and have been generated by me as the result of my own original research.

AGRICULTURAL DROUGHT ASSESSMENT USING MULTIPLE INDICES UNDER CLIMATE CHANGE, OVER PAKISTAN

I confirm that:

1. This thesis is composed of my original work, and contains no material previously published or written by another person except where due reference has been made in the text;
2. Wherever any part of this thesis has previously been submitted for a degree or any other qualification at this or any other institution, it has been clearly stated;
3. I have acknowledged all main sources of help;
4. Where the thesis is based on work done by myself jointly with others, I have made clear exactly what was done by others and what I have contributed myself;
5. None of this work has been published before submission.
6. This work is not plagiarized under the HEC plagiarism policy.

Signed: Maryam Arif

Date: 08.10.2024

DEDICATION

To

Allah Almighty

&

My loving parents, my supportive husband, and our precious little one

Thank you for bearing the stressful moments I had, for the prayers and support to overcome them and for the endless encouragement. This achievement is a tribute to the remarkable family Allah has granted me. This thesis is a sincere expression of my heartfelt gratitude.

ACKNOWLEDGEMENTS

As I stand at the end of my master's journey, humbled and overjoyed, I express my deep and sincere gratitude to everyone who has played a crucial role in the completion of my research.

I am thankful to Dr. Muhammad Azmat, my research supervisor, for providing his constant help during the entire research work. With his expertise in the field, he provided me with innovative ideas and helped in formulating my thesis scientifically. His precious guidance and support helped me in completing my thesis systematically.

To my father and mother, for their unwavering support, love, and sacrifices which have been the foundation of my success. To my siblings, your constant encouragement and belief in me have been invaluable. I am forever grateful to each of you for being my pillar of strength. I feel proud that I could make my family proud of my performance.

To my husband, you have been my constant support. I am forever grateful for your patience and encouragement.

To my precious little one, you motivate me to continue striving for the better and provide you with the best possible future.

Maryam Arif

Table of Contents

LIST OF TABLES

LIST OF FIGURES

LIST OF ABBREVIATIONS

Abbreviation	Explanation
GIS	Geographic Information System
RS	Remote Sensing
MODIS	Moderate Resolution Imaging Spectroradiometer
NDVI	Normalized Difference Vegetation Index
SPI	Standardized Precipitation Index
PDSI	Palmer Drought Severity Index
SDI	Stream flow Drought Index
SWSI	Surface Water Supply Index
VCI	Vegetation Condition Index
VHI	Vegetation Health Index
TCI	Temperature Condition Index
GEE	Google Earth Engine
EVI	Enhanced Vegetation Index
ML	Machine Learning
CMIP6	Coupled Model Intercomparison Project Phase 6
RF	Random Forest
SSPs	Shared Socio-economic Pathways
AHP	Analytical Hierarchy Process
SPEI	Standardized Precipitation and Evapotranspiration Index

CWSI	Crop Water Stress Index
SMADI	Soil Moisture Agriculture Drought Index
GCMs	General Circulation Models
WCRP	World Climate Research Program
MLR	Multiple Linear Regression
PDI	Palmer Drought Index
MDPI	Modified Palmer Drought Index
SMOS	Soil Moisture and Ocean Salinity
ESI	Evaporation Stress Index
SAI	Standardized Anomaly Index
GLDAS	Global Land Data Assimilation System
CHIRPS	Climate Hazards Group Infrared Precipitation with Station Data
IMERG	Integrated Multi-satellite Retrievals for GPM
ERA-5	Fifth generation ECMWF atmospheric Reanalysis of the global climate
TRMM	Tropical Rainfall Measuring Mission

SUSTAINABLE DEVELOPMENT GOALS (SDGs)

The Sustainable Development Goals (SDGs) are a universal call to action to end poverty, protect the planet, and ensure that all people enjoy peace and prosperity. These 17 Goals build on the successes of the Millennium Development Goals, while including new areas such as climate change, economic inequality, innovation, sustainable consumption, peace and justice, among other priorities. The SDGs are interconnected – often the key to success on one will involve tackling issues more commonly associated with another.

This research aligns with the following SDGs set by the United Nations:

The research addresses the critical need for resilient agricultural practices. It helps in identifying vulnerable regions by utilizing multiple drought indices and provide developing strategies to ensure sustainable food production, ultimately contributing to food security in drought-prone areas.

By examining the impacts of drought on water resources essential for agriculture. Analysing soil moisture and water availability through advanced indices, the research contributes to better water management practices, ensuring efficient use of water in agriculture, and preventing water scarcity in affected regions.

Future climate projections and the use of machine learning model, will provide awareness about how climate change will exacerbate drought conditions, its severity and frequency in Pakistan, educating about climate adaptation and mitigation strategies to reduce the impact of extreme weather events on agriculture.

The research aligns with SDG 15 by focusing on the impact of drought on land degradation and agricultural sustainability. A comprehensive assessment of drought's effects on ecosystems by integrating various drought indices. It offers strategies for land conservation and combating desertification.

This research offers valuable contributions towards achieving these Sustainable Development Goals by improving drought monitoring and prediction, promoting resilient agricultural practices, sustainable water management, and effective climate adaptation strategies to mitigate the impacts on vulnerable ecosystems and communities.

ABSTRACT

Climate change impacts global ecosystems, agriculture, health of individuals, and water availability. The most severe effect of climate change is drought, which is becoming severe and intense. Drought and associated risk management are typically tracked using a variety of drought indices. The key components in determining drought are temperature, precipitation, and other hydro-meteorological factors. Four agriculture drought indices – VCI, TCI, SPEI, and SMADI, were computed and analysed over 12 years (2010-2021) using Earth Engine. The possible future changes in the intensity and spatial distribution of agricultural droughts were analysed based on the MME mean of thirteen GCMs of CMIP6 in two different warming scenarios (SSP 2-4.5 and SSP 5-8.5) using the Random Forest algorithm to improve the prediction accuracy. A Drought Composite Map was generated by an innovative method using AHP established MCDM approach. Each index was given AHP-derived weightage with a consistency ratio of 3.10% and a consistency index of 2.79. The study also integrates multiple satellite products, including CHIRPS and IMERG rainfall, MODIS, and ERA-5 temperature datasets, used for the quantification for the period 2010-2021 across different agro-climatic zones. The results showed significant spatial and temporal variability in drought severity, with arid and semi-arid regions being the most vulnerable. Quetta, Kalat, and Panjgur are the most affected areas under current conditions; under future scenario (SSP 2-4.5), Badin, along with Kalat is severely affected by drought, and under SSP 5-8.5, and all these regions are under extreme drought conditions in 2100. Effective drought management requires simple, applicable models that consider multiple factors and can accurately forecast agricultural droughts despite meteorological outliers.

CHAPTER 1: INTRODUCTION

1.1 Background

1.1.1 Droughts

Climate change hugely affects worldwide ecosystems, agriculture, human well-being and water supplies (*European Climate Risk Assessment*, 2024). The most severe effect of climate change is droughts, which have become frequent and intense, impacting water resources and crop yields globally (Trenberth et al., 2014). A long duration of insufficient precipitation causing water scarcity is known as drought. The most susceptible regions to drought are arid, semi-arid, dry sub-humid, often referred to as "dry lands" based on the United Nations Convention to Combat Desertification (UNCCD) (*Convention | UNCCD*).

1.1.2 Droughts situation in Pakistan

Droughts have a vast effect on world economies, societies and ecosystems. In Asia, specifically in South and Southeast Asia, droughts are intense because of rising temperatures and unpredicted rainfalls (*European Climate Risk Assessment*, 2024). It is essential to understand the drought situation in Pakistan because it affects our agriculture sector, economy, and water reserves. Pakistan is a country with diverse agro-climate zones, ranging from arid deserts to fertile lands; its GDP is majorly based on agriculture, which calls for immediate actions to reduce the consequences of droughts and mitigate their effects (Zaman et al., 2023). The analysis of climate change and its impacts on vegetation and hydrology indicates the need for adaptive measures to cope with the threat of drought (Ishaq et al., 2024). Therefore, thorough studies are important for devising effective strategies and management practices for sustainable agricultural development in Pakistan.

1.1.3 Types of droughts and their impact

Droughts are categorized into four main categories: hydrological, agricultural, socioeconomic, and meteorological. Understanding the various types is crucial to effectively manage and mitigate their impacts effectively. **Meteorological drought** occurs when there is severely low precipitation over a long time in a particular region, which lowers surface water levels and soil moisture (Torabinezhad et al., 2023). **Hydrological drought** is the amounts of water in lakes, reservoirs, and aquifers drop below average levels, influencing water

availability for human consumption, agriculture, and industrial use (Essa et al., 2023). Insufficient amount of soil moisture to sustain agricultural growth, resulting in reduced crop productivity and risk of famine is known as **Agricultural drought** (Baral et al., 2023)**. Socioeconomic drought** is defined by the consequences of water scarcity on human activities and the economy, including both direct effects on agriculture and water supply as well as broader impacts on food prices, employment, and economic stability (Rashid, 2023).

Droughts cause significant threats to the environment as they cause water shortage, biodiversity loss, soil degradation, and elevated risks of wildfires (Vicente-Serrano et al., 2020). These environmental impacts, combined with social and financial influence, cause significant economic losses in agriculture, leading to food insecurity and inflation, thus displacing populations, causing health issues and provoking conflicts over water resources (Ghamghami & Irannejad, 2019). Affective drought monitoring and assessment is crucial to reduce these impacts, involving monitoring indicators such as hydrological levels, soil hydration, and water reservoir levels ("Droughts: Things to Know | U.S. Geological Survey," June 8, 2018).

1.2 Problem Statement

1.2.1 Drought impact

Droughts have far-reaching impacts on the environment, economy, and society. Environmentally, they lead to water scarcity, biodiversity loss, soil degradation, and increased risks of wildfires (López-Moreno et al., 2013). Socially, they can displace populations, cause health issues due to poor water quality, and trigger conflicts over water resources. Economically, droughts are responsible for significant losses in agriculture and, therefore impact food security through hikes in commodity prices (Edwards et al., 2019). Drought has a significant influence on developing countries' economies, which rely largely on agricultural products (Brown et al., 2011). Furthermore, climate change and harsh weather conditions might exacerbate the drought and general socioeconomic factors (IPCC, 2013). Affective drought management is important to mitigate these impacts. It involves monitoring indicators such as rainfall, soil moisture content, and water storage levels to predict and manage drought conditions effectively (Wilhite, 2006).

1.3 Tools to combat drought

Efficient irrigation, rainwater harvesting, and recharge of groundwater are a few ways to combat drought. Hence, water management techniques may improve water conservation (Mahan & Lascano, 2016). Drought-resistant crop varieties should be introduced to ensure that agriculture thrives under water-scarce conditions (Shengxue et al., 2023). Soil management practices, including mulching, no-tillage farming, and composting, all improve soil's capacity to conserve moisture and reduce water losses (Pengfei et al., 2023). A check on policy and governance also plays a vital role in water-use regulations, encouraging sustainable water-use practices and strengthening community awareness through outreach activities (Pengfei et al., 2023). Technological innovations, such as desalination, water recycling, and cloud seeding, can be alternative ways to access water (O'Brien, 2015).

1.3.1 GIS & RS approach

Geographic Information Systems (GIS) and Remote Sensing (RS) are significant tools for evaluating and monitoring droughts. They provide different operations on a larger scale for monitoring, examining, and visualizing over time and space. Landsat, MODIS, and Sentinel are a few of the satellites that provide real-time data on surface water bodies, soil moisture content, and vegetation cover (TOPÇU & GÜVEL, 2021). Drought severity is evaluated using the Normalized Difference Vegetation Index (NDVI) and the Standardized Precipitation Index (SPI) (Wei et al., 2021). We can access the precipitation patterns over time by using SPI and the Palmer Drought Severity Index (PDSI) (Bakke et al., 2023). The Stream flow Drought Index (SDI) and the Surface Water Supply Index (SWSI) are used to calculate hydrological droughts by analysing stream flow and reservoir capacity (Kartal & Nones, 2024). Analysing vegetation state and impact of temperature on crop productivity, indices like Vegetation Condition Index (VCI), Vegetation Health Index (VHI), and the Temperature Condition Index (TCI) are used (Tsiros et al., 2004). A comprehensive assessment of drought severity can be achieved by incorporating a variety of indices that encompass meteorological, hydrological, and agricultural standpoints, each offering valuable insights through the analysis of remote sensing data and certain environmental factors.

1.3.2 Google Earth Engine

Google Earth Engine (GEE) is a cloud-based platform that allows for the analysis and visualization of a massive amount of environmental data from all around the world. It helps in the study of changes on Earth, such as deforestation, climate change, and urbanization, by combining large amounts of satellite images and other geospatial data with powerful computation tools. It allows scientists, researchers and developers to run complex analyses quickly, make interactive maps, and retrieve results in multiple formats (Gorelick et al., 2017). GEE plays an important role in drought monitoring by allowing large-scale analysis of satellite data such as MODIS and Sentinel (Gorelick et al., 2017). For example, MODIS data in GEE was utilized to calculate indices including NDVI and the Enhanced Vegetation Index (EVI), which are crucial for identifying the vegetation conditions and drought regions (Son et al., 2014). Agricultural droughts are computed in GEE by integrating Landsat data such as soil moisture and crop cover, thus allowing for monitoring changes in land surface conditions (Ejaz et al., 2023). Recent advancements in GEE, such as its integration with machine learning, have improved its accuracy of drought prediction (Elnashar et al., 2020). It has become such a powerful tool that improves our ability to comprehend, predict, and mitigate the effects of drought on ecosystems and societies.

1.4 Future Projections under SSP 2-4.5 & SSP 5-8.5 using Random Forest

Drought is a climate change-related phenomenon. Present and future knowledge about climate change at the local, regional, and global levels is important for devising national and international strategies to mitigate natural disasters such as droughts (Miao et al., 2011). Predicting the future spread of droughts until 2100 is a significant challenge for scientists and policymakers related to climate change (Cook et al., 2020). However, the current situation depends on advanced climate models such as those provided by the Coupled Model Intercomparison Project Phase 6 (CMIP6). This model, which incorporates different emissions of greenhouse gases, changes in land use, and socio-economic pathways, is crucial in projecting future climate conditions. It indicates an increase in the frequency and severity of droughts globally, with significant variations among regions (Cook et al., 2020; Eyring et al., 2016). General Circulation Models (GCMs) have become a crucial tool for researching climate change processes (IPCC, 2013). GCMs can accurately simulate current climate change and

predict future climate changes based on various scenarios by different radiative forcing. The CMIP, established by the World Climate Research Program (WCRP), offers simulated data derived from a range of climate models. The project's significance lies in its ability to facilitate the establishment of a Multi-Model Ensemble (MME) mean, which allows for comparisons to be made (Hongmei et al., 2011).

Future drought conditions are predicted using machine learning (ML) approaches, which are renowned data-driven techniques like the Random Forest (RF) method (Pradhan et al., 2019). ML models have recently achieved notable progress in several industries, including data reconstruction, hydrological modelling, climate change research, and other areas (Bennett & Nijssen, 2021). The most used ML models are Multiple Linear Regression (MLR), Support Vector Machine (SVM) Long Short-Term Memory (LSTM), and RS. RF models can handle large datasets and capture intricate relationships between different climatic and environmental parameters, thus improving prediction accuracy (Omar & Kawamukai, 2020). It constructs an ensemble of decision trees based on previous trends in drought, soil moisture level, precipitation, and temperature. It gives a very close estimation of future droughts (Zarei et al., 2023). For instance, one can use RF to improve regional-scale drought predictions obtained from the CMIP6 projections by considering local climatic variations (Shah et al., 2017).

Future predictions of droughts under CMIP6 Shared Socio-economic Pathways (SSPs) 2-4.5 and 5-8.5 indicate significant fluctuations in drought's frequency and intensity (An, Park, Jung, & Jang, 2022). Drought occurrences increase moderately under the SSP 2-4.5, a stabilizing scenario that projects moderate greenhouse gas emissions and socio-economic changes (An et al., 2022; Su et al., 2021). Droughts are frequent and severe under SSP 5-8.5, marked by high emissions and rapid economic growth. Studies performed using RF models have shown that the Mediterranean, the southern United States, and areas of Australia are especially vulnerable in these circumstances (Bachmair et al., 1947).

In Pakistan, there is an increased likelihood for more prolonged drought, especially in particularly in semi-arid and arid areas, as they get more water-stressed, according to CMIP6 projections from (Adnan et al., 2022). Under both SSPs 2-4.5 and 5-8.5, Pakistan is projected to encounter a rise in the occurrence of droughts that will lead to significant damage to

agriculture, water resources, and socio-economic stability which calls for immediate and robust climate change adaptation measures (Ishaq et al., 2024; Zaman et al., 2023). Under these circumstances, it becomes necessary that strong climate adaptation and mitigation be put in place to address the upcoming risks associated with increased drought conditions.

1.5 Composite Drought Analysis using AHP

The Analytical Hierarchy Process (AHP) is a reliable technique for evaluating and ranking the many effects of droughts. This approach combines a number of indicators, including rainfall level, soil moisture levels, and agricultural productivity, to provide a detailed assessment of the impact of drought and its possible impacts (Saaty, 2004). By using AHP, researchers are able to systematically weigh and synthesize the various factors in a way that extends more accurate and informed decision-making (Palchaudhuri & Biswas, 2016). Various research has employed Multiple-Criteria Decision Making (MCDM) to determine drought conditions (Liu et al., 2019; Mokarram et al., 2021). Several studies have generated drought sustainability maps, which include studies of (Al-Faifi et al., 2019; Jianing et al., 2015; Pandey et al., 2023; Taherdoost & Madanchian, 2023).

In this hierarchical structure, the technique can include expert judgement and local knowledge, which is very reliable and relevant to the study of Saaty (2004). Composite drought analysis through Multi-Criteria Evaluation (MCE) technique within AHP will add much strength to the development of effective strategies for drought mitigation and adaptation, which is important for managing water resources and ensuring agricultural sustainability in the climate change conditions (Bhushan & Rai, 2004).

1.6 Research gap and way forward

Multiple studies have been undertaken on the performance of different drought indices in Pakistan. However, a few gaps remain in the current state of research. One such important gap is that indices need to be more validated and calibrated in a variety across a variety of the country's agro-climatic situations. Furthermore, there is a lack of established protocols that define which indices to select with regard to certain characteristics of drought and their effects on agriculture (Adnan Ullah et al., 2017). There is a need for an adequate understanding of drought propagation, meaning its Spatiotemporal trend and intensification, as a key ingredient

in comprehensive drought management (Pulwarty et al., 2014). Future work should focus on improving both the temporal and spatial resolution of these structures and bringing advanced remote sensing technologies together with in-situ observations closer to the ground (Ahmad et al., 2004). In addition, a comparison of the calculated drought indices of Pakistan with those from other regions having the same climatic conditions will be carried out.

In this study, we aim to compare several satellite products and gauge observations to determine their accuracy. This will help us select the most accurate climate products for further incorporation in drought studies. Furthermore, we will compare several prominent drought indices, including the Soil Moisture Agricultural Drought Index (SMADI), Crop Water Stress Index (CWSI), Standardized Precipitation and Evapotranspiration Index (SPEI), TCI, and VCI.

1.6.1. Performance comparison of multiple drought indices around the world

Pakistan, with diverse climatic conditions from arid to sub-humid climates, require effective drought monitoring and analysis. Drought conditions in various agro-climatic zones are being analysed globally using multiple drought indices, including SMADI, SPEI, VCI, and TCI. This research will compare the performance of several indices among countries, examining the similarities between the weather patterns in Pakistan and their possible usefulness in improving the ability to withstand droughts and sustain agriculture in the area. For instance, in a study done by Sánchez et al (2016), SMADI is effectively utilized to assess drought in semi-arid areas of southeastern Spain, which encounters irregular precipitation patterns. This index was able to perform reasonably in the Duero Basin during irregular climatic conditions, like high temperature and low precipitation, which resembles those found in some areas of Pakistan, such as Balochistan, due to its integration of several parameters that are important for managing agriculture. This is further validated by Dunne and Kuleshov (2023), in their study on the Murray-Darling Basin in Australia, which has variable precipitation, recurring droughts, and temperature fluctuations throughout the year. These factors result in extreme drought conditions, similar to those in parts of Pakistan, which are solely dependent on seasonal precipitation, especially monsoon. VCI is utilized in Brazil to evaluate the vegetation health of the Amazon rainforest (Vilanova et al., 2020). Amazon rainforest is characterized by a tropical climate, where VCI was applied as part of the VHI to evaluate the vegetation health. (Rawat et al., 2012) studied 10 out of 15 agro-climatic zones of

India, identifying that VCI is effective for monitoring vegetation health in geographically non-homogenous areas. VCI is effective in varying climates, which signifies its utility in agricultural drought monitoring. In the Midwestern area of the United States, a prolonged and severe drought occurred from 2011 to 2013, which affected agriculture severely. This was studied by Zhang et al. (2017) in which they performed TCI. The study area comes under temperate and arid zones where TCI was able to highlight the regions with high temperatures that intensify droughts (Domínguez-Castro et al., 2019). The paper discusses the region of Spain with has significant variability in climatic conditions, having hot, dry summers and mild, wet winters. SPEI was used to measure drought which effectively captures the severity and duration of droughts that correlate with agricultural impacts.

By calculating these indices concurrently, we can achieve a nuanced understanding of drought dynamics in Pakistan. Each index measures drought differently, so relying on a single index may not fully represent this complex phenomenon. The multi-index approach, however, significantly enhances the accuracy of drought assessment and aids in identifying the most suitable index for specific climatic conditions. This approach, along with composite analysis, which combines multiple indices into a single framework, will present an improved and holistic view of drought conditions. This study is essential for identifying drought-prone regions and projecting future precipitation and temperature changes throughout Pakistan's agro-climatic regions. Using an MME mean from CMIP6, we will analyse future drought characteristics, including duration, frequency, and intensity changes under SSP 2-4.5 and SSP 5-9.5 scenarios.

1.7 Objectives

This study aimed to:

1. To examine the accuracy of precipitation and temperature data of different satellite-based products over Pakistan.
2. To estimate multiple agricultural drought indices, i.e. SMADI, SPEI, VCI and TCI, under current and future scenarios using CMIP6 GCMs (SSP 2-4.5 & SSP 5-8.5).
3. Assessment of Agricultural drought based on Composite Drought Analysis using AHP under current scenarios and future scenarios using CMIP6 GCMs (SSP 2-4.5 & SSP 5-8.5).

CHAPTER 2: LITERATURE REVIEW

This chapter provides a comprehensive overview of existing knowledge and scholarly work done on the subject of the current research, which includes theories, models, and relevant empirical studies to highlight gaps in existing knowledge and set the context for the current research. Agricultural drought is a severe threat to food security, water availability, and overall agricultural productivity, especially in regions like Pakistan, where diverse climatic conditions highlight its impacts. A variety of indices must be calculated to determine the level of drought in agriculture in this regard. This work has been carried out using different drought indices in order to evaluate agricultural drought fully in a changing climate environment in Pakistan. This research is tailored to improve the level of precision of drought monitoring. A review of the existing literature was undertaken on several articles based on studies of the effects of climate change on agricultural droughts in Pakistan. A summary of various papers related to multi-index agriculture drought assessment is presented below.

In a study by Shahabfar and Eitzinger (2011), they evaluated the performance of Palmer Drought Index (PDI) and Modified Palmer Drought Index (MDPI) using MODIS data over 10 agro-climatic zones in Iran, from 2000 to 2005 and compared them with EVI and VCI and further correlated with five water balance parameters for winter wheat. The results showed that PDI and MDPI had significant correlations with water balance parameters and performed better than EVI and VCI for drought stress detection, especially at sensitive growth stages of winter wheat. These findings suggest that PDI and MDPI are best tools, to assess drought in the semi-arid and arid regions. Ghaleb et al. (2015) monitored the condition of drought by calculating VCI and TCI based on VHI in Lebanon from 1982 to 2014 using Landsat imagery. The results indicated severe to moderate drought occurrences in the northern part of Lebanon, while mild drought in the valley of Bekaa and the Tyr region on 2014, which shows the good ability of VHI for regional drought assessment.

Baig et al. (2020) measured meteorological and agricultural droughts in the Chitral Kabul River Basin (CKRB) over the period 2000 to 2018 using indices like Precipitation Condition Index (PCI), Soil Moisture Condition Index (SMCI), and VCI. The results showed 2000 and 2004 as the hardest years of drought and high vulnerability of basins in the northwest due to low monsoonal rainfall. A decreasing drought trend from 2000 to 2018, projected to continue

until 2030. The study emphasizes the interdependence of meteorological and agricultural droughts and suggests that integrating various datasets could enhance drought monitoring and management. The only drawback is the limited number of weather stations which hinders in the data validation, indicating a need for more observation stations to improve drought assessment.

Shahzaman et al. (2021) conducted a study on the monitoring of agricultural drought in South Asian countries. The study specifically examined remote sensing indices including Evaporation Stress Index (ESI), VHI, EVI, and Standardized Anomaly Index (SAI). These indices were compares to evaluate drought development patterns from 2002 to 2019. It was shown that the ESI exhibits more sensitivity to immediate moisture deficiencies compared to vegetation-based indices. The findings indicated that ESI in the most precise indicator for identifying locations that are impacted by drought. This conclusion is supported by the strong link seen between the ESI and anomalies in crop yield, particularly in wheat, rice, and maize, in Pakistan, India, Bangladesh, and Afghanistan.

Wolteji et al. (2022) assessed agricultural drought in the Rift Valley Region of Ethiopia by using multiple drought indices from 2015 to 2019. The NDVI is a metric that monitor the health of vegetation. It demonstrates that higher NDVI values imply healthy plants, while lower values suggest stress from a lack of moisture. The VCI and TCI were also used, with VCI being particularly effective for monitoring agricultural drought, whereas TCI provides valuable information on the effects of temperature on vegetation. The VHI, which integrates the TCI and VCI, has detected severe and extreme drought conditions in many regions and years, particularly in 2015 and 2016. The study indicated that there was higher occurrence of severe droughts in the low-lying regions, particularly in the eastern parts of the Rift Valley. The combination of these indices offered a thorough evaluation of drought patterns, highlighting their usefulness in monitoring agricultural drought and emphasising the significance of including several indices for precise drought assessment.

Pan et al. (2023) analysed the reliability of several drought indices for agriculture in China during 2000 to 2019 to determine which one works best in both wet and dry conditions. The Drought Severity Index (DSI), Soil Moisture Anomaly (SMA), VCI, SPI, and SPI were

computed and compared for this purpose. The results indicated that DSI from Global Land Data Assimilation System (GLDAS) is most accurate under all climatic regions. They key findings are that Northern arid and semi-arid areas, The Northeast China Plain, and the Huang-Huai-Hai Plain suffered from frequent moderate to severe droughts. There was an overall reduction in the occurrence of droughts over the Northern arid zones and a significant increase risk on Yunnan-Guizhou Plateau from 2002, which stresses the importance of reliable remote sensing based datasets for effective monitoring and future planning measures towards sustainable agricultural practices.

Khalil et al. (2023) assessed drought impacts on environmental flow (EF) in twenty-seven Indus Basin's catchments from 1980 to 2018 using SPEI and Principal Component Analysis (PCA). The results indicated significant alterations, especially in the Lower Indus Basin (LIB). Drought's frequency and intensity increased in extreme low flow (ELF) and low flow (LF). Moderate droughts affected ELF and LF in the Upper and Middle Indus Basin at shorter timescales. This study highlights the importance of sustainable water management to mitigate drought effects on EFs.

Al Shoumik et al. (2023) highlighted the intricate dynamics between meteorological and agricultural droughts in drought-prone regions of Bangladesh. Various indices, such as SPI, Palmer Drought Severity Index (PDSI), and SPEI, have been widely used to evaluate meteorological drought. Similarly, agricultural drought has been assessed using indices like NDVI, VCI, TCI, and VHI. The results indicated that rainfall during pre-monsoon increased in the northwest Bangladesh. SPI and SPEI shows increasing while PDSI shows decreasing trend. The results offer a complex interplay between meteorological and agricultural droughts, especially in regions with extensive irrigation practices.

Bilal et al. (2023) investigated the Spatio-temporal trend of drought in three most arid zones of Balochistan, Pakistan using SPI, agricultural SPI (aSPI), and SPEI. DrinC software and SPEI calculator was used to measure these indices over temporal scales of 3, 6, 9, and 12 months. NOAA precipitation data from 1992 to 2021 was analysed. The results showed severe and extreme drought years, hitting areas of Dalbandin, Quetta, Sibbi, Kalat, Khuzdar, and

Zhob. The comparison between indices reveals that SPI was the best performing index, with high suitability in capturing drought occurrence.

Sánchez et al. (2016) elaborated a new index called the SMADI, which uses data from Soil Moisture and Ocean Salinity (SMOS) mission. This index was validated in Spain and demonstrated that it has a greater strength to integrate soil moisture data seamlessly, thus identifying agricultural drought conditions. The results confirms that SMADI is a reliable indicator of drought and much advanced as compared to traditional vegetation indices owing to the improvement in the accuracy of assessing drought through direct soil moisture measurements.

Shahzada et al. (2016) investigated the precipitation and drought climatology in South Central Asia by using data from Pakistan between 1951 and 2010. They applied indices and statistical calculations to reveal six sub-regions and further analyse trends in precipitation. Results showed two major drought events i.e., 1971 and 2000-2002 and a severe drought in 1952. The region A5 (northeast South-Central Asia) was found to be the most drought prone. The monthly trends indicate that precipitation has increased in September and June in the regions A3 (central Asian region) and A5, whereas the mean values present a decreasing tendency in January and August for the region A4 (north-eastern parts of India). Decadal analysis showed a decreasing trend in the region A4 and increasing trends in Pakistan and region A5, highlighting the need for improved water management and agricultural planning.

In another study by Shahzada et al. (2016) , they analysed shifting agro-climatic zones and drought vulnerability in Pakistan through precipitation and temperature trend analysis, over the period from 1951 to 2014. The results indicated that maximum temperatures in severely arid and humid regions have increased significantly, as has yearly precipitation in arid regions. The semi-arid zone is highly vulnerable to drought, with the most severe events recorded in 1952, 1969, 2000, and 2002. The findings also showed that 87% of Pakistan is severely or semi-arid, posing challenges for crop water requirements due to rising temperatures. Understanding these patterns is essential for sustainable agriculture and water management in the face of climate variability.

Chattopadhyay et al. (2020) developed a Combined Drought Index (CDI) by integrating meteorological, land-based, and remote sensing data to improve drought prediction and monitoring. The CDI was successfully tested from 2014 to 2016 in five Indian states during the monsoon season. It accurately measured the severity of drought and its impacts on crop productivity. The data showed consistency with other indices like the SPI, NOAA drought index, indicating its potential for practical application in drought early warning and management systems.

Yangyang et al. (2022), they used ML for drought assessment in Shandong Province, China with multi-source remote sensing data. This research evaluated the efficiency of three ML techniques, which are Bias-Corrected Random Forest (BRF), Extreme Gradient Boosting (XGBoost), and Support Vector Machines (SVM) in SPEI estimation. Spatial distribution of SPEI BRF is the most effective and is the best data to estimate spatial structure. The results demonstrated that BRF can monitor drought accurately, even in regions without observational data to support ground truth of drought assessment. ML models, particularly BRF model can enhance the quality and spatial resolution of drought monitoring using information from optical sensors.

Abd El-Hamid and Alshehri (2023) analysed drought vulnerability in El-Dammam city using Landsat satellite data from 2014 to 2022. They aimed to simulate and predict drought using PDI, Normalized Difference Drought Index (NDDI), evaluating SVM and Partial Least Square (PLS) techniques. Results indicated that NDDI and PDI are inversely correlated with NDVI and the Normalized Difference Water Index (NDWI), and positively correlated with Normalized Difference Snow Index (NDSI) and Stress Index (SI). PCA revealed that PC-1, PC-2, and PC-3 accounted for 98% of the data. PLS and SVM models were effective in drought predictions with R^2 values of 0.95 and 0.98, respectively. Severe drought was predicted in the Southern areas. The study concluded that NDVI, NDSI, SI, and NDWI are effective drought indices and machine learning techniques like PLS and CVM are reliable for drought prediction.

Tladi et al. (2022), who assessed the effectiveness of reanalysis rainfall data for drought monitoring over Upper Olifants sub-basin in South Africa. To evaluate National Centres for Environmental Prediction Climate Forecast System Reanalysis (NCEP-CFSR) and European

Centre for Medium-Range Weather Forecasts (ECMWF) ERA5 rainfall estimates, we compared them against observed data using Mean Error (ME), Nash-Sutcliffe Efficiency index (NSE), and percentage of bias (PBIAS). The results showed that the data of ERA5 is better correlated with observed data (R^2 = 0.78) then CFSR (R^2 = 0.57). The SPI analysis further supports ERA5's superiority in detecting major droughts, making it a preferable choice for meteorological drought monitoring and predictive modelling. Also, it performs better in non-winter months not only because of finer spatiotemporal resolution but also higher reliability regarding major droughts.

Ejaz et al. (2023) showcased the potential of GEE platform in several hydro-meteorological studies like drought evaluation. Numerous studies have proven the efficiency of this cloud-based solution in satellite data processing by deriving RS retrieved Drought Indices (RSDIs) using MODIS, Landsat, and Sentinel datasets. The RSDIs such as VCI, TCI, and VHI are compared with SPEI which is a meteorological drought index. Pearson correlation coefficient (CC) was determined for the SPEI and RSDIs. The results showed that VHI and SPEI have greater correlations with drought indices and are appropriate for evaluating drought in the data-scarce hyper-arid regions. For instance, Pham-Duc et al. (2023) utilized GEE to analyse drought in Vietnam using Landsat derived indices, while Benzougagh et al. (2022) used GEE data to monitor drought in Morocco, highlighting the utility of these indices for regional drought evaluation. These methodologies address significant data scarcity issues in arid regions, such as the Al-Lith watershed in Saudi Arabia, where traditional gauge data is insufficient. By incorporating satellite-derived indices and GEE, these studies will enhance the spatial and temporal environmental studies to help device strategies for drought mitigation.

Khan et al. (2021) created a global drought monitoring dashboard using GEE. The main objective was to compute and visualize drought indices including TCI, VCI, SMCI, and PCI. The methodology involved processing satellite data to generate these indices and evaluate drought conditions across various regions and time periods. Significant drought events were identified, including severe drought in Australia in 2002, extreme drought in Northeast Brazil in 2013, and notable drought in Thailand in 2019. The study concluded that the interactive dashboard effectively captures and visualizes drought conditions, providing valuable insights for drought management and planning.

An integrated analysis for the prediction and assessment of landslide susceptibility was presented by Nath et al. (2021) using AHP, logistic regression, random forest models in Darjeeling-Sikkim Himalaya. The primary objective was to prepare precise landslide susceptibility maps with a combination of multiple thematic layers in GIS platform. AHP was employed to determine weights of landslide-causing factors and a comparison matrix was formed. The RFs model achieved highest prediction accuracy, with an accuracy of 0.871. The logistic regression and AHP models had accuracies of 0.803 and 0.774, respectively.

Tang et al. (2021) examined the projected changes in extreme precipitation in the INCSC (Democratic Nationalist Republic of South China and Indochina Peninsula), using an MME mean of 26 CMIP6 models. This research focuses on evaluating how the projections of four extreme precipitation indices differ between two MME mean estimates obtained from rank-based weighting and simple multi-model averaging under SSPs. The results indicated that both schemes provide similar projections.

Most of the research reviewed can be improved upon with different methodologies when focusing on extreme weather scenarios. A single index for monitoring drought often results in incomplete results; also, choosing climate products with higher accuracy can get us the most reliable results. The reviewed studies underscore the importance of using multiple drought indices for monitoring agricultural droughts. By comparing various indices and integrating them into a composite, along with high-accuracy climate products data, these methodologies can be enhanced. Additionally, advanced tools like GEE and ML techniques can improve drought assessments. Moreover, the CMIP6 model is currently the most precise source of climate change data, and this will be used in the research instead of CMIP5 or any other previous climate model data, which has now become obsolete. Moreover, the study will span a longer time, and future projections will be given up to the year 2100, which will be beneficial for future studies.

CHAPTER 3: MATERIALS AND METHODS

This Chapter explains the methodology used to achieve the study's objectives. Therefore, it covers the theoretical framework, data collection procedure, and analysis techniques.

3.1 Study Area

Pakistan is situated in South Asia, with latitudes ranging from 24° to 37° N and longitudes ranging from 60° to 77°. It is bordered by the Arabian Sea to the south, China to the north, Afghanistan and Iran to the west, and India to the east (Tariq et al., 2021). It is the 33rd largest country in the globe and has a total area of approximately 881,913 square kilometers (Hussain et al., 2023).

The Pakistan Bureau of Statistics reports that land utilization in Pakistan is varied. The agricultural sector uses 47% of the total area, 24% as rangelands, and 19% is classified as forest land, leaving behind 6% as urban areas that contemplate urbanization (*Pakistan Bureau of Statistics*).

Pakistan's topography encompasses a wide variety of landscapes, from the mountainous regions of the Himalayas and Karakoram ranges in the north to the plains and bountiful lands along the Indus River in the south, is a key factor in understanding the country's agriculture. These geographic variations greatly impact the local climate and agricultural practices (Syed et al., 2022).

Pakistan's climate changes significantly from arid to semi-arid, along with considerable changes in the temperature and precipitation, which are affected by the monsoon, western disturbances, and varied topography (Syed et al., 2022).

Rainfall varies significantly, both spatially and temporally, with the monsoon season, which spans from July to September. The average annual rainfall of Pakistan is about 494 mm, with considerable regional variations (Ahmad et al., 2023). The distribution of rainfall throughout different provinces is as follows: Punjab receives moderate to heavy rainfall during the monsoon, between 400-700 mm annually (Abbas et al., 2021). Lower rainfall patterns in Sindh, between 100-200 mm annually during monsoon (Saddique et al., 2022). Khyber Pakhtunkhwa

receives much rain, benefitting from monsoon and winter rainfall, with annual averages between 500-1000 mm (Ullah et al., 2018). Balochistan, following the same trend as Sindh, is the driest region and receives 50-200 mm annually (Ahmad et al., 2023). The Indus River and its tributaries are the major source of water, which is important for agriculture. Groundwater also contributes to these sources, especially in places with limited surface water (Ahmad et al., 2023). Temperature changes are also noticeable, ranging from the cold northern highlands to the hot southern plains, with an average annual temperature of 13°C to 25°C (Zahid & Rasul, 2012).

Pakistan's economy is mainly dependent on Agriculture, which contributes up to 20% of the GDP, and employs up to 42% of the workers. The major crops include wheat, rice, cotton, and sugarcane (Raza et al., 2012).

The rate of urbanization in Pakistan is 36.4 %, and it has a population of more than 220 million people. This rapid urbanization results in the destruction of infrastructure, pollution, and increased resource demands (Farooq et al., 2024). This situation leads to stress on natural resources such as water, leads to land degradation, and exacerbates socio-economic disparities. These problems are made worse due to inadequate urban planning and urban growth (Mangi et al., 2018). All this situation is leading to droughts, which are more likely to happen in Balochistan, Sindh and parts of Southern Punjab, characterized by arid and semi-arid climates, irregular rainfall, and high temperatures (Mangi et al., 2018).

Pakistan is selected as a study area because of its contrasted geomorphologic features and climatic divisions from the very wet Himalayan region including permanent snow–glacial region to the very dry regions. The study was focused on drought indices, which were assessed using climatic data (temperature and precipitation) collected over 12 years (2010-2021) across Pakistan. Pakistan was divided into eight agro climatic zones which are extremely arid, arid, dry semi-arid, wet semi-arid, dry sub-humid, wet sub-humid, humid and very humid. It helps to determine the different features of a region. The classification is useful for providing valuable insight to formulate strategies related to crop growth, hence benefitting our country's agriculture. The map of the study area is given in Figure 1.
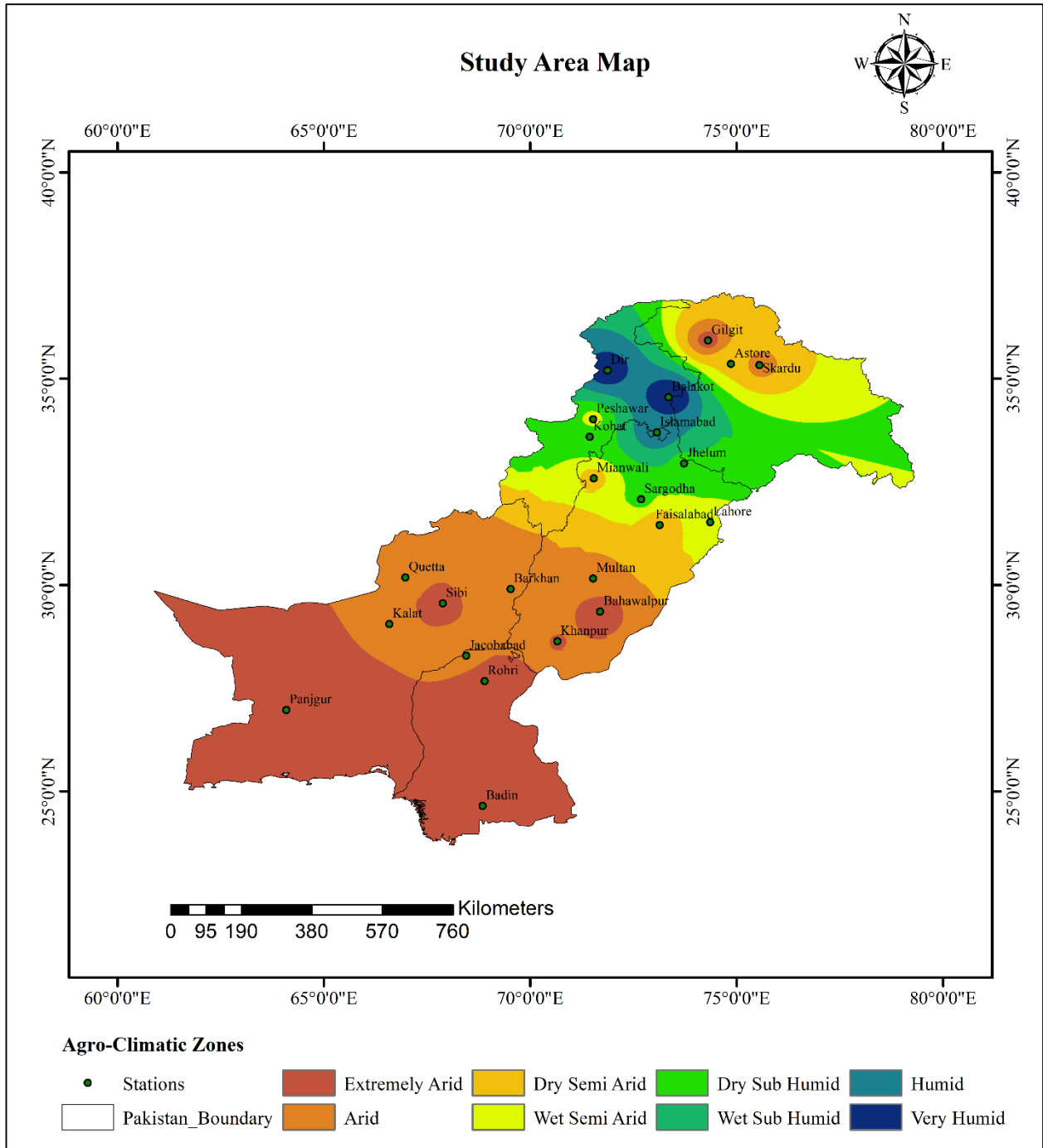
Figure 1: Study Area Map

3.2 General Methodological Design

The general methodological design of the research is as follows: In this study, eight climatic zones were delineated based on De Martonne's aridity index, using daily temperature and precipitation data from 24 weather stations across Pakistan. Climate data products (CHIRPS, IMERG, MODIS and ERA-5) were sourced from GEE and validated against gauge data. The datasets considered in this study are discussed in detail in the following sections. To evaluate the performance of these satellite-derived products, several statistical indices were calculated, including coefficient of correlation (CC), BIAS, relative BIAS (rBIAS), Root Mean Square Error (RMSE), Mean Absolute Error (MAE) and coefficient of Slope (β_1). Following this, four agricultural drought indices were computed, including the VCI, TCI, SPEI, and SMADI for drought monitoring. The processing of drought indices was carried out on GEE with Java Scripting, which allows us to retrieve satellite imagery as well as RS-derived products and process them in the cloud. A Spatiotemporal variability analysis was performed for each index, and the indices were compared with gauge precipitation and temperature data to assess the impact of these hydrological parameters over time. Subsequently, future drought predictions for each index were generated using a Random Forest Regressor. Historical index data from 2010 to 2021 and future climate projections from the CMIP6 dataset under two scenarios (SSP 2-4.5 & SSP 5-8.5) from 2022 to 2100 were used. The results of these predictions were used to create composite drought maps, integrating various indices. Weights were assigned to each index using AHP and pairwise comparison, enabling a comprehensive evaluation of the contribution of each index to the overall drought conditions. The results of the study are given in the form of maps, tables, and charts that are processed using ArcGIS 10.8.2 and Microsoft Excel. Figure 2 shows the overall methodology of this research work.

The flowchart contains the following text:

Objective 1

Observed Data (PMD) (2010-2021)

Satellite Products (2010-2021)

Climatic Variables Comparison

Precipitation → CHIRPS, IMERG

Temperature → MODIS, ERA 5

Statistical Indices:
- Correlation Coefficient
- Bias
- Relative Bias
- Root Mean Square Error
- Mean Absolute Error
- Coefficient of Slope

Objective 2

Agricultural Drought Assessment

Current Scenario

VCI   TCI   SPEI   SMADI

Future Scenario CMIP6 (SSP 2-4.5 & SSP 5-8.5)
- BIAS Correction
- MME mean
- Projections (Random Forest)

$$VCI = \frac{NDVI_i - NDVI_{min}}{NDVI_{max} - NDVI_{min}} * 100$$

$$TCI = \frac{LST_i - LST_{min}}{LST_{max} - LST_{min}} * 100$$

$$D = P - PET$$

$$SMADI = SMCI_i \frac{MTCI_i}{VCI_{i+1}}$$

Spatio-temporal Variability
- Observed Temperature
- Observed Precipitation

Objective 3

Multi Criteria Evaluation Technique

Calculated Drought Indices

SSP 2-4.5   SSP 5-8.5

Pairwise Comparison Matrix

Criteria Weighting ← Analytical Hierarchy Process

Drought Composite Map

Full Forms

CHIRPS = Climate Hazards Group Infrared Precipitation with Station Data
IMERG = Integrated Multi-Satellite Retrievals for GPM
MODIS = Moderate Resolution Imaging Spectroradiometer
ERA-5 = Fifth Generation ECMWF Atmospheric Reanalysis of the Global Climate
VCI = Vegetation Condition Index
TCI = Temperature Condition Index
SPEI = Standardized Precipitation Evapotranspiration Index
SMADI = Soil Moisture Agricultural Drought Index
CMIP6 = Coupled Model Intercomparison Project Phase 6
SSP = Shared Socio-economic Pathway

Figure 2: Methodology Flowchart

21

3.3 Data Collection

3.3.1 Gauge Data

There are very few gauge-based datasets kept by various organizations in Pakistan. The daily temperature and precipitation data from Jan 2010 to Dec 2021 were acquired from the Pakistan Meteorological Department (PMD). PMD has three types of observatories: Pilot-based, aerometric, and meteorological observatories (*Pakistan Meteorological Department*). After thorough evaluations, the daily precipitation and temperature data of 24 stations across Pakistan were considered and used to calculate drought for this study. The locations of gauging stations are shown in Table 1.

Table 1: Inventory of Climate Stations

Sr. No	Gauge	Elevation (meters)	Latitude	Longitude	Average Precipitation (mm)	Average Temperature (°C)
1	Skardu	2,500	35.3247	75.551	2370.0	68897.5
2	Bahawalpur	110.00	29.3544	71.6911	2497.4	113031.1
3	Faisalabad	185.6	31.4504	73.135	5523.6	107746.3
4	Islamabad	535.84	33.6937	73.0649	15288.6	104922.7
5	Jhelum	287.19	32.9425	73.7257	9488.1	100269.9
6	KhanPur	88.41	28.6332	70.6574	3207.0	111822.6
7	Lahore	214.00	31.5204	74.3587	8451.0	105573.4
8	Multan	121.95	30.1575	71.5249	3495.4	101232.4
9	Astore	2,546	35.357	74.8624	4735.7	73321.3
10	Barkhan	1,100	29.8995	69.5246	4821.0	104389.5

11	Badin	159	24.6459	68.8467	3028.9	113298.1
12	Dir	1420	35.1977	71.8749	15392.1	91402.4
13	Sargodha	155	32.074	72.6861	6835.0	76964.9
14	Sibi	30	29.5532	67.8808	3059.7	119935.6
15	Jacobabad	59	28.2823	68.4472	4000.1	112247.7
16	Rohri	186	27.6687	68.8943	1577.7	93023.7
17	Panjgur	980	26.9706	64.0887	900.8	103435.1
18	Balakot	974	34.5482	73.3532	16411.3	88112.2
19	Quetta	1,680	30.1798	66.975	2533.9	79881.0
20	Kalat	1989.75	29.0523	66.5879	1991.0	62662.9
21	Peshawar	331	34.0151	71.5249	5943.8	77922.8
22	Mianwali	215	32.5839	71.537	5317.8	88404.7
23	Kohat	489	33.5889	71.4429	7345.5	80431.7
24	Gilgit	1,500	35.9202	74.308	1891.4	89358.1

Reference: (*Pakistan Meteorological Department*)

3.3.2 Satellite Data / Climate Products

The TRMM (Tropical Rainfall Measuring Mission) satellite was jointly launched by NASA (National Aeronautics and Space Administration) and JAXA (Japan Aerospace Exploration Energy) in 1997. The TRMM was the earliest mission to focus on the generation and analysis of data related to precipitation and evapotranspiration, which measures and monitors drought conditions and water availability (Huffman & Bolvin, 2013). Several SPEs have become operational to monitor precipitation from space on a regular grid with near-global coverage as a result of this mission (Huffman & Bolvin, 2013). These SPEs have been

successful in monitoring regional drought conditions and conducting long-term hydrological surveys (Allafta et al., 2021; Bayissa et al., 2017).

The satellite precipitation daily data of Climate Hazards Group Infrared Precipitation with Station Data (CHIPRS) and **The Integrated Multi-satellite Retrievals for Global Precipitation Measurement (GPM) (**IMERG) version 6 were used in this work. Two well-known temperature datasets, which are (MODIS) and the Fifth Generation ECMWF atmospheric reanalysis of the global climate (ERA-5), were employed in this study. These datasets, downloaded from reputable sources, were then aggregated to annual values. The extraction of data was carried out using GEE, a trusted method in the field of climate research.

3.3.3 CHIRPS

Climate Hazards Group Infrared Precipitation with Station Data (CHIRPS) is a quasi-global precipitation time series data set covering 43 years developed for monitoring seasonal drought and global hydrological changes (Funk et al., 2015). These datasets contain global daily, ten days, and monthly precipitation data from 1981 to the present, having spatial resolutions of 0.05°, less bias and an extended record (Xinmeng et al., 2023). CHIRPS has been assessed against ground observations and is extensively used for climate, hydrological, and water resources studies, as well as for drought monitoring (Funk et al., 2015). The details of the dataset used in this study are given in Table 2.

3.3.4 IMERG-version 6

The Integrated Multi-satellite Retrievals for GPM IMERG version 6 techniques are quasi-real-time products that have been present from 2006 till the present and are used to compute precipitation levels throughout a major area of the Earth's surface using data from the GPM satellite constellation (Huffman et al., 2020)**.** Version 6, when compared with previous versions, has been improved and modified to perform better in data processing, algorithms and validations (Huffman et al., 2020). With the addition of GPM Microwave Imager (GMI) and Dual-frequency Precipitation Radar (DPR), this version has improved detection accuracy effectively (Skofronick-Jackson et al., 2017). The spatial resolution is 0°, and temporal resolutions are available in many options such as 30 minutes, 3 hours, one day, 7 days and 1 month, making it suitable for evaluating precipitation patterns throughout the day (Yu et al.,

2021). We used a temporal resolution of 1 day, as detailed in Table 2. This technology is beneficial in areas with few typical precipitation monitoring tools (Jiang & Bauer-Gottwein, 2019).

3.3.5 MODIS

The Moderate Resolution Imaging Spectroradiometer (MODIS) is a medium-resolution imaging spectrometer aboard NASA's Terra and Aqua satellites. It plays a pivotal role in the U.S. Earth Observing System (EOS) program. It is used for monitoring global biological and physical operations as well as agricultural drought assessment (Muhammad & Thapa, 2021). It detects electromagnetic energy in a broad spectral range to study the Earth's environmental, meteorological and hydrological conditions (Jing & Sun, 2017). With its wide spectral range from visible to thermal infrared wavelengths, MODIS offers detailed insights into land surface conditions relevant to drought monitoring, precise delineation of vegetation health and soil moisture content changes, which all help to identify drought-prone areas and assess crop stress levels. It has high spatial resolutions (250 meters to 1 kilometer) and temporal resolutions of every 1 to 2 days (Wang et al., 2020). MODIS offers different products based on critical indicators like land surface temperature (LST), vegetation indices (e.g., NDVI), evapotranspiration rates, and surface reflectance (Fagua & Ramsey, 2019; Huete et al., 2011). These products have been available from about 2000 till the present day (Khan & Gilani, 2021). The datasets details used in this study are presented in Table 2.

3.3.6 ERA-5

ERA-5, developed by ECMWF, a fifth generation, offers a comprehensive global atmospheric reanalysis from 1950 to near-real-time (Hersbach, Bell, Berrisford, Hirahara, et al., 2020). Assimilating diverse observational data, it provides high-resolution atmospheric fields with a spatial resolution of about 31 kilometers and a temporal resolution of one hour (Tan et al., 2023). It is widely used in weather forecasting, climate research, and environmental monitoring (Peng et al., 2023). ERA-5 facilitates understanding of past climate trends and prediction of future scenarios. Its accessibility to the public fosters collaboration and innovation in atmospheric and climate sciences worldwide (McNicholl et al., 2022). The dataset details utilized in this study are outlined in Table 2.

3.3.7 FLDAS-Soil Moisture

FLDAS stands for Famine Early Warning Systems Network Land Data Assimilation System. It is a customized version of NASA's Land Information System (LIS) used for assessing the environment, food security, data flow, monitoring, and prediction in developing countries with limited data (Khorrami et al., 2023; McNally et al., 2017). It contains global monthly soil moisture data in different depths from 1982 till date, along with information on elevation, vegetation cover, and albedo (Khorrami et al., 2023).

In this study, we employed a unique approach, using the monthly soil moisture datasets for the period 2010 to 2021 from FLDAS, GIOVANNI, which have a 0.1° spatial resolution and a depth of 40-100 cm underground. This dataset was combined with VCI and MTCI indices to generate the SMADI, a novel combination that allowed us to gain new insights. The specifics of the soil moisture data are summarized in Table 2.

3.3.8 Future Prediction Data-CMIP 6

General Circulation Models (GCMs) are important for accessing long-term climate change situations (Verma et al., 2023). A large number of GCMS are covered by the Climate Model Intercomparison Project (CMIP), which is designed to understand climate change more effectively (Ali et al., 2023). Previously, CMIP5 has been widely used to examine drought phenomena. However, CMIP6 is the newest of climate projections based on various socio-economic assumptions and has better parameterization that efficiently models climate projections (Eyring et al., 2016). CMIP6 have multiple strengths with additional improved models, higher spatial resolutions, fewer biases and better representations of climate phenomena (Iqbal et al., 2021). The new set of emissions from the CMIP6 for future emission scenarios called Shared Socio-economic Pathways (SSP), is a combination of Representative Concentration Pathway (RCP) and other pathways of socioeconomic development (O'Neill et al., 2016). These SSPs show different possible futures for greenhouse gas emissions and land use change based on data from integrated assessment models with SSP1-2.6, SSP2-4.5, SSP4-6.0, and SSP5-8.5 known as sustainable, moderate, severe, and extreme scenarios respectively (Eyring et al., 2016).

CMIP6 future observations (2022-2100) of precipitation and maximum and minimum temperature of SSP 2-4.5 (Moderate scenario) and SSP 5-8.5 (extreme scenario) were used to estimate agricultural droughts based on five different indices (i.e., VCI, TCI, SPEI, CWSI, and SMADI). These climate variables were obtained from multiple GCMs at daily time scales. Because the outcomes of these GCMs vary widely within the scenarios, the Multi-Model Ensemble (MME) mean was applied. These models are ACCESS-CM2, CMCC-ESM2, CNRM-ESM2-1, EC-Earth3-CC, EC-Earth3-Veg-LR, INM-CM4-8, INM-CM5-0, MIROC6, MIROC-ES2L, MPI-ESM1-2-LR, MRI-ESM2-0, NESM3, and NorESM2-MM. The selection of these models is based on the availability of future projections. The details of the GCMS of CMIP6 used in this study are given in Table 3.

The climatic variables at different spatial resolutions were initially re-gridded to a 1km resolution. The MME of 13 different GCMs were used instead of using an individual GCM, which benefits in terms of more reliable estimates, eliminating model uncertainties and variances, and decrease in spatial error and variability (Shrestha et al., 2020; Weigel et al., 2008). All models were averaged using the Equal Weight (EW) method of the MME which involves averaging the values for each model (Sun et al., 2024). For the Bias correction of the projected CMIP6 data, the variance scaling method was employed, which is used to adjust the statistics such as mean, variance, and standard deviation, of the climate model to better match the observed statistics for a certain period (Supharatid et al., 2022). Afterwards, the power transformation technique is used to correct the skewness and other non-normal characteristics of model data distributions. It makes the data more symmetrical and closer to the normal distribution (Eyring et al., 1937).

This way, the prediction obtained from this dataset is considered as a fair interpretation of all the GCMs, leading to more reliable and accurate climate projections. The datasets used in this study are summarized in Table 2.

Table 2: Datasets Used

Datasets	Description	Temporal Resolution	Spatial Resolution	Time Period	Source
CHIRPS **Climate Hazards Group Infrared Precipitation with Station Data**	Precipitation	Daily	0.05mm	2010-2021	GEE
IMERG **Integrated Multi-Satellite Retrievals for GPM - Early**	Precipitation	Daily	0.1mm	2010-2021	GEOVANNI-Earth NASA
MODIS **Moderate-resolution Imaging Spectroradiometer**	Temperature	Daily	250m	2010-2021	GEE
ERA-5 **Fifth Generation ECMWF Atmospheric Reanalysis of the Global Climate**	Temperature	Daily	0.1°×0.1°	2010-2021	GEE
FLDAS **Famine Early Warning Systems Network Land Data Assimilation System**	Soil Moisture	Monthly	0.1°×0.1°	2010-2021	GEOVANNI-Earth NASA
CMIP6 **Coupled Model Intercomparison Project**	Precipitation & Temperature	Daily	1km	2022-2100	Earth System Grid System-ESGS

Table 3: CMIP6 Models Used

Model	Developed by	Resolution (lat * lon)
ACCESS-CM2	CSIRO and BOM, Australia	$1.875° \times 1.25°$
CMCC-ESM2	CMCC, Italy	$0.75° \times 0.75°$
CNRM-ESM2-1	CNRM, France	$1.4° \times 1.4°$
EC-Earth3-CC	EC-Earth Consortium	$0.7° \times 0.7°$
EC-Earth3-Veg-LR	EC-Earth Consortium	$0.7° \times 0.7°$
INM-CM4-8	Institute of Numerical Mathematics, Russia	$1.5° \times 2°$
INM-CM5-0	Institute of Numerical Mathematics, Russia	$1.5° \times 2°$
MIROC6	JAMSTEC, AORI, NIES, and R-CCS, Japan	$1.4° \times 1.4°$
MIROC-ES2L	JAMSTEC, AORI, NIES, and R-CCS, Japan	$2.8° \times 2.8°$
MPI-ESM1-2-LR	Max Planck Institute for Meteorology, Germany	$1.875° \times 1.875°$
MRI-ESM2-0	Meteorological Research Institute, Japan	$1.125° \times 1.125°$
NESM3	Nanjing University of Information Science & Technology, China	$1.875° \times 1.875°$
NorESM2-MM	Norwegian Climate Centre, Norway	$1.25° \times 0.9375°$

3.4 Data Pre-processing

Climate classification organizes areas with single or multiple climatic parameters to determine the affinities in the area (Griffiths, 1976). Classification is different for different areas across the globe based on various techniques by climatologists. Agroecological zones are areas with similar environmental properties that are suitable for cultivation. These zones are developed based on the ecological requirements of the particular crops, climatology, hydrology, plant productivity and soil characteristics (Haider & Adnan, 2014). To compute drought indices efficiently, it is important to identify areas with similar climates. A **climate territory** can be defined by its characteristics, such as temperature, rainfall, humidity, radiation, wind, etc. (Funk et al., 2015).

The present study is conducted in Pakistan. It was divided into major climatic zones, mainly Arid, semi-arid, sub-humid and humid. The classification into zones showed that largest area is extremely arid i.e. 36.84 %, while 22.39% is arid. 10.48% is dry semi-arid, 9.66% is wet semi-arid, 12.35% is dry sub-humid, 3.70% is wet sub-humid, 3.33% is humid, and only 1.25% is very humid. After the spatial distribution of weather stations across the country, Inverse Distance Weighting (IDW) Interpolation was employed to predict values at unknown locations, resulting in interpolated values that created a continuous spatial representation of climate across the study area. De Martonne aridity index (E, 1926) presented in Equation 1 below was then used to classify the climate:

$$I = \frac{P}{(T+10)} \qquad \qquad \text{Equation 1}$$

Where P and T are the mean annual rainfall (millimeters) and the mean annual temperature (degree Celsius), respectively (Rahimi et al., 2013; Taheri Qazvini & Carrion, 2023).

3.5 Statistical Analysis

A comprehensive calculation of evaluation measures, including Coefficient Correlation (r), Root Mean Square Error (RMSE), Bias, Relative Bias (r-Bias), R-squared (r^2), Mean Absolute Error (MAE), and Slope of Coefficient (B_1) was used to examine and verify the accuracy and efficiency of rainfall products. These statistical indices examine the precision of satellite precipitation products.

Coefficient Correlation (r):

R measures the strength and direction of a linear relationship between two variables, such as observed values (Asuero et al., 2006). The value of r ranges from -1 to +1. A value of +1 shows a perfect positive relation, whereas a value of -1 shows a perfect negative relation. A 0 value means no correlation (Ratner & marketing, 2009).

$$r = \frac{\sum_{i=1}^{N}(X_{si}-\bar{X}_s)(Y_{oi}-\bar{Y}_o)}{\sqrt{\sum_{i=1}^{N}(X_{si}-\bar{X}_s)^2}\sqrt{\sum_{i=1}^{N}(Y_{oi}-\bar{Y}_o)^2}}$$
    Equation 2

Coefficient of determination (r²):

It tells us how well the satellite data matches the observed data. The value of r^2 ranges from 0 to 1, with 0 stating unsatisfactory results and 1 showing very good results (Belayneh et al., 2020).

$$r^2 = 1 - \frac{\sum_{i=1}^{N}(Y_{oi}-\hat{Y}_{oi})^2}{\sum_{i=1}^{N}(Y_{oi}-\hat{\bar{Y}}_o)^2}$$
    Equation 3

Mean Absolute Error (MAE):

It quantifies the mean magnitude of the error by measuring the difference between the satellite and observed data. Its values range from 0 to infinity, with lower values predicting that the satellite product values are more closer to observed data values, suggesting a better fit of the model (Ghajarnia et al., 2015; Sadiq et al., 2018).

$$MAE = \frac{1}{N}\sum_{i=1}^{N}|X_{si} - Y_{oi}|$$
    Equation 4

Root Mean Square Error (RMSE):

RMSE assigns more weight to larger errors compared than MAE and measures the mean magnitude of the error. RMSE values function the same way as MAE values, indicating that higher values have greater variation between satellite and observed data (Belayneh et al., 2020).

$$RMSE = \sqrt{\sum_{i=1}^{N} \frac{(X_{si} - Y_{oi})^2}{N}} \qquad \text{Equation 5}$$

Bias:

It is the difference between observed and satellite data. It is either positive, indicating overestimation, or negative, indicating underestimation (Belayneh et al., 2020; Quan & Bansal, 2021).

$$Bias = \frac{1}{N}\sum_{i=1}^{N}(X_{si} - Y_{oi}) \qquad \text{Equation 6}$$

Relative Bias (R-Bias):

It is the systematic bias of the satellite and observed data and behaves the same as bias (Quan & Bansal, 2021). The positive bias overestimates and the negative bias underestimates the observed data, and zero bias indicates a perfect agreement between the model and the observations.

$$rBias = \frac{\sum_{i=1}^{N}(X_{si} - Y_{oi})}{\sum_{i=1}^{N} Y_{oi}} \times 100 \qquad \text{Equation 7}$$

Coefficient of Slope (β):

The slope of the regression line is directly linked to the r and is defined by the quantitative measurement of the vertical change for every unit of horizontal change. This slope of regression is also known as the fitted line. It indicates whether the dependent variable increases or decreases as r increases. When the value of r is negative, the **β** is negative and, when the correlation is positive, the **β** is positive (Sahoo et al., 2020). The coefficient of slope can be determined from a linear regression Equation 8.

$$Y_{oi} = \beta . X_{si} + \alpha \qquad \text{Equation 8}$$

Where, the formula for **β** as shown in Equation 9 is:

$$\beta = \frac{\sum_{i=1}^{N}(X_{si} - \bar{X}_s)(Y_{oi} - \bar{Y}_o)}{\sum_{i=1}^{N}(X_{si} - \bar{X}_s)^2} \qquad \text{Equation 9}$$

Where,

X_{si} = Satellite data for the ith daily event.

Y_{oi} = Observed data for the ith daily event.

N = Total number of observations.

$\overline{X}_s$ = Mean of satellite data.

$\overline{Y}_o$ = Mean of observed data.

α = intercept.

$|X_{si} - Y_{oi}|$ = Absolute error for each prediction.

3.6 Agricultural Drought Assessment

3.6.1 Vegetation Condition Index (VCI)

The Vegetation Condition Index (VCI) is a key indicator used in monitoring vegetation health, particularly in the context of drought assessment. It quantifies the relative greenness of vegetation compared to its typical condition, offering insights into plant stress levels (Kogan, 1997). VCI is typically derived from remote sensing data, such as satellite imagery, and is calculated based on metrics like NDVI (Khan & Gilani, 2021). By analyzing temporal changes in vegetation greenness, VCI provides valuable information on the onset, severity, and duration of drought impacts on ecosystems(Jiao et al., 2016). This index is widely utilized in agricultural monitoring, environmental management, and early warning systems, aiding decision-makers in mitigating the effects of droughts on food security, biodiversity, and ecosystem services (Jiao et al., 2016).

VCI was computed using the values of NDVI from MOD13A2.006 product with 1km spatial resolution as shown in Equation 10 (Jiao et al., 2016; Karimi et al., 2022)

$$VCI = \frac{NDVI - NDVI_{min}}{NDVI_{max} - NDVI_{min}} \times 100 \qquad \text{Equation 10}$$

Where, NDVI is the current value of the pixel, $NDVI_{min}$ and $NDVI_{max}$ is the minimum and maximum values of the NDVI time series. The value ranges from 0 to 100 with lower values for extremely unfavorable conditions to higher values being good conditions.

3.6.2 Temperature Condition Index (TCI)

The Temperature Condition Index (TCI) is pivotal in agricultural drought monitoring and evaluating temperature anomalies' impact on vegetation health (Li et al., 2024). It provides insights into stress levels experienced by crops and natural vegetation, enhancing understanding of thermal conditions affecting agricultural areas (Zeng et al., 2022). Land surface temperatures affect the vegetation cover and underground water tables. Therefore, after VCI, this index suggested as free of cloud contamination and air moisture. Integrated with metrics like NDVI, TCI offers a holistic view of vegetation conditions amidst changing temperature patterns (Tsiros et al., 2004). Its inclusion in drought monitoring frameworks improves early warning systems' accuracy, enabling timely interventions to mitigate agricultural losses and ensure food security (Cunha et al., 2019). TCI plays a vital role in safeguarding agricultural productivity by providing actionable information for drought management and adaptation strategies (Li et al., 2024).

TCI was computed using Land Surface Temperature data from MOD11A1 product with 1km spatial resolution as shown in Equation 11 (Kogan, 1997).

$$TCI = \frac{LST - LST_{min}}{LST_{max} - LST_{min}} \times 100$$
Equation 11

Where, LST is the current value, LST_{min} and LST_{max} are the minimum and maximum values of LST for the time period of the study respectively (Alamdarloo et al., 2018).

3.6.3 Standardized Precipitation-Evapotranspiration Index (SPEI)

The Standardized Precipitation-Evapotranspiration Index (SPEI) is a comprehensive drought assessment tool that integrates precipitation and evapotranspiration data (Beguería et al., 2014; Shukla & Wood, 2008). Unlike other indices, SPEI incorporates temperature effects, making it adaptable to diverse climates (Vicente-Serrano et al., 2010). It standardizes precipitation and evapotranspiration over a specified timeframe, revealing deviations from historical patterns and indicating drought severity (Beguería et al., 2014). This index, widely

employed in drought monitoring and water resource management, offers insights into drought intensity, duration, and spatial extent. SPEI's versatility and accuracy make it invaluable for decision-making and adaptation strategies in regions vulnerable to water scarcity and climate variability (Danandeh Mehr & Vaheddoost, 2020). SPEI is a variant of the Standard Precipitation Index, which contains information on evapotranspiration as well and is therefore used to determine the major impact of temperature rise on water need (Danandeh Mehr & Vaheddoost, 2020). To calculate SPEI, we use the water balance equation which is given in Equation 12:

$$D = P - PET$$
<div align="right">Equation 12</div>

Where, D is the difference between precipitation and Potential Evapotranspiration.

3.6.4 Soil Moisture Agricultural Drought Index (SMADI)

The Soil Moisture Agricultural Drought Index (SMADI) stands as a crucial tool for accurately assessing agricultural drought by focusing on soil moisture dynamics (Mercedes et al., 2021). By precisely measuring the moisture content in the root zone, SMADI provides essential insights into the immediate availability of water for crops, directly influencing their growth and productivity (Sánchez et al., 2016). Effective utilization of SMADI enables timely interventions such as irrigation scheduling, crop selection, and drought-resistant farming practices, empowering farmers and policymakers to proactively manage drought impacts and enhance agricultural resilience in the face of changing climate patterns (Zhao et al., 2022).

The index depends on the remote sensing data sources and is computed using the soil moisture (SM), LST and Vegetation Index (VI) (Sánchez et al., 2016). The connection of LST and VI with soil moisture makes it necessary to consider it for the calculation of SMADI (Yang et al., 2024). First, we normalize the NDVI, LST and SM to achieve VCI, MTCI Equation 13, and SMCI Equation 14. Then, SMADI is calculated using Equation 15 which focuses on the inverse relationship between the LST and NDVI (Salvia et al., 2020; Sánchez et al., 2016).

$$MTCI = \frac{LST - LST_{min}}{LST_{max} - LST_{min}} \times 100$$
<div align="right">Equation 13</div>

$$SMCI = \frac{SM_{max} - SM}{SM_{max} - SM_{min}} \times 100$$
<div align="right">Equation 14</div>

$$SMADI = SMCI \; \frac{MTCI}{VCI}$$
<div align="right">Equation 15</div>

Where, LST_{min}, LST_{max}, SM_{min} and SM_{max} represent the minimum and maximum values of LST and SM for the study period.

Drought severity classification range for each index is given in Table 4.

Table 4: Drought Severity Classification Index

Class	VCI	TCI	SPEI	SMADI
Extreme Drought	0 to 10	0 to 10	≤ -2.0	> 4
Severe Drought	11 to 20	11 to 20	-1.5 to -1.9	3 to 4
Moderate Drought	21 to 30	21 to 30	-1 to -1.4	2 to 2.99
Mild Drought	31 to 50	31 to 50	-0.5 to -0.9	1 to 1.99
Normal	51 to 70	51 to 70	-0.1 to -0.4	0.5 to 1
Excellent Vegetation	71 to 100	71 to 100	≥ 0.0	0 to 0.49

Reference: (Zhao et al., 2022)

3.7 Spatio-temporal Trend Analysis

Precipitation, temperature, soil moisture, and other hydrological parameters are important for drought identification (Shahzada et al., 2018). The impact of temperature and precipitation on drought indices is also known as temperature and precipitation variability or correlation. The long-term monthly average of precipitation, temperature, and drought indices (TCI, VCI, SPEI, and SMADI) from 2010 to 2021 was used to compute the spatiotemporal trend.

3.8 Future Drought Predictions

Future drought predictions aid in preventive resource management and agricultural planning, which makes people more ready and helps deal with mitigating economic and environmental consequences (Mishra & Singh, 2010). They enable prompt decision-making

to minimise negative consequences and ensure sustainability (Weltzin et al., 2003). Future predictions can be done using statistical analysis such as time series and trend extrapolation, which involves historical climate data to identify patterns and, based on these patterns, predict future trends and conditions. However, with Machine Learning (ML) and Artificial Intelligence (AI), these predictions are enhanced and improved by analysing complex climate data patterns and timeliness of forecasts.

Machine learning (ML) includes a wide number of methods that include making prediction models and looking for trends in them. Its purpose is to model human perception to recognize patterns (Greener et al., 2022). It is the most accurate method in RS for solving complex problems including sorting out large datasets, making them most suitable for satellite image analysis (Belgiu et al., 2016; Han et al., 2019). Random Forest (RF), Convolutional Neural Network (CNN), Artificial Neural Network (ANN) Boosted Regression Tree (BRT), and Multivariable Linear Regression (MLR) are some of the types of ML used in remote sensing (Han et al., 2019). RF is the most accurate method compared to other ML algorithms, and it is better at dealing with missing data and huge datasets (Choi et al., 2023).

3.8.1 Random Forest Regressor

Random forest is a machine learning algorithm that is widely used for two major purposes, i.e., regression and classification. RFR is a collective tree-type classifier that uses different decision trees combined to improve classification accuracy (Belgiu et al., 2016; Prasad et al., 2006). The principle of RF is to build multiple decision trees during training by choosing a subset of explanatory variables and averaging their predictions for effective regression performance (Belgiu et al., 2016). Two important variables for generating the model are the dependent variable, also known as the number of trees desired (k), and the independent variable, known as the number of prediction variables (m) (Breiman, 2001; Rodriguez-Galiano et al., 2012).

In this study, we used the RF algorithm to generate a number of decision trees. For the regression, the algorithm takes the average of all the predictions from each tree to produce the final result. In the data preparation, historical data from 2010 to 2021 of the indices calculated were given to the model. Also CMIP6 future data of temperature (minimum and maximum)

and precipitation from 2022 to 2100 was used. All of these datasets were included in the training samples, precipitation and temperature serving as input features, which were then aggregated to produce yearly average outputs. The decision trees used the input features and split them into subsets guided by the target data values. This method makes predictions and analyses more accurate, even when the data is complicated and changes over time (Breiman, 2001). RFR is given in the Equation 16.

$$RF\ model_{trained} = fit(RF\ model, X_{train}, Y_{train})$$ Equation 16

Where, fit represents the training process, X_{train} and Y_{train} are the training data features and the target values, respectively.

The advantages of RF include handling large datasets with high accuracy, which makes it suitable for image analysis, reduces over-fitting, and handles missing values and outliers (Soyoung & Kim, 2019) .

Future predictions for each index were done using historical index data and CMIP6 future data under two scenarios, i.e. SSP 2-4.5 and SSP 5-8.5. However, the future projections of VCI were generated solely from historical VCI values; some key differences occur, such as prediction accuracy and uncertainty levels. The RFR uses only calculated historical VCI values to project future VCI, which assumes that past patterns and trends will continue into the future and, thus, does not take into account any potential impacts of future climate change. In terms of climate change sensitivity, the future predictions of VCI are just hypothetical because they are based on stationary climate, which can underestimate or overestimate future drought conditions. Regarding uncertainty, VCI's uncertainty arises from historical data's variability and trends and does not consider additional extreme conditions in the future climate. Other indices such as TCI, SPEI, and SMADI were predicted using CMIP6 data, which takes into account the future climate variability and trends and, therefore, responses to shifts in climate change, giving us more accurate and reliable results. Predicted results will help us analyze the differences in drought indices patterns and calculations and reveal significant strengths and limitations of each index.

3.9 Multi-Criteria Evaluation (MCE)

MCE is a method of decision-making that assesses numerous criteria that conflict with each other in order to evaluate various options or alternatives. This is particularly valuable in complex scenarios where a decision must consider multiple elements simultaneously, such as environmental, economic, and social impact (Malczewski, 2006). MCE facilitates the integration of both qualitative and quantitative data, which results in a thorough examination of the various criteria (Mendoza et al., 2000). This method is widely used in fields such as urban planning, resource management, and environmental studies as well.

AHP is a specific technique within MCE that helps complex decision problems into a hierarchy of criteria and sub-criteria. It is widely used in various applications, including project prioritization, risk assessment, and resource collection (Kumari et al., 2023).

3.9.1. Analytical Hierarchy Process (AHP)

The Analytical Hierarchy Process (AHP) multi-criteria approach was employed in this study to compare the factors as per their relative importance over one another and to ascertain priorities. It is the most widely used approach presented by Saaty in 1990 (Pandey & Srivastava, 2019). It works on the principle of setting evaluation criteria and offers multiple options to choose the best among them. Sometimes, the best-chosen option yields only optimized results when all criteria and parameters are taken into account. Therefore, in such cases, AHP proves to be a versatile and effective tool for conducting pairwise analysis with criteria and rankings (Chakraborty et al., 2019). The method involves three major steps, which include calculating the weightage scale, quantifying optional scoring sources and determining ranking options for values (Rahman & Saha, 2008). The parameters involved are VCI, TCI, SPEI, and SMADI. A pairwise comparison matrix was performed to calculate the weightage factor of each parameter.

The *pairwise comparison matric (PWCM)* rates the factors based on their relationship with other factors and the extent of impact they have on drought severity. For this, a scale of values ranging from 1 to 9, developed by (Saaty, 1977) is used. The highest and the lowest ratings, i.e. 9 and 1, respectively, show how much a certain factor is dominating over other factors and vice versa. Based on previous studies as a reference, expert opinion and subject-specific

experience are also taken into consideration when deciding the criteria for the factors involved. Moreover, VCI was given the least weight as its future projections are hypothetical based solely on historical VCI values and do not consider any future climate aspect.

Consistency Ratio (CR) is defined as a singular numeric index used to assess the consistency of PWCM. If CR is equal to or less than 0.10, the consistency result is acceptable (Saaty, 1977). CR is calculated using Equation 17.

$$CR = \frac{CI}{RI}$$
Equation 17

Where, *CI* is the consistency index and *RI* is the random inconsistency index.

To calculate CI, we use Equation 18:

$$CI = \frac{\lambda_{max} - 1}{n - 1}$$
Equation 18

Where, λ_{max} is the principal eigenvalue and *n* is the total number of criteria.

The RI values proposed by (Saaty, 1977) were used by (Jiao et al., 2019; Kalambukattu et al., 2018; Zagade & Umrikar, 2021) in their research studies. The pairwise comparison matrix were designed based on AHP scale given in Table 5 and the final criteria weight based on MCDM AHP method is given in Table 6.

Table 5: AHP Derived Pairwise Comparison Matrix And Standardization Results.

	VCI	SPEI	SMADI	TCI
VCI	1	0.33	0.33	0.25
SPEI	3	1	0.5	2
SMADI	3	2	1	3
TCI	4	0.5	0.33	1
Average	0.09	0.27	0.44	0.20
Principal Eigenvalue = 4.22, **random inconsistency index (RI)** = 0.9 , **number of comparisons** = 6				
Consistency Index (CI) = 2.79, **Consistency Ratio (CR)** = 3.10%				

Table 6: Final Main Criteria Weight Based On Multi-Criteria Decision Making AHP Method

Sr. No	Criteria/Category	Priority	Rank
1	VCI	8.9%	4
2	SPEI	27.4%	2
3	SMADI	43.8%	1
4	TCI	19.9%	3

3.10 Software and Tools Used

For this study, several key software programs were used to analyse drought indices which include ArcMap 10.8.2, Google Earth Engine, and Microsoft Excel.

ArcMap 10.8.2

ArcMap 10.8.2 was used in this study. It is a product of Esri's ArcGIS desktop suite and is a powerful GIS program for mapping, spatial analysis, and data visualization. It is beneficial in environmental studies, urban planning, resource management, and disaster response. We used the ArcMap Spatial Analyst toolbox to study and visualize drought-related data, integrating diverse datasets such as precipitation data, soil moisture data, and vegetation indices.

Google Earth Engine

Google Earth Engine (GEE) is a cloud-based platform that offers powerful tools for processing and analysing geospatial data at scale (Gorelick et al., 2017). It contains multiple components that help with geospatial analysis, including elements such as a data catalog, code editor, Earth engine library, code repository, visualization tools, and Earth engine apps. The tool was used to acquire climate data such as CHIRP, IMERGE-E, MODIS, etc. for the period 2010 to 2021. We used GEE to compute drought indices such as VCI, TCI, and SPEI, and supplementary data for the calculation of SMADI were also acquired from it.

Microsoft Excel

Microsoft Excel was used to organize data acquired from multiple sources and employed to perform preliminary analysis and statistical calculations. Furthermore, it was used to create graphs and charts to represent the data.

CHAPTER 4: RESULTS AND DISCUSSION

4.1 Comparison of Gauge Data with Climate Products

4.1.1 Comparison of Gauge Precipitation with CHIRPS and IMERG Version 6

Figure 3 & Figure 4 displays scatter plots that compare monthly averaged precipitation data from two satellite-based products (CHIRPS and IMERG) with gauge precipitation data. Each graph displays a fitted line and several statistical metrics to illustrate the correlation and evaluate the performance of each satellite product.

Analysis of CHIRPS

Figure 3 assesses the CHIRPS product. The scatter plot shows the relationship between CHIRPS monthly averaged precipitation on the y-axis and PMD monthly averaged precipitation on the x-axis (ground truth). The coefficient of determination (R2) indicates the amount of variation in the dependent variable (CHIRPS) that is predicted from the independent variable (PMD). The graph shows that (R^2) is 0.78, which means that observed data can explain 78% variation in CHIRPS data. R^2 may vary from 0 to 1, with values closer to 1 suggesting a better fit. The correlation coefficient (CC) measures the strength and direction of the linear relationship between the two variables. A value of 0.88 indicates a strong positive linear correlation between the two datasets. Bias measures the average difference between CHIRPS and PMD values. A Bias of 0.52, indicates that CHIRPS values are slightly higher on average as compared to PMD measurements. The values of Bias range from negative to positive, with 0 indicating no bias. The relative bias (rBias) is the bias normalized by the mean of the observed values. A rBias of 1.31 or 31% further confirms this overestimation.

RMSE measures the standard deviation of the residuals (prediction errors). The RMSE of 16.34mm shows the standard deviation of the prediction errors, showing the model's accuracy. The RMSE scales from zero to infinity, with lower values indicating greater model performance. MAE measures the average of the squares of the errors. An MAE of 11.15mm^2 represents the average squared difference between the observed (PMD) and predicted (CHIRPS). The coefficient of regression (β_1) measures the strength and direction of the relationship between the independent (PMD) and the dependent (CHIRPS) variable. The β_1 of

0.73 indicates that CHIRPS is a reasonably good predictor of actual precipitation as measured by PMD gauges. In general, the value of β_1, if closer to 1 or -1, shows a stronger relationship.
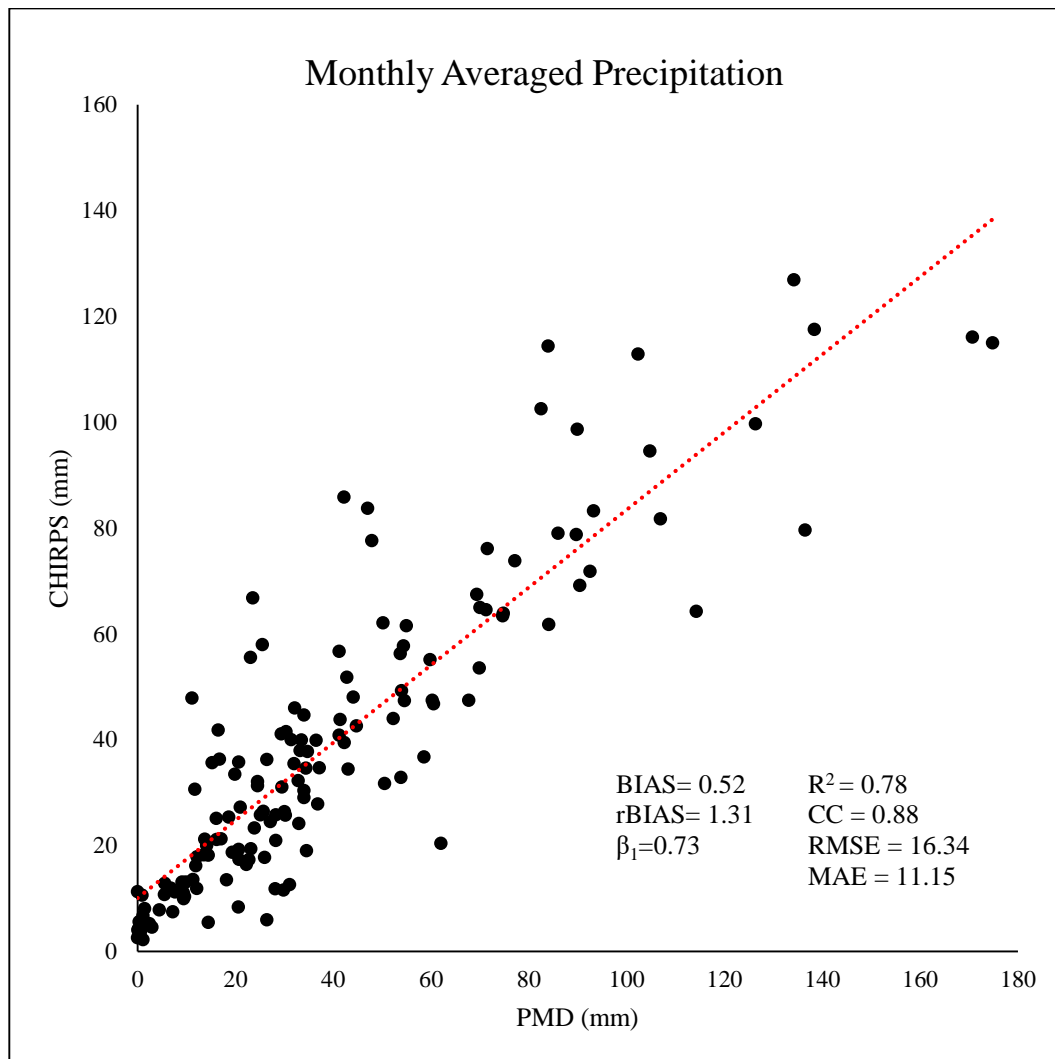

Figure 3: Comparison of gauge precipitation and CHIRPS

Analysis of IMERG

Figure 4 assesses the IMERG product. The scatter plot shows the relationship between IMERG monthly averaged precipitation on the y-axis and PMD monthly averaged precipitation on the x-axis (ground truth). The R^2 value of 0.72, i.e., 72%, shows the variance in the gauge data is covered by the IMERG data, which is slightly lower than the R^2 for CHIRPS. The CC of 0.85 shows a strong positive correlation, slightly weaker than CHIRPS. In this graph, the trend line has a steeper slope β_1 of 1.33. The statistical metrics include a bias of -24.01 and a rBias of -60.35, confirming significant underestimation by IMERG compared

to PMD. RMSE of 38.70mm shows that IMERG data has a large average error compared to PMD data, and an MAE of 26.44mm^2 shows significant variation between the datasets.

Although IMERG shows a good correlation with PMD, as indicated by CC, it shows higher errors and significant negative bias. CHIRPS, on the other hand, exhibits better performance than IMERG. This is confirmed by high R^2 values and lower error metrics (RMSE and MAE). The smaller values of bias and rBias for CHIRPS also align closely with the PMD measurements.
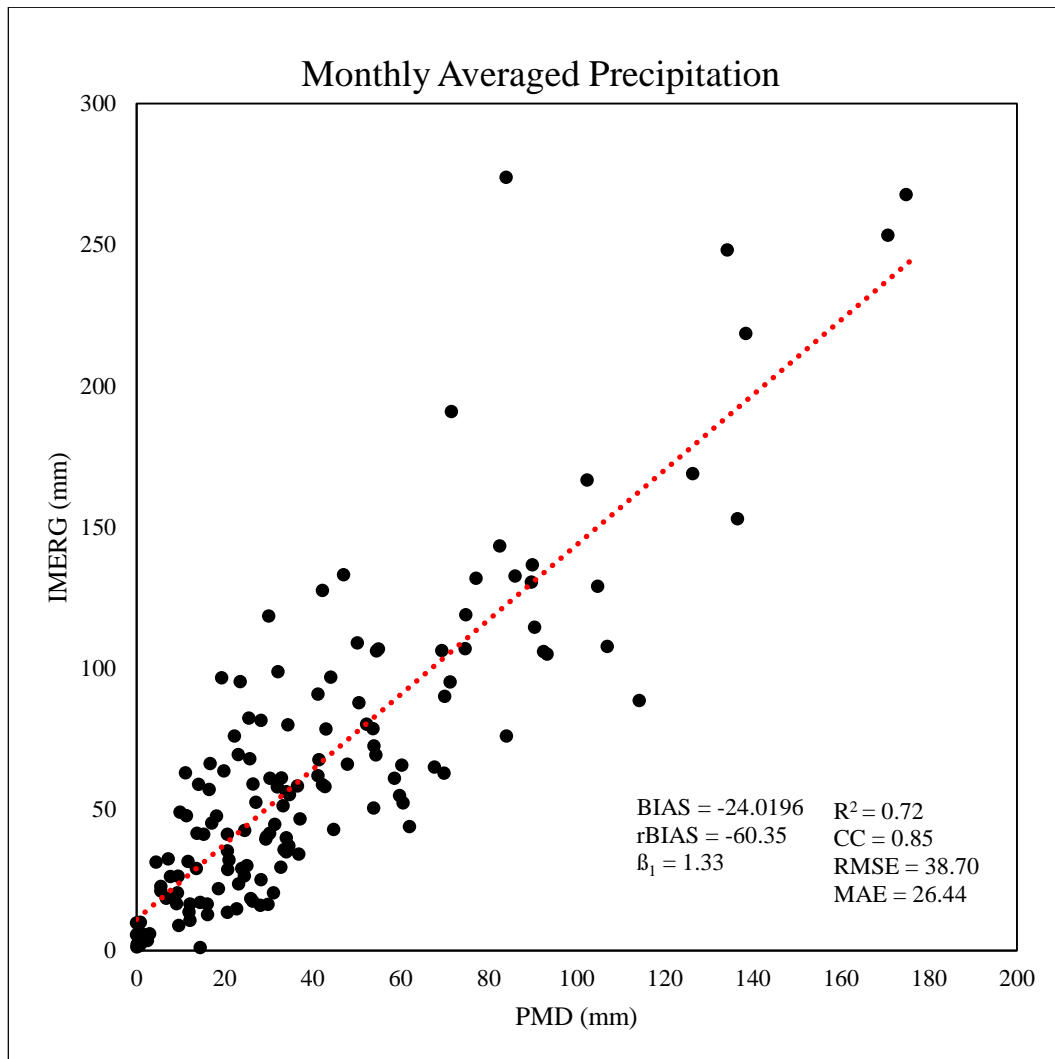
Figure 4: Comparison of gauge precipitation with IMERG

Therefore, CHIRPS provides more accurate and reliable estimates and IMERG. These results are also confirmed by several studies done by (Duan et al., 2019; Nashwan et al., 2019), which evaluated several precipitation products with rain gauge station data, and their results showed that while CHIRPS and IMERG are the most used satellite products for hydrological studies, CHIRPS products performed better and gave more similar results with gauge data.

4.1.2 Comparison of Gauge Temperature with MODIS and ERA-5

Figure 5 and Figure 6 displays scatter plots that compare monthly averaged temperatures from two satellite-based products (MODIS and ERA-5) with gauge temperature data. Each graph displays a fitted line and several statistical metrics to evaluate the performance of MODIS and ERA-5 in predicting surface temperatures.

Analysis of MODIS

Figure 5 assesses the MODIS product. The scatter plot shows the relationship between MODIS monthly averaged temperature on the y-axis and PMD monthly averaged temperature on the x-axis (ground truth). The graph shows that (R^2) is 0.73, meaning that observed data can explain 73% variation in MODIS data. A CC value of 0.85 indicates a strong positive linear correlation between the two datasets. A bias of 10.29 signifies that MODIS values are higher on average than PMD measurements. A rBias of 30.17 further indicates a substantial deviation. The RMSE of 2.94°C and an MAE of 2.67°C^2 shows a moderate level of agreement. The β_1 of 60.92 shows a linear relationship with a positive slope.
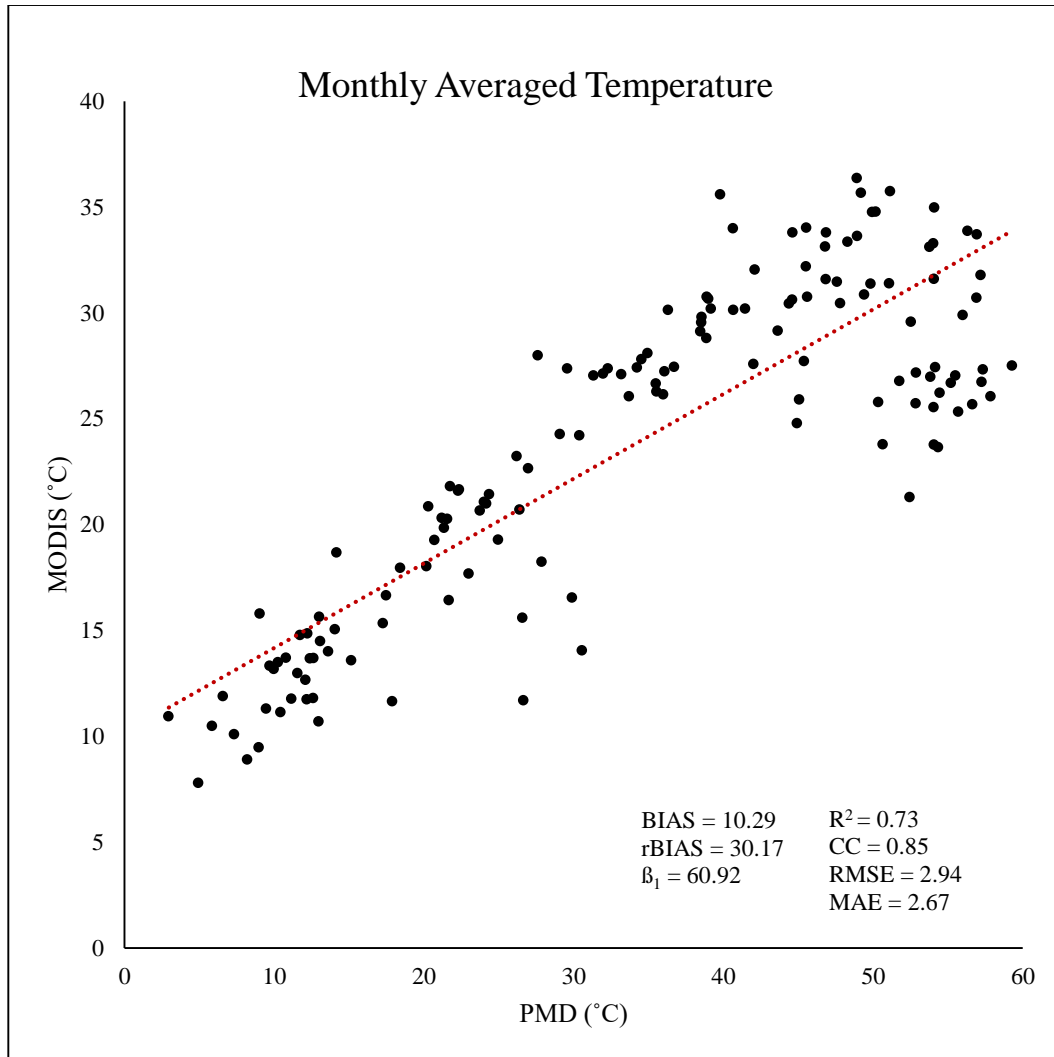
Figure 5: Comparison of gauge temperature with MODIS

Analysis of ERA-5

Figure 6 assesses the ERA-5 product. The scatter plot shows the relationship between ERA-5 monthly averaged temperature on the y-axis and PMD monthly averaged temperature on the x-axis (ground truth). This figure shows a stronger linear relationship than MODIS. The statistical measures demonstrate a strong level of agreement, i.e., R^2 = 0.95, CC=0.97, RMSE=2.12°C, and MAE=1.93°C^2. A bias of 16.08 shows that ERA-5 estimates, on average, are higher than PMD measurements. The rBias of 47.15 signifies a significant deviation.

ERA-5 shows a greater association with PMD values than other data, as seen by higher R^2 and CC values. Although ERA-5 has higher bias and rBias values, still outperforms MODIS in estimating surface temperatures.
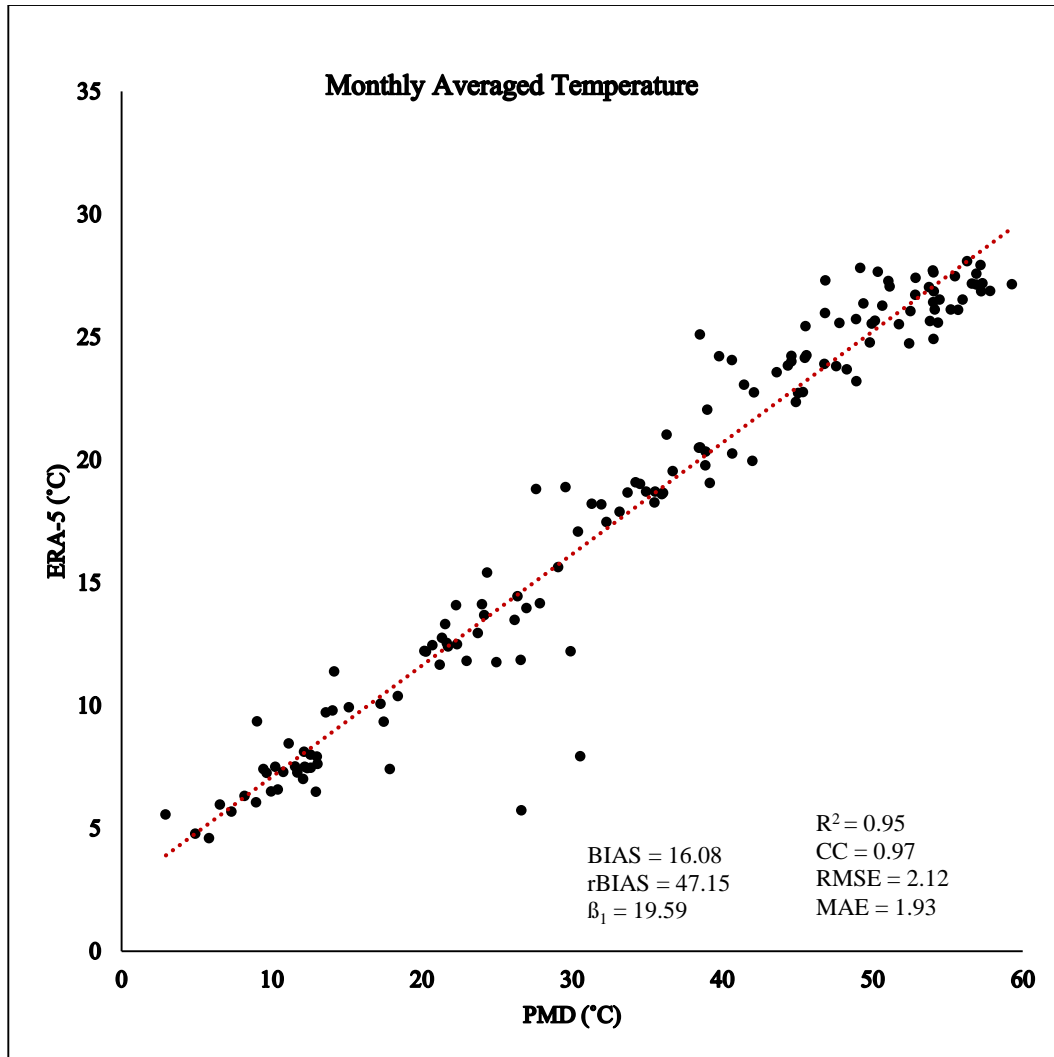
Monthly Averaged Temperature

R^2 = 0.95
CC = 0.97
RMSE = 2.12
MAE = 1.93

BIAS = 16.08
rBIAS = 47.15
β_1 = 19.59

Figure 6: Comparison of gauge temperature with ERA-5

4.2 Spatio Temporal Variability Analysis

The spatio-temporal variability analysis of each drought index, and observed temperature and precipitation over long-term monthly averages shows how these variables change across different regions and time periods. This involves statistical and geospatial techniques to identify patterns, trends, and anomalies. Multiple drought indices are used to quantify drought conditions, while temperature and precipitation data aid in understanding the wider climatic context. This analysis aims to assess how these factors interact, identify drought vulnerable areas, and evaluate the impact of climate variability and change on water supply and agricultural productivity.

The graph for each analysis illustrates the relationship between precipitation (mm), temperature (°C), and index over a year taken as long-term monthly averages. The x-axis represents the long-term monthly averages, while the y-axis on the left indicates values for precipitation and temperature, and the y-axis on the right shows the index. Precipitation reaches its maximum in the middle of the year, with values observed in July, which indicates a typical seasonal trend. In the seasonal pattern, precipitation increases during specific months, likely corresponding to a rainy season. Following the peak, there is a significant decline towards the end of the year. Temperature, on the other hand, displays a more consistent and gradual increase from January, reaching stability between May and August, implying higher temperatures in the summer. Following this trend, temperature gradually declines towards December, indicating a shift towards the cooler months.

4.2.1 Spatio-temporal Variability of VCI

In Figure 7, the x-axis represents the long-term monthly averages. At the same time, the y-axis on the left indicates values for precipitation and temperature, and the y-axis on the right shows the VCI. The VCI shows an initial rise from January, peaking around May, indicating better vegetation conditions. Following that, there is a slight decline, followed by another increase in September, before a steady decrease towards the end of the year. These fluctuations are closely associated with changes in precipitation and temperature, suggesting that vegetation conditions improve with increased precipitation and moderate temperatures.

The temporal trend of these parameters shows great interdependence. The peak in precipitation values aligns with high VCI values, indicating the importance of water availability for vegetation health. On the contrary, the decline in VCI towards the end of the year corresponds with a decrease in temperature and precipitation. Overall, the data highlights the variability of precipitation and temperature and their direct influence as indicated by the VCI. This is important for managing agricultural practices and projecting ecological responses to climate change.
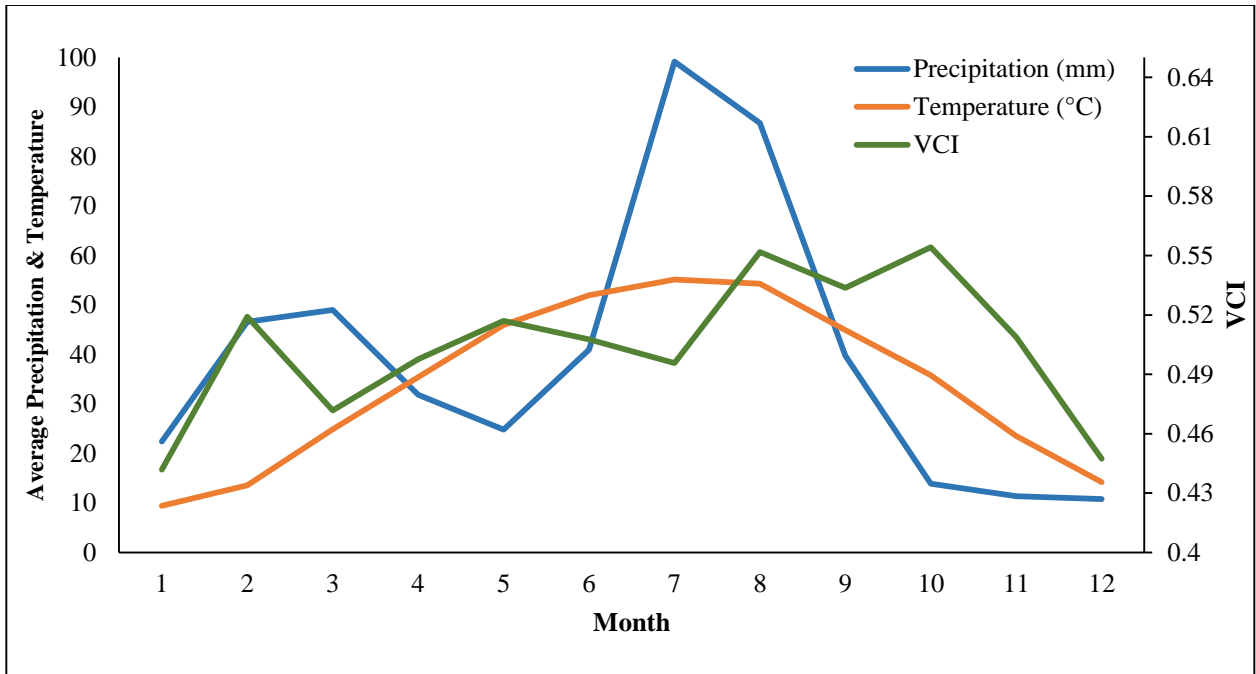
Figure 7: Spatio-temporal variability of VCI

4.2.2 Spatio-temporal Variability of TCI

In Figure 8, the x-axis represents the long-term monthly averages. At the same time, the y-axis on the left indicates values for precipitation and temperature, and the y-axis on the right shows the TCI. The TCI begins with a moderate value in January, rises to its peak in May, and then fluctuates throughout the year with prominent peaks in August and September. The index then declines towards December. These fluctuations suggest that while TCI reflects overall temperature conditions favorable for vegetation, it also corresponds distinctly to precipitation changes.

The graph shows the relationship between the parameters, where the peak in precipitation during the midyear correlates with the highest TCI values, indicating the impact of rainfall on temperature conditions beneficial for vegetation. On the contrary, the decline in precipitation and temperature towards the end of the year indicates less favourable conditions for vegetation. Overall, the seasonal variations in precipitation and temperature significantly influence the TCI. This highlights the importance of hydrologic factors in determining vegetation health, with TCI acting as a critical indicator of these conditions.
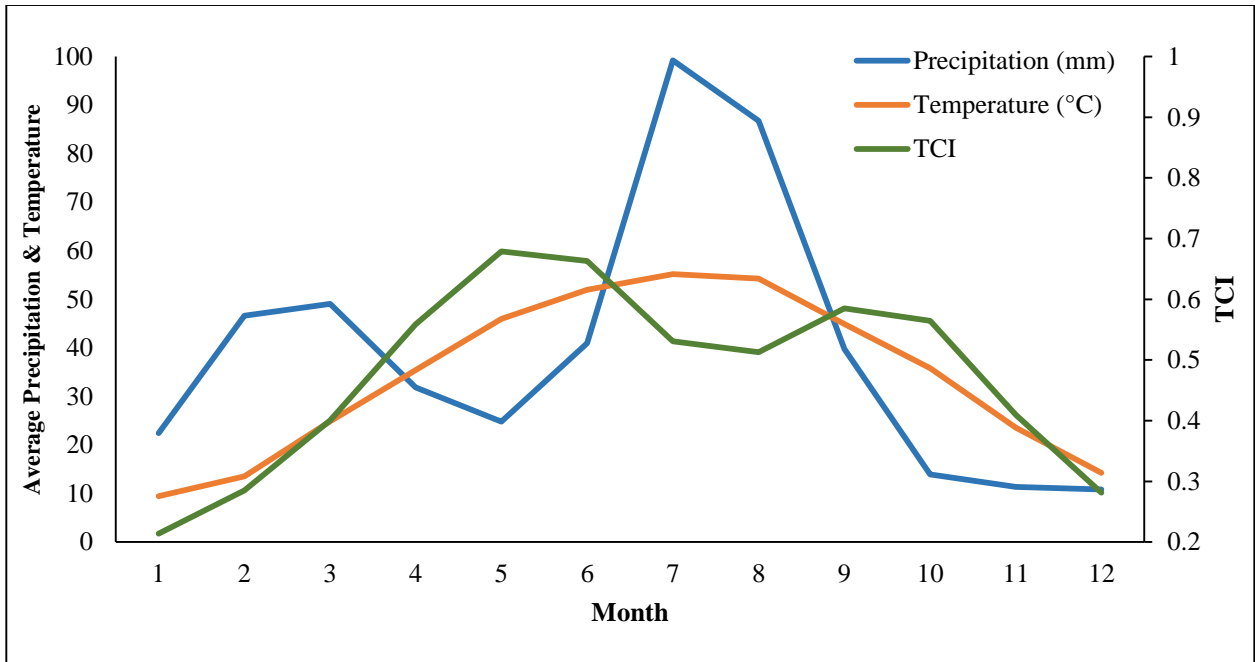
Figure 8: Spatio-temporal variability of TCI

4.2.3 Spatio-temporal Variability of SPEI

In Figure 9, the x-axis represents the long-term monthly averages. At the same time, the y-axis on the left indicates values for precipitation and temperature, and the y-axis on the right shows the SPEI values. The SPEI values increase from the beginning of the year, peaking around June, and then fluctuate moderately before declining towards the end of the year. SPEI values during midyear show improved moisture conditions, probably due to increased precipitation and moderate temperatures. On the contrary, the decline in SPEI towards the end of the year indicates worsening drought conditions as precipitation decreases and temperature drops.

Overall, the graph illustrates a clear seasonal cycle, with midyear marked by high precipitation and temperatures, contributing to favourable moisture conditions (higher SPEI). In the subsequent months, the decrease in precipitation and temperature indicates drier conditions (lower SPEI). This is important for understanding the local climate patterns and their consequences for water resource management, agriculture, and ecosystem sustainability.
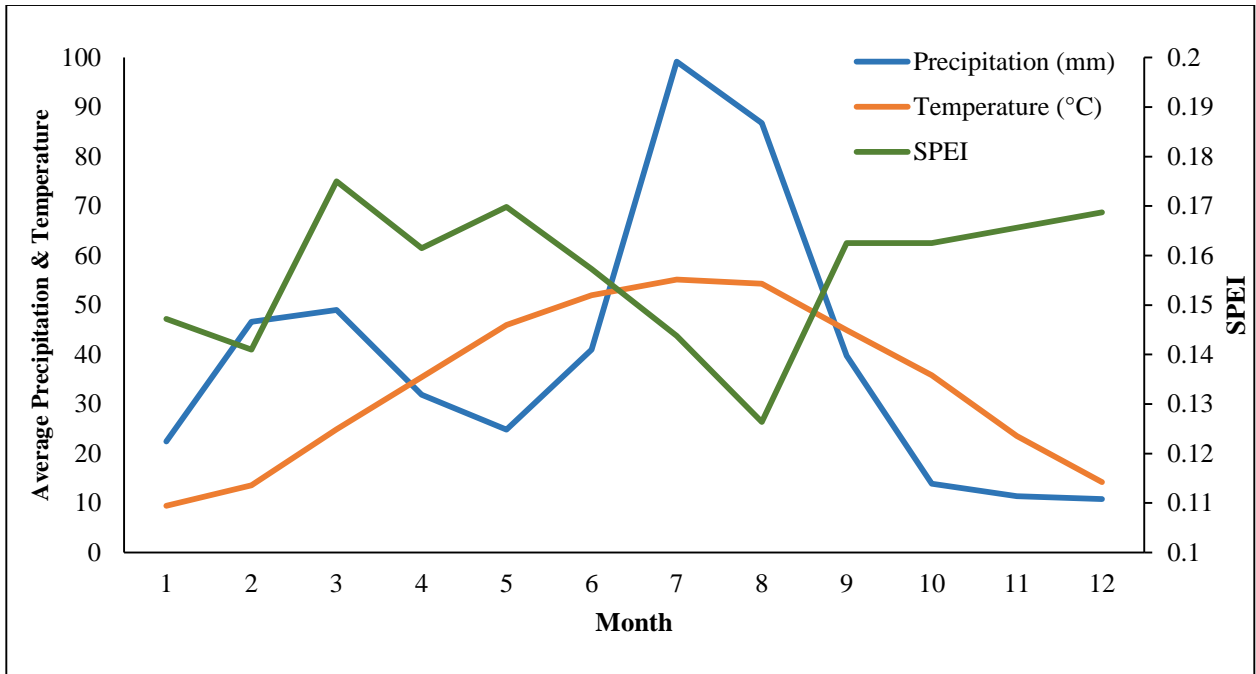
Figure 9: Spatio-temporal variability of SPEI

4.2.4 Spatio-temporal Variability of SMADI

In Figure 10, the x-axis represents the long-term monthly averages. At the same time, the y-axis on the left indicates values for precipitation and temperature, and the y-axis on the right shows the SMADI values. SMADI significantly declines in January, dropping from 7 to around 4.5 by February. This is followed by slight fluctuations and a gradual decline until April. From May onwards, SMADI rises steadily, peaking again in December at 6.5. This trend indicates a cyclic pattern of drought intensity, with lower values during the middle year months and higher values towards the beginning and end of the year.

Overall, the graph shows distinct seasonal patterns for these variables. Precipitation shows significant variability with two major peaks, while temperature follows a more consistent seasonal pattern of increase and decrease. SMADI displays a cyclic pattern, highlighting periods of varying drought intensity throughout the year. This data is essential for understanding the climate patterns and their potential impacts on the studied area.
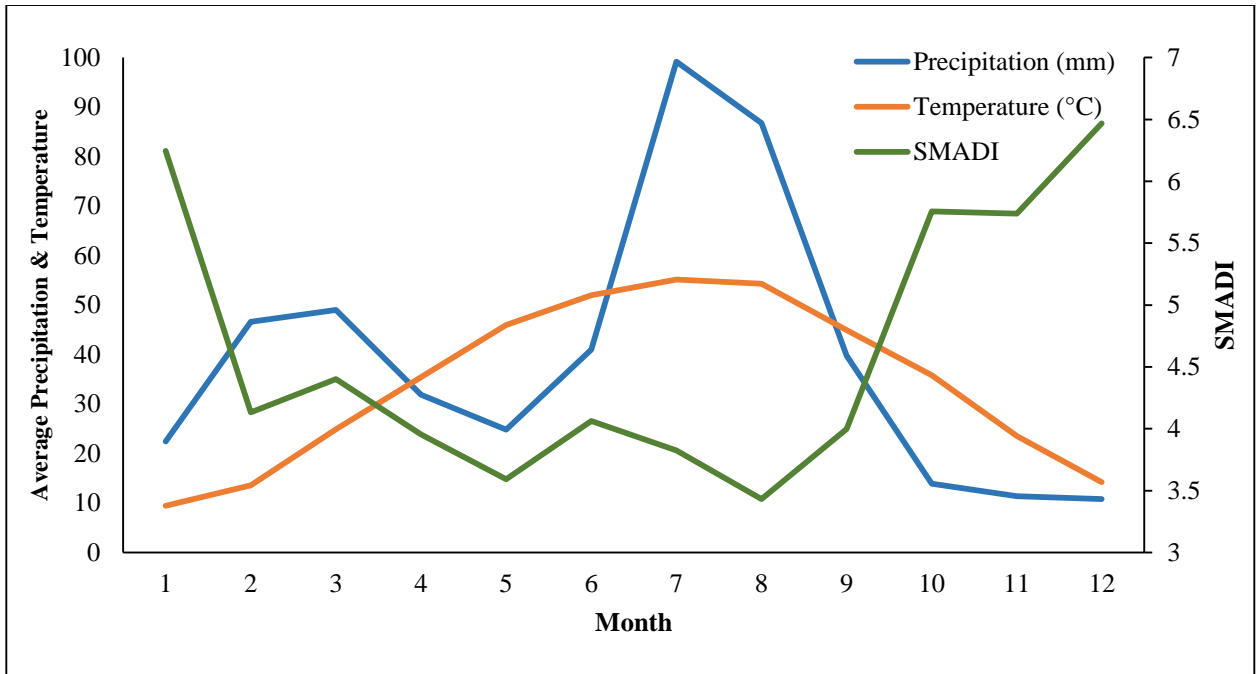
Figure 10: Spatio-temporal variability of SMADI

4.3 Spatial Distribution and Intensity of Drought Indices

In this study, we assessed global meteorological, hydrological, and agricultural drought from 2010 to 2100 based on four drought indices (VCI, TCI, SPEI, and SMADI), with the period of 2010 to 2021 being the historical period and 2022 to 2100 being the future period under SSP 2-4.5 and SSP 5-8.5. The CMIP6 SSP 2-4.5 scenario was used in these projections, representing a "middle-of-the-road" future in which social, economic, and technological trends do not change significantly from historical patterns. This scenario assumes moderate mitigation efforts to reduce greenhouse gas emissions. When this scenario is applied to predict the indices, it assesses under moderate climate change impact. This intermediate pathway aids researchers and policymakers in assessing the resilience and adaptability of ecosystems in response to gradual environmental shifts. The CMIP6 SSP 5-8.5 is a high-emission scenario, which represents a future of rapid economic growth, overconsumption, and carbon-intensive usage. This scenario considers minimal climate policies, leading to substantial global warming. It predicts severe impacts, with a huge sea level rise, extreme weather events, reduced water availability, and significant risks to ecosystems, agriculture, water supply, food security, human health, and infrastructure. When this scenario is applied, the prediction results indicate a significant increase in the frequency, distribution, and severity of drought events. Drought

indices calculated on the study area showed spatial distribution and variation of drought intensity across different regions. This is visualized through varying maps that help us identify major drought-prone regions and the varying degrees of drought severity. These visualizations help us identify major drought-prone areas, which help us make strategies for mitigation and adaptation to manage and reduce the adverse impacts of droughts.

4.3.1 Spatial Distribution and Intensity of Vegetation Condition Index (VCI)

Figure 11 and Figure 12 show the VCI of Pakistan for four different time intervals under SSP 2-4.5 and SSP 5-8.5: the present, 2050, 2075, and 2100, respectively. These maps visually represent how the vegetation condition is expected to change over time. The green points on the maps represent the locations of observed stations used for data collection, and the color-coded regions clearly classify drought severity; red implies severe drought, orange denotes moderate drought, light green represents near normal drought, and dark green signifies normal vegetation.

The current scenario

Figure 11 provides a detailed assessment of vegetation health across the country. This index ranges from extreme drought conditions to moist and healthy vegetation, considering the impact of various climatic factors on vegetation. The map shows a heterogeneous distribution of vegetation health throughout Pakistan. In the southwestern part of Balochistan, particularly around Quetta, Kalat, and Rohri in Sindh, vegetation is severely affected, and extreme drought conditions are present. This is due to prolonged periods of inadequate rainfall and high temperatures. The central and south-eastern regions, including Jacobabad and Badin, show severe drought conditions, and the vegetation is stressed. In the northern and north-western parts of Pakistan, regions such as Peshawar, Islamabad, and adjacent areas show near-normal drought conditions. In these areas, vegetation health is relatively stable, considering that the climatic conditions are more favourable, having adequate rainfall and temperature. The distribution of vegetation health across the map highlights significant regional variations, emphasizing the diverse climatic and environmental conditions across Pakistan.
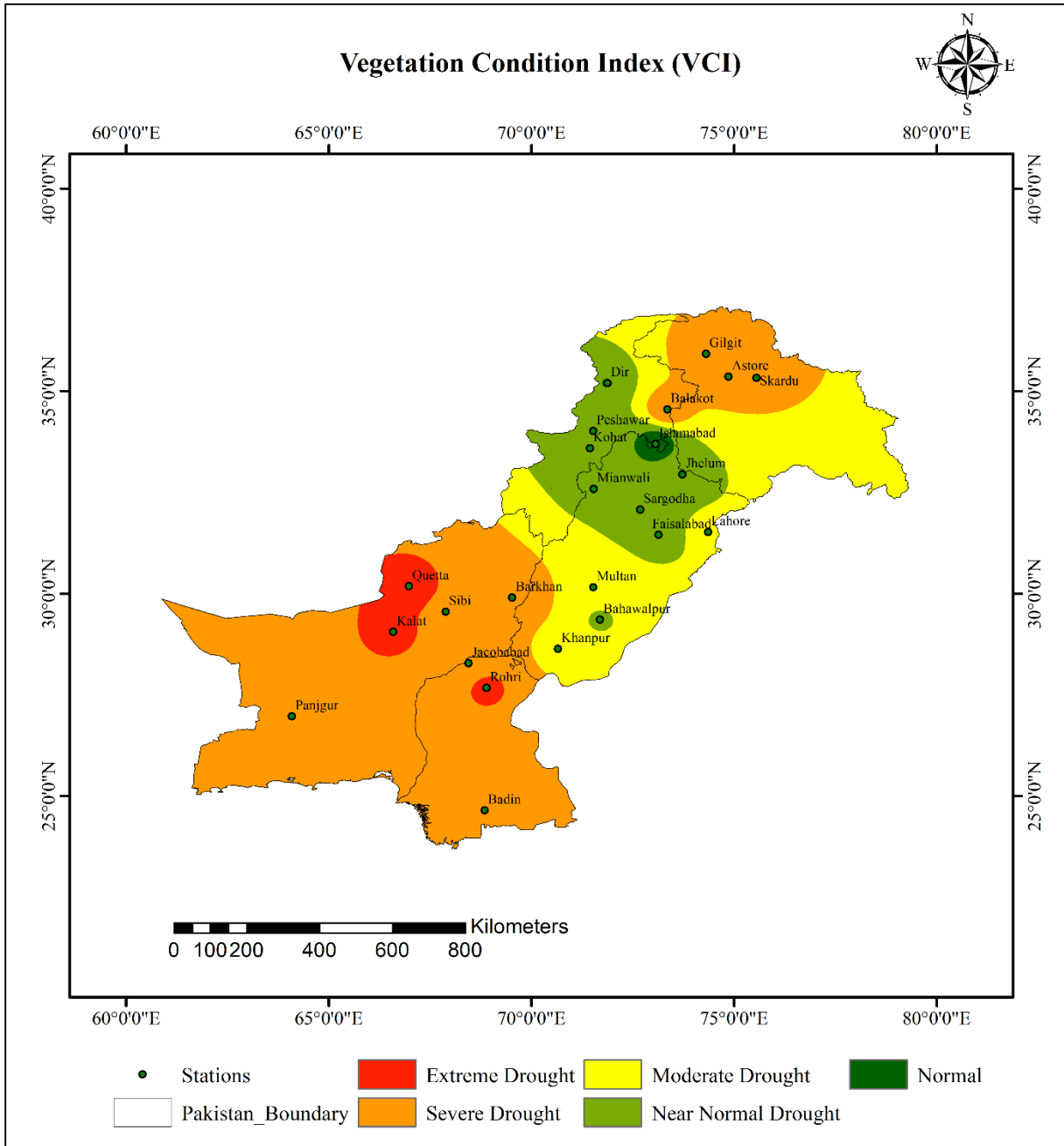
Vegetation Condition Index (VCI)

Figure 11: Spatial distribution and drought intensity under VCI current scenario

Future Projections under SSP 2-4.5 & SSP 5-8.5

Figure 12 compares VCI predictions under two climate scenarios, SSP 2-4.5 and SSP 5-8.5, using CMIP6 data for the years 2050, 2075, and 2100. ***Map (a) 2050 SSP 2-4.5 vs. Map (d) SSP 5-8.5:*** **F**ig.12a & 12d illustrates projected changes in vegetation health across Pakistan under two scenarios. The normal and healthy vegetation regions are the same in both maps, primarily in the federal capital. However, these two maps show noticeable differences in the extent and severity of drought conditions. In 12a, most of Balochistan and Sindh faced severe drought conditions except for a few areas such, as Quetta and Sibbi, which faced extreme drought in terms of vegetation. Northern Pakistan, i.e., Gilgit Baltistan, also faces severe drought conditions. Moderate drought conditions are seen in central Punjab. In 12d, the severe scenario, Quetta and Kalat still experience extreme drought, and the area affected by severe drought is reduced compared to Fig.12a. The regions experiencing moderate drought are more extensive, including parts of central and southern Punjab. ***Map (b) 2075 SSP 2-4.5 vs. Map (e) SSP 5-8.5:*** In Fig.12b, the areas experiencing extreme drought are still prominently visible, with key regions being Quetta, Kalat, and Rohri in Balochistan and Gilgit in Gilgit Baltistan. Panjgur, Sibbi, and nearby regions, including northern Pakistan, are facing severe drought conditions. Regions like Islamabad and Faisalabad are still under near-normal vegetation conditions. Fig. 12e under SSP 5-8.5 shows more pronounced extreme and severe drought conditions, indicating higher stress levels on vegetation, whereas Fig. 12b under SSP 2-4.5 shows significant droughts, suggesting a slight improvement in some regions, especially areas of moderate and near normal drought conditions. ***Map (c) 2100 SSP 2-4.5 vs. Map (f) SSP 5-8.5:*** In 2100, VCI predictions are less severe in extreme scenarios than in moderate scenarios under 2-4.5. In Fig. 12c, a small region around Quetta faces extreme drought conditions, with areas such as Kalat and parts of southern Pakistan, including Jacobabad and Rohri, under severe drought. Most of Pakistan is under near-normal drought, with Islamabad, Peshawar, Kohat, Dir, Lahore, and Badin included in healthy vegetative areas. In the extreme scenario, Fig. 12f, the regions experiencing extreme drought have expanded to include Kalat and Quetta. The severe drought regions have also spread further and cover additional regions such as Sibbi and parts of central and southern Pakistan. The regions of moderate drought conditions remain the same but show a slight increase in central areas. Overall, the moist regions in the northern

parts of Pakistan are stable, which means they are less affected by the increasing drought stress observed in other parts of the country.
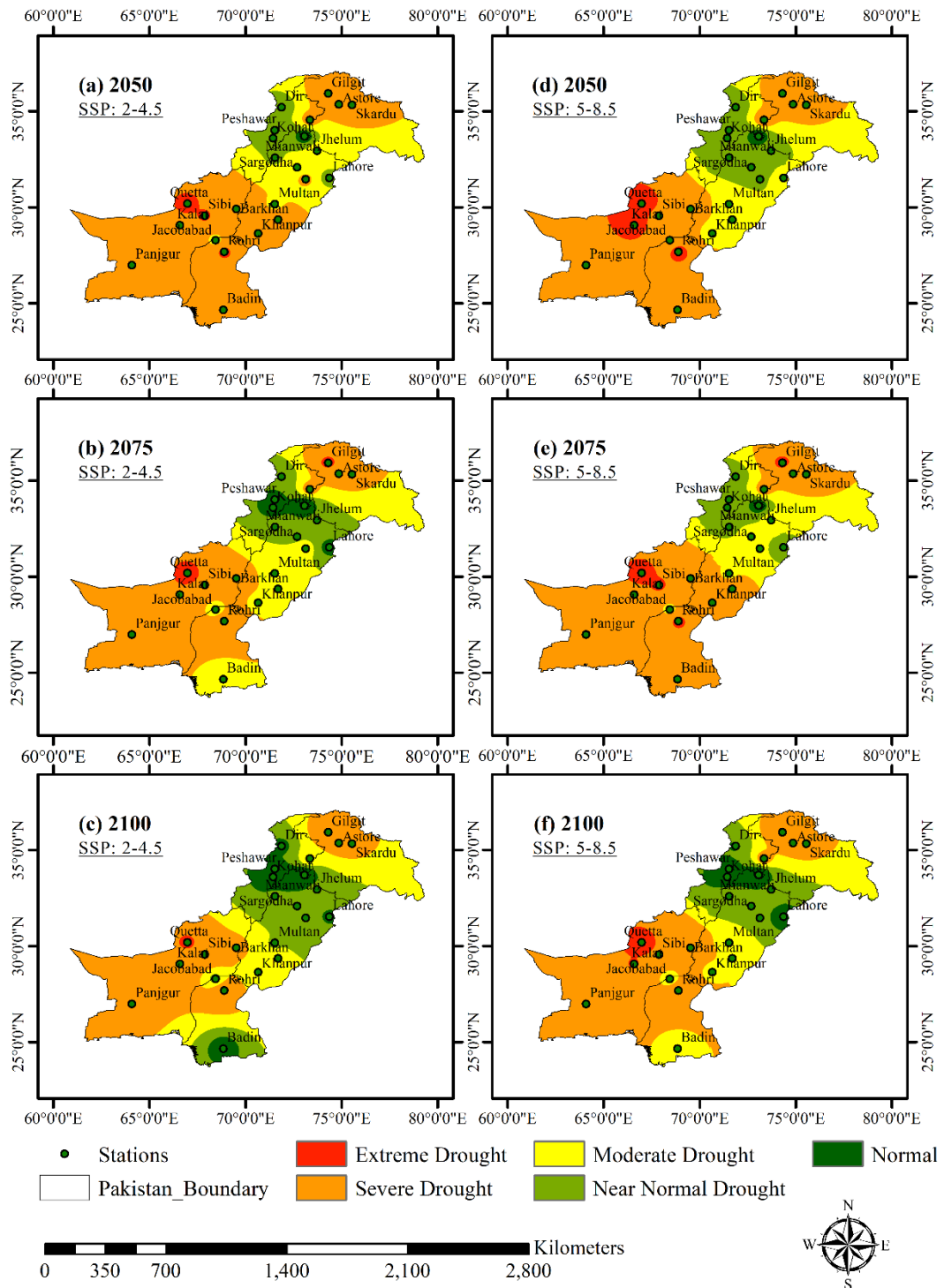
Figure 12: Spatial distribution and drought intensity under VCI future projections

In conclusion, these maps provide a projection of the VCI in Pakistan from the current day to 2100, indicating a gradual enhancement in vegetation conditions. The projections imply a decrease in areas affected by severe drought and an increase in regions with wet conditions. This indicates a potential reduction in drought severity over long-term, although some regions will still experience moderate drought conditions.

Upon comparing the performance of VCI in Pakistan with other countries or regions, it shows that while VCI is focused more on evaluating the vegetation health over different areas, such as in Amazon rainforest, its use in Pakistan is solely based on agricultural drought monitoring in arid and semi-arid climates, as is the case of (Rawat et al., 2012) which also focused on monitoring drought in the states of Maharashtra and Karnataka, where monsoon variability affects crop production.

4.3.2 Spatial Distribution and Intensity of Temperature Condition Index (TCI)

Figure 13 and Figure 14 displays the Temperature Condition Index in Pakistan at four different time intervals under SSP 2-4.5 and SSP 5-8.5: the present, 2050, 2075, and 2100. TCI is an important measure use to evaluate the impact of temperature-related stress on vegetation, indicating varying levels of drought severity. These maps show how temperature conditions are expected to change over specific time frames.

The Current scenario

In Figure 13, the map shows a wide range of temperature conditions across Pakistan. Regions such as Panjgur, Kalat, Sibbi, and Khanpur are currently experiencing extreme drought. Quetta, Badin, and several regions in southern Pakistan are facing severe drought conditions. The yellow regions, including Lahore and Faisalabad, show moderate drought

conditions. The northern regions, specifically Gilgit and Skardu, shows no signs of dryness and have no drought.
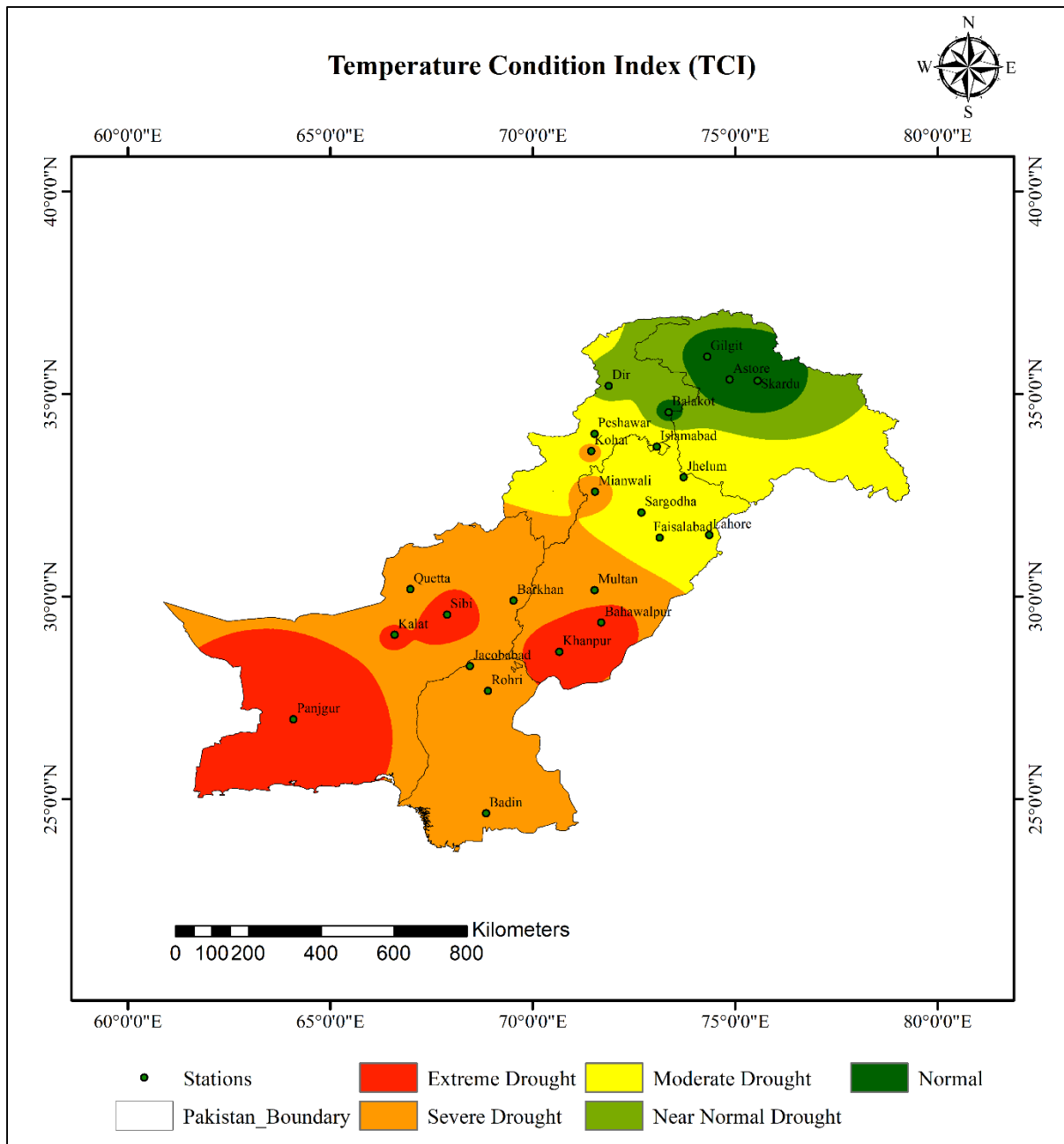

Figure 13: Spatial distribution and drought intensity under TCI current scenario

Future Projections under SSP 2-4.5 & SSP 5-8.5

Map (a) 2050 SSP 2-4.5 vs. Map (d) SSP 5-8.5: According to the 2050 projections, as shown in Fig. 14a, Kalat, Sibbi, Panjgur and Khanpur continue to face extreme drought conditions, while severe drought conditions persist in areas like Barkhan. The same drought conditions persist in the Lahore and Multan areas and Peshawar and Sargodha region as in the current scenario. The northern regions remain unaffected by drought. In Fig. 14d, southwestern regions are experiencing extreme drought under the extreme scenario. Furthermore, there are slight differences in the distribution and extent of the drought severity levels. Regions such as Jacobabad and Rohri have transitioned from extreme drought to severe drought, indicating an improvement over time. *Map (b) 2075 SSP 2-4.5 vs. Map (e) SSP 5-8.5:* The 2075 forecasts, as shown in Fig. 14b indicate a slight increase in the prevalence of extreme drought conditions, particularly in regions like Panjgur and Jacobabad, where the impact remains substantial. Severe drought conditions have extended slightly and persist in Mianwali, Kohat, and Jhelum. Central regions and areas like Peshawar and Sargodha follow the same trend as in previous periods. The northern region continues to exhibit no drought conditions. In the second map, i.e., Fig. 14e, the TCI data predicts extreme drought conditions in Pakistan. The map indicates that southern western regions, including Quetta, Kalat, Sibbi, and Jacobabad, are experiencing extreme drought. Northern Punjab and federal face moderate drought conditions, central Punjab faces severe drought conditions, while northern Pakistan remains unaffected. The comparison of both these scenarios indicates a temporal change in the temperature conditions, which impacts the severity of drought in Pakistan. Under SSP 2-4.5, the map shows improvement in terms of drought severity instead of SSP 5-8.5, which suggests a severe and widespread drought period. *Map (c) 2100 SSP 2-4.5 vs. Map (f) SSP 5-8.5:* According to projections, harsh drought conditions are expected to worsen by 2100, as shown in Fig. 14c, particularly in Panjgur and Sibbi. Severe drought conditions persist in Quetta and are spreading to nearby regions. Other regions, such as the central and northern regions and areas like Peshawar, follow the same conditions. Fig. 14f, shows intensified drought conditions. The extent of extreme drought has increased significantly, covering large areas in southwestern and central Pakistan, with regions like Rohri and Khanpur now included. The area under moderate droughts and near-normal conditions has also decreased, suggesting a worsening drought. The moist regions remain the same.
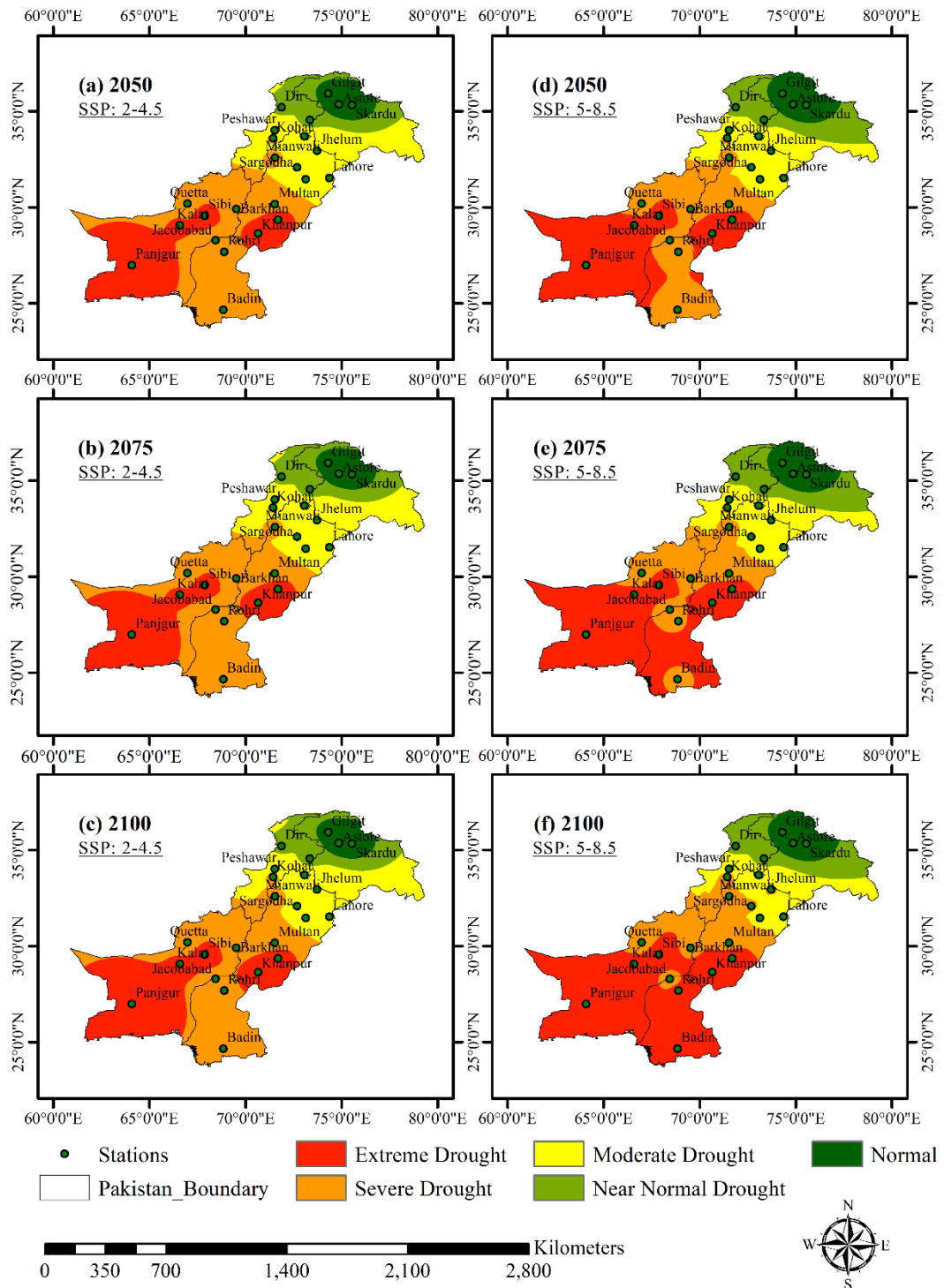
Temperature Condition Index (TCI)

Figure 14: Spatial distribution and drought intensity under TCI future projections

Overall, these maps predict the TCI in Pakistan from 2010 to 2100. They show that drought conditions will become more severe over time, with a noticeable increase in areas experiencing extreme and severe drought. This also signifies the increasing pressure on agriculture caused by an increase in temperature and calls for urgent need and adaptive strategies to reduce the negative effects of climate change on agriculture and natural ecosystems.

Almost all Pakistan faces significant temperature variations, particularly in hot and dry agro-climatic zones, like Balochistan. TCI effectively detected temperature stress on agriculture and yielded the best results in cities like Jacobabad and Sibbi.

4.3.3 Spatial Distribution and Intensity of Standardized Precipitation Evapotranspiration Index (SPEI)

The map in Figures 15 and 16 visualizes the Standardized Precipitation Evapotranspiration Index (SPEI) across Pakistan at four distinct time intervals: the present, 2050, 2075, and 2100. SPEI is a reliable measure for monitoring drought conditions as it combines precipitation and potential evapotranspiration, providing valuable information about the climatic water balance.

The Current scenario

The present scenario, Figure 15, displays extreme drought conditions in Panjgur, Jacobabad, and Rohri. Moderate drought conditions are visible in Quetta, Khanpur, Sibbi, and Kalat. Near Normal drought conditions are shown in regions like Badin, Barkhan and northern Pakistan. Northern Punjab and Federal capital are experiencing moist conditions.
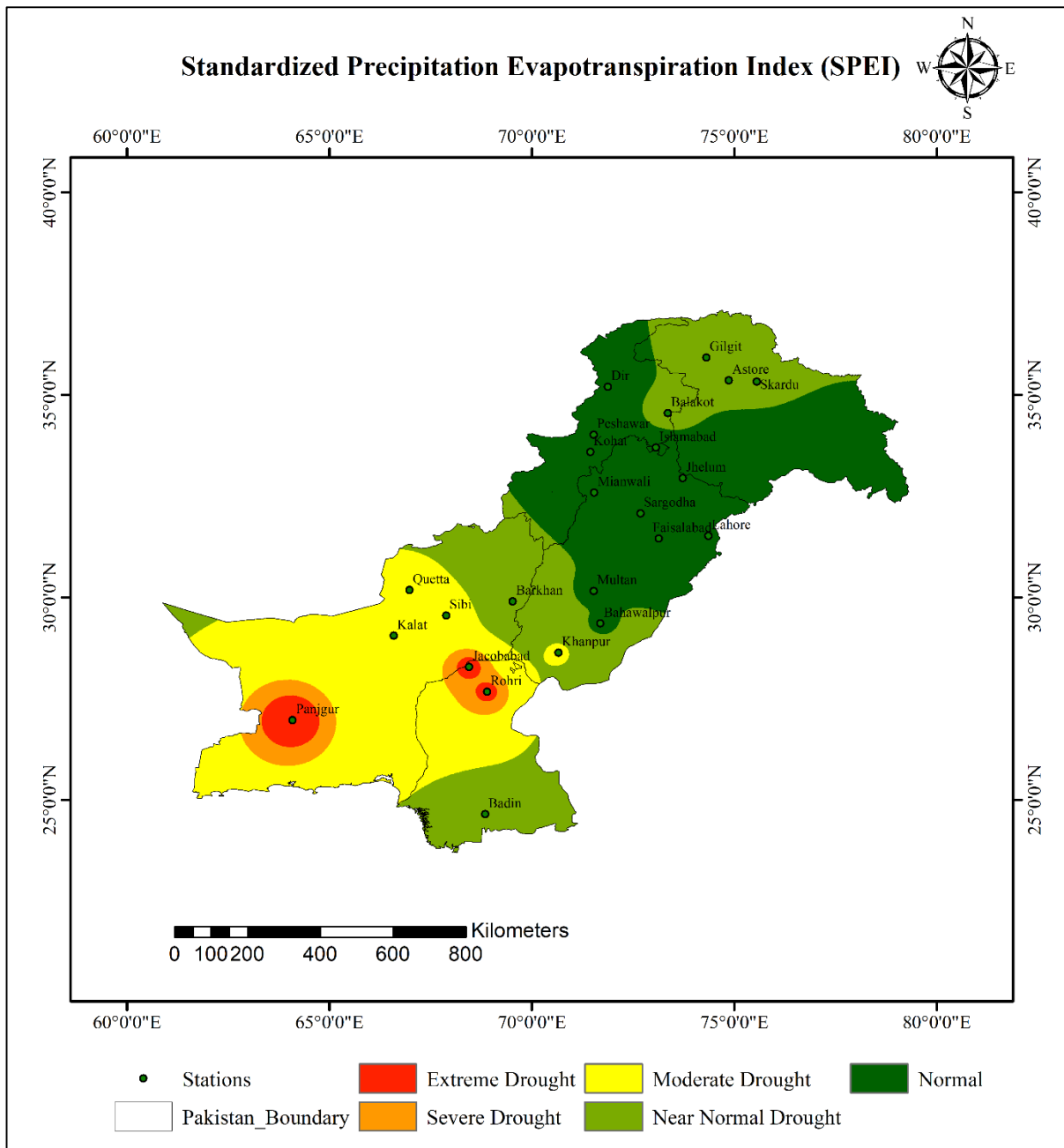

Figure 15: Spatial distribution and drought intensity under SPEI current scenario

Future Projections under SSP 2-4.5 & SSP 5-8.5

      Map (a) 2050 SSP 2-4.5 vs. Map (d) SSP 5-8.5: Fig. 16a and Fig. 16d illustrate the projected drought conditions in Pakistan for the year 2050, based on two scenarios using SPEI. Under SSP 2-4.5 in Fig. 16a the majority area is covered by near-normal to normal conditions. The northern and eastern parts of Pakistan, including Lahore, Faisalabad, and Gilgit, are projected to remain normal with no significant drought. The southern and southwestern regions exhibit greater variability, with moderate drought conditions observed in areas such as Quetta and Kalat. There are severe drought conditions in specific regions near Jacobabad and Rohri, while extreme drought is around Panjgur. The situation appears much more severe under the extreme scenario, as shown in map (d). There is a change in extent between near-normal and normal conditions. The southern and southwestern regions are further intensified with extreme drought conditions spreading further in cities like Jacobabad and Sibbi. Quetta and Kalat are expected to undergo moderate to severe drought conditions. *Map (b) 2075 SSP 2-4.5 vs. Map (e) SSP 5-8.5:* The given maps depict expected drought conditions for Pakistan in 2075. Fig. 16b indicates moderate drought conditions in the southern and southwestern parts of Pakistan, such as Panjgur, Kalat, and Quetta, where severe to extreme drought conditions are present. The central and northern parts of the country show near-normal to normal conditions. Fig. 16e highly exaggerates the projections. Drought severity escalated in the southern and southwestern regions, with a wider distribution of severe and extreme drought conditions. *Map (c) 2100 SSP 2-4.5 vs. Map (f) SSP 5-8.5:* Fig. 16c under SSP 2-4.5 shows extreme drought in southern Pakistan, specifically near Quetta, Panjgur, and Kalat, while severe drought is seen in adjacent areas and further extends into Sibbi and the surrounding territories of Jacobabad. Central and southern Pakistan is under a moderate drought, including certain areas of Sindh province around Badin. Normal conditions are seen in most of northern and eastern Pakistan. Under SSP 5-8.5, in Fig. 16f, extreme drought becomes more extensive than in moderate scenario. Severe drought becomes more widespread, encompassing areas like Kalat and Sibbi, leading to less coverage by moderate droughts. Normal drought conditions persist in the northern regions of Pakistan.
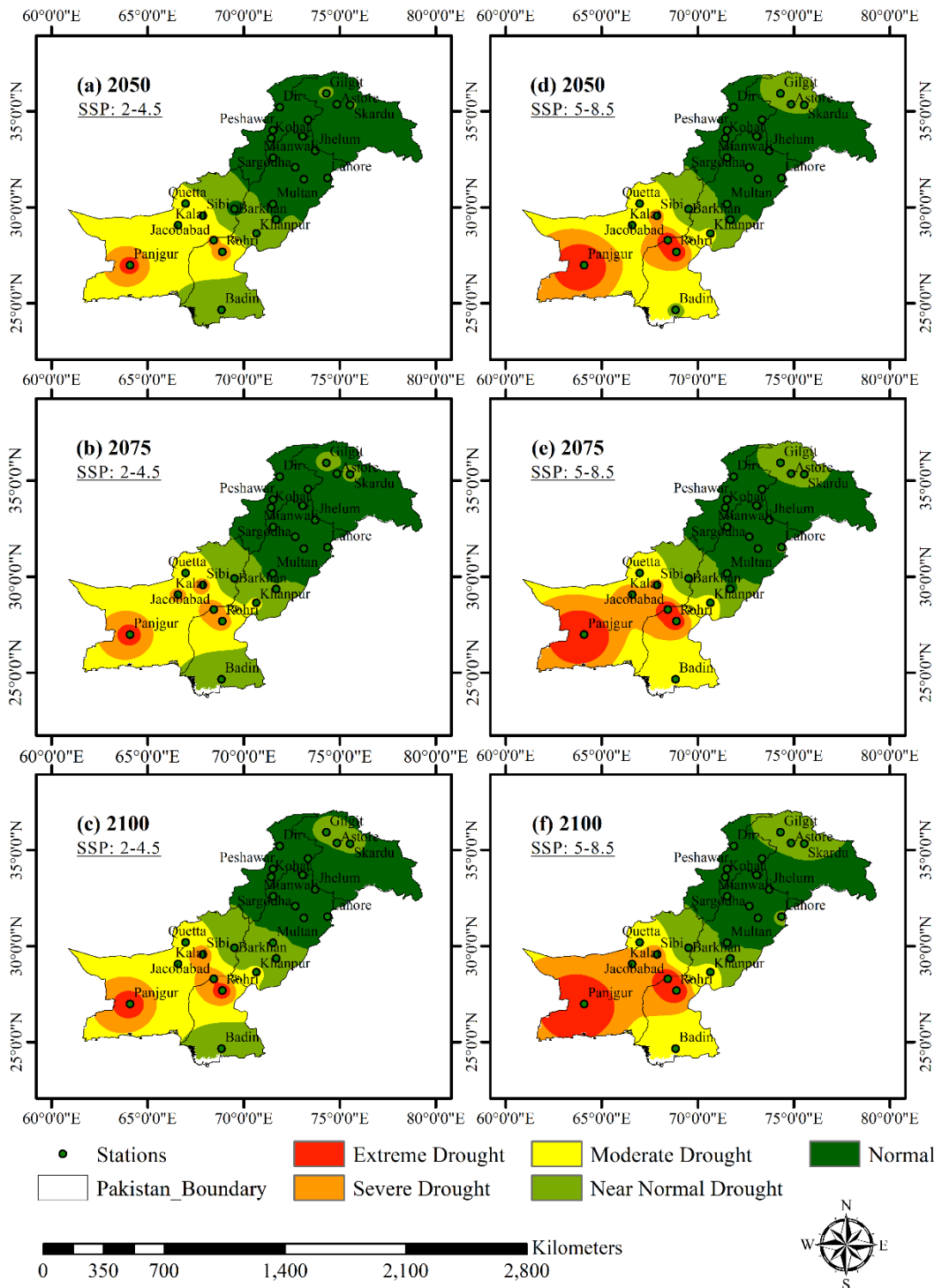
Figure 16: Spatial distribution and drought intensity under SPEI future scenario

Upon comparing the two scenarios, it becomes clear that the extreme scenario predicts a considerably more intense and extreme drought throughout Pakistan by the year 2100. This will lead to increased water scarcity and result in vast areas experiencing severe drought conditions, posing significant threat to agriculture and water resources.

SPEI is designed to evaluate drought conditions using both precipitation and evapotranspiration, making it effective for areas having high climatic variability, such as discussed in the paper by (Domínguez-Castro et al., 2019). Upon comparing with Pakistan, SPEI will be a valuable index to measure drought dynamics especially in areas influenced with monsoon. On the other hand, its performance is different in the arid southern regions of Pakistan where evapotranspiration plays a different role.

4.3.4 Spatial Distribution of Soil Moisture Agricultural Drought Index (SMADI)

The provided Figure 17 and **Error! Reference source not found.** illustrates the Soil Moisture Agricultural Drought Index (SMADI) for Pakistan, presenting the current situation and future forecasts for the years 2050, 2075, and 2100. SMADI is essential for soil moisture deficit assessment, which impacts on agricultural output. It shows how changes in soil moisture levels affect drought conditions over time.

The current scenario

Currently, areas facing normal drought, as shown in Figure 17, are primarily located in southern and central parts of Pakistan. A major portion of the study area is covered with near-normal drought conditions under this index, which indicates regions with slight deviations from average soil moisture levels. Areas experiencing mild droughts are spread across various parts, particularly in northwest and central regions. Moderate droughts are recorded in the southern and northern regions. The areas with severe drought are concentrated in the southwestern regions like Quetta and Kalat. The presence of extreme drought is limited to a

few crucial areas that are experiencing substantial deficits in soil moisture.

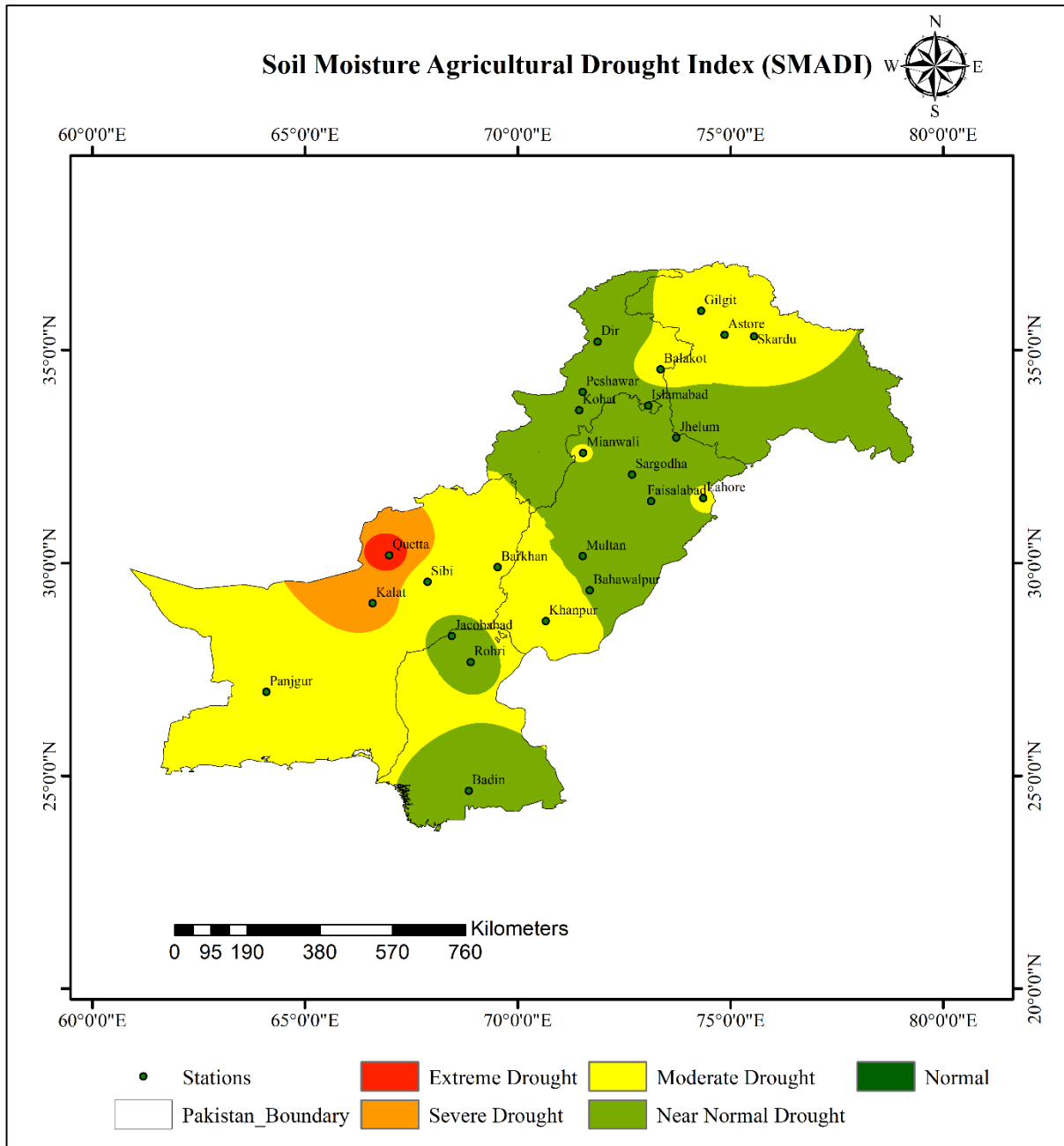*Figure 17: Spatial distribution and drought intensity under SMADI current scenario*

Future Projections under SSP 2-4.5 & SSP 5-8.5

Map (a) 2050 SSP 2-4.5 vs. Map (d) SSP 5-8.5: By 2050, as shown in Fig. 18a, the projections suggest an improvement in soil moisture conditions. Near-normal drought conditions remain significant but are more concentrated in the central and southern regions.

Moderate drought regions become more confined. Severe and extreme drought areas decrease significantly, showing a favourable trend in soil moisture levels. Under SSP 5-8.5, mild drought conditions are seen all across Pakistan, with northern regions, including areas of Gilgit Baltistan, experiencing moderate drought. ***Map (b) 2075 SSP 2-4.5 vs. Map (e) SSP 5-8.5:*** In 2075, as shown in Fig. 18b under moderate scenario, the trend of improvement continues, and the areas of moderate drought are slightly increasing. Although drought conditions persists, they are less prevalent. The extreme drought region is almost non-existent. As in the case of SSP 5-8.5, the overall trend shows moderate drought conditions in northern Pakistan and parts of southern Pakistan, including areas such as Panjgur, Quetta, and Sibbi. ***Map (c) 2100 SSP 2-4.5 vs. Map (f) SSP 5-8.5:*** By 2100, as shown in Fig. 18c, the overall condition changes drastically, and now the major parts of the country are under moderate drought conditions, with severe and extreme conditions visible in Quetta, Astore, and parts of Gilgit. Some scattered mild drought condition can be seen in Islamabad, Badin, Dir, Kalat, Peshawar, Sargodha, and Faisalabad. In the extreme scenario, as shown in Fig. 18f, Pakistan is under moderate drought conditions, with a few areas such as Panjgur, Quetta, Mianwali, Astore, and parts of Gilgit facing severe drought conditions. No region is left under normal vegetation. This indicates a significant worsening of soil moisture conditions rapidly across Pakistan.

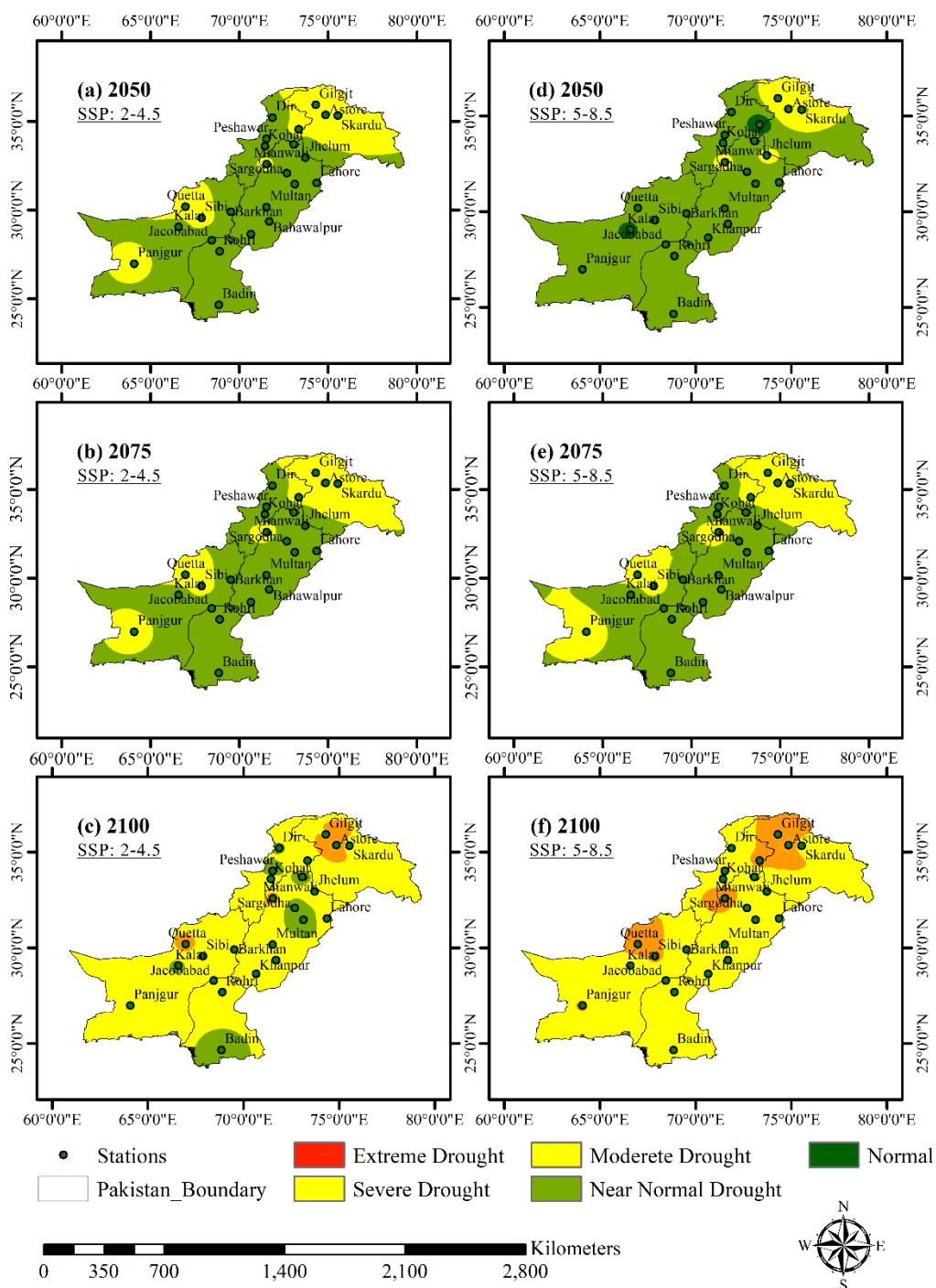# Soil Moisture Agricultural Drought Index (SMADI)

Figure 18: Spatial distribution and drought intensity under SMADI future projections

Overall, the figure shows an initial improvement in soil moisture conditions by the middle of the century, followed by a slight increase in drought severity towards the end of the century. These findings highlight the significance of implementing sustainable water management methods and adaptive agricultural solutions to reduce the effects of soil moisture fluctuations on agricultural productivity in Pakistan.

Pakistan's arid and semi-arid regions, such as Balochistan and Sindh, have similar climatic conditions to southeastern Spain and the Murray-Darling Basin, as indicated by (Dunne & Kuleshov, 2023; Mercedes et al., 2021) in their studies, making SMADI a suitable index for monitoring drought in Pakistan. The values of SMADI are very much affected by its parameters, as it is expected that higher SMADI showing extreme/severe drought come from a combination of very low VCI, high SMCI, and high MTCI. In the semi-arid regions, SMADI is more dependent on soil moisture than temperature, which is also stated by (Scaini et al., 2015). The seasonal pattern is determined by temperature, whereas the soil moisture conditions determine the intensity of drought.

4.4 Drought Composite Map

A drought composite map was created to provide a thorough overview of drought conditions. It integrates multiple drought indices, such as VCI, TCI, SPEI, and SMADI. The integration of these indices was based on weighted scores for each criterion. VCI represents the health of vegetation and moisture sensitivity, and TCI measures the effects of temperature extremes on the plants. To understand the long-term drought trends, SPEI is used, which evaluates the drought severity over different time periods by using precipitation and ET data. Understanding the effects of drought on agriculture is largely based on SMADI, which focuses on anomalies in soil moisture. This DCM provides a multi-dimensional perspective on drought by combining these indices, making it easier to evaluate and control the risks associated with drought in different geographical areas.

Current Drought Composite Map

Figure displays a drought composite map of Pakistan, showing different regions experiencing drought. The most affected cities are Quetta, Kalat, and Panjgur, especially in Pakistan's southwest, which is under severe to extreme drought. Contrary to that, Peshawar, Mianwali, and Lahore, including other northern parts, are under normal vegetation or mild drought conditions. Moderate or average conditions persist in the central and northern parts of Pakistan.
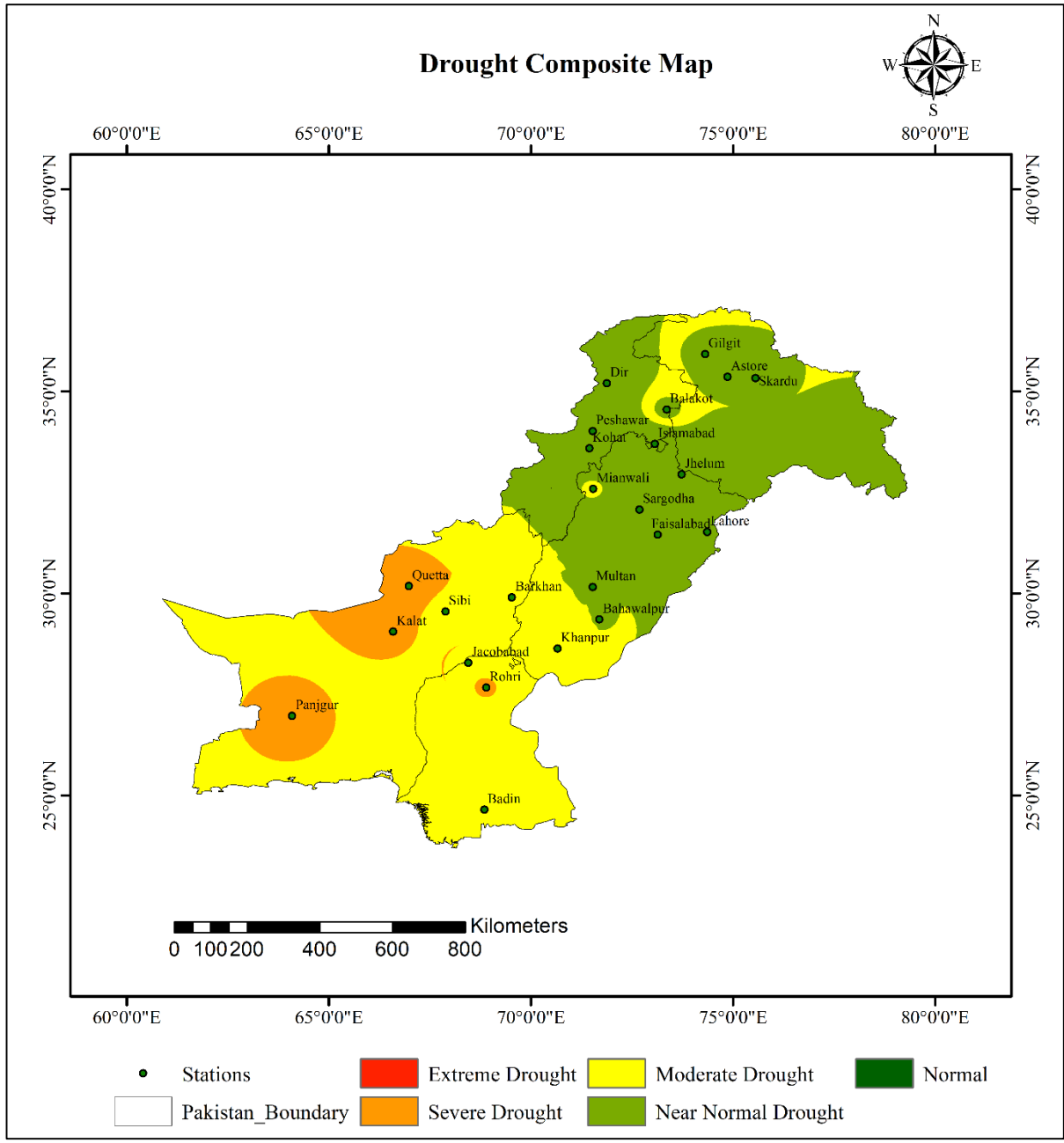
Figure 19: Drought Composite Map current scenario

Future Drought Composite Maps under CMIP6 SSP 2-4.5 & SSP 5-8.5

Map (a) 2050 SSP 2-4.5 vs. Map (d) SSP 5-8.5: Figure 20 shows future drought projections for 2050 under two SSPs. Under SSP 2-4.5, the Fig. 20a depicts moderate and mild drought conditions. Panjgur comes under severe drought conditions, whereas the rest of the area across Pakistan exhibits normal vegetation. No noticeable areas experiencing extreme drought are shown in this scenario. Under SSP 5-8.5, Fig. 20d shows more widespread and

severe drought conditions than moderate scenarios. Panjgur and Rohri are under extreme and severe drought conditions, while the rest of the country shows moderate drought conditions. The regions surrounding Islamabad, Lahore, and Gilgit are experiencing normal vegetation conditions. This comparison shows how the two scenarios differ significantly in severity, with the higher scenario indicating a more concerning situation. ***Map (b) 2075 SSP 2-4.5 vs. Map (e) SSP 5-8.5:*** Fig. 20b and Fig. 20e show predictions for the year 2075 under two SSPs representing varying climate change scenarios based on various levels of greenhouse gas emissions. A moderate drought situation is depicted in Fig. 20b under SSP 2-4.5. The southern region has severe to mild drought conditions, especially in Quetta, Kalat, and Panjgur. The rest of the country comes under moderate drought conditions, while the northern region exhibits healthy vegetation. SSP 5-8.5 shows a more severe scenario. According to this prediction, there is a greater widespread drought throughout Pakistan. A considerable area of Pakistan, particularly in the south and southwest, shows moderate drought, with areas surrounding Quetta, Kalat, Sibbi, and Panjgur under extreme and severe drought. The spread of moderate drought conditions is more noticeable than SPP 2-4.5. However, the northern region is under normal conditions. In comparison, the drought will be more widespread by 2075 under SSP 5-8.5, but both scenarios imply serious drought conditions in the southern regions. ***Map (c) 2100 SSP 2-4.5 vs. Map (f) SSP 5-8.5:*** The Fig. 20c & Fig. 20f illustrates the future projections for the year 2100. Under SSP 2-4.5, severe drought conditions are present in the southwestern regions surrounding Kalat, Jacobabad, and Panjgur. Islamabad, Mianwali, Gilgit, and northern and central parts of the country are under normal conditions. Under SSP 5-8.5, a significant portion is under extreme and severe drought, which includes Quetta, Kalat, Sibbi, and Panjgur. This shows that the worst drought conditions are anticipated to occur in these areas while most of the area is under moderate drought encompassing northern and central regions like Gilgit, Islamabad, and Lahore. ,

Based on the overall pattern, most of Pakistan will be severely stressed by drought, with very few areas having normal circumstances. These projections emphasize how critical it is to implement policies for both climate mitigation and adaptation to effectively manage the future water and agricultural issues brought on by extreme drought.
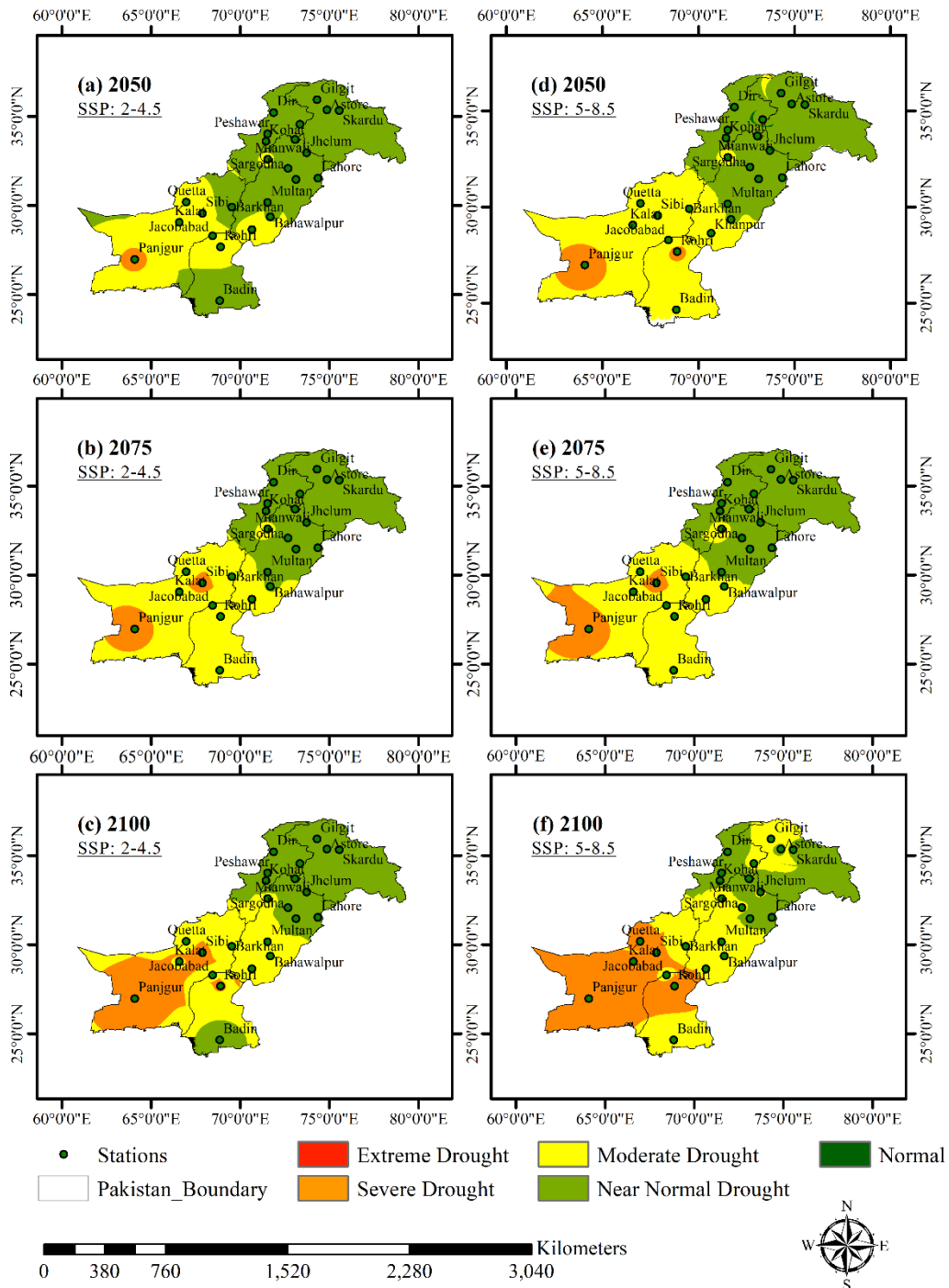
Figure 20: Drought Composite Map future scenario under SSP2-4.5 and SSP 5-8.5

CHAPTER 5: CONCLUSION AND RECOMMENDATIONS

Droughts significantly affect the present ecosystem, agricultural produce, human survival, and economic uplift. It has the potential to lead to long-term climate change and desertification. Hence, it is important to investigate the essence of drought calamities, thoroughly analyse their spatial and temporal attributes, and employ scientific approaches to avoid and mitigate drought. The investigation into drought severity and intensity remains inconclusive since it mainly focuses on a single drought index and rarely examines the collective impact of various elements contributing to drought. Effective agricultural drought management of agricultural drought is important due to its direct impact on food security. Therefore, multiple models have been created to forecast agricultural drought. Despite the high quality of a model, inaccuracy might occur in predicting droughts due to meteorological outliers *(Park et al., 2019)*. The model for predicting droughts should be simple, practical, and useful to establish effective mitigation efforts.

5.1 Conclusion

The comparative analysis of satellite products and gauge-based datasets, including CHIRPS, IMERG, MODIS, and ERA-5, provides several key findings in their performances, particularly for Pakistan. CHIRPS outperformed IMERG in estimating precipitation, as indicated by higher r^2 values, reduced RMSE and MAE, and negligible bias. CHIRPS combines satellite data with gauge data, allowing it to adjust better and correct its estimates, especially in complex terrain regions such as Pakistan. IMERG, on the other hand, tends to overestimate or underestimate precipitation in areas where precipitation is highly variable, giving less accurate results. In terms of temperature data analysis, ERA-5 had superior performance compared to MODIS in the estimation of surface temperatures, showing a greater correlation with the observed data. ERA-5 offers a thorough atmospheric reanalysis, including land surface and air temperatures at different altitudes. These data are obtained from a diverse set of observations that are integrated into a global model. Therefore, ERA-5 can accurately represent larger climate patterns and offer uninterrupted and reliable temperature data over time *(Hersbach, Bell, Berrisford, Dahlgren, et al., 2020)*. These findings emphasize the importance of choosing the most accurate datasets for climate modeling and analysis, particularly in areas with meteorological variables such as Pakistan.

Unlike previous studies, this research took all of Pakistan as the study area and analysed the overall drought severity and intensity spatially and temporally by combining multiple drought indices, considering several factors, such as rainfall, temperature, vegetation health, and soil moisture. The current and future predictions (using the MME mean of several GCMs of CMIP6) of drought indices such as VCI, TCI, SPEI, and SMADI show a comprehensive assessment of drought patterns, emphasizing their value in monitoring agricultural drought and focusing on the importance of using many indices for accurate drought evaluation. These indices combined suggest that Pakistan's central and southern regions are very susceptible to drought, and the situation is projected to worsen by the end of the century under both mild and extreme climate scenarios. The projected drought from CMIP6 future precipitation and temperature data under moderate and extreme scenarios is a fair representation of all the GCMs with low uncertainty and variability.

AHP can allocate weights to various drought indices according to their significance in drought assessment. These weights impact the overall estimate of drought severity by assigning greater significance to some indices than others. Combining multiple drought indices using AHP into a Drought Composite Map creates a comprehensive tool for evaluating and addressing drought hazards. The higher weights of SMADI and SPEI signify the importance of soil moisture and evapotranspiration, particularly in agricultural regions. The results clearly state that climate change will increase the severity and intensity of agricultural droughts, but it depends on the regions and index being used in the study. This research provides critical insight for improving and verifying the models for predicting drought conditions.

It is important to note that the number of criteria and their respective weights can vary according to the size, scale, or specific objective of the study. AHP is limited by the fact that as the number of criteria increases, the analysis becomes more complex because of the need for a greater number of pairwise comparisons. To address this complication, this study only considered the most important and influential drought indices for computation and evaluation. Despite its limits, utilizing MCE and AHP provides a valuable framework for effectively incorporating various criteria into an integrated assessment, improving the comprehension and management of drought impacts.

5.2 Recommendations

1. Given the superior performance of CHIRPS and ERA-5, integrating these climate datasets with existing gauge data improves the accuracy and reliability of precipitation and temperature estimates. The combination of data with RS methods provides promising results. Also, with the recent effects of climate change in unpredictable climate conditions such as extreme drought or extreme floods, a dynamic monitoring system using high temporal and spatial resolutions of climate data will be beneficial for implementing quick measures to reduce the severe effects of climate calamities on agriculture.

2. Though this study utilized various drought indices, including VCI, TCI, SPEI, and SMADI, the inclusion of additional indices such as the Palmer Drought Severity Index (PDSI), Evaporation Stress Index (ESI) would further enhance the impact assessment of drought.

3. To understand future climate scenarios more clearly, it is advisable to integrate long-term climate models with updated emission scenarios, which will enhance the scope of possible results and enhance the evaluation of hazards linked to various pathways of greenhouse gas emissions and socio-economic progress.

4. Future research should prioritise detailed regional and area-specific analyses within Pakistan that are particularly susceptible to drought. Such research topics can be the impact of drought on specific crops, water resource management in arid regions, or the socio-economic consequences for populations relying on agriculture. Such studies will yield practical and effective information for specific actions. Furthermore, it could also explore the use of AI-driven models for analysing large datasets to predict droughts with more precision and accuracy. Another aspect of future research is integrating socio-economic factors into drought impact assessments that will provide researchers a more complete picture of the possible effects of drought on the population. Future investigations could examine the interplay of variables such as population growth, land-use changes, and economic policies with climate factors to determine their impact on drought vulnerability.

REFERENCES

Abbas, S., Mayo, Z. A. J. E., Development, & Sustainability. (2021). Impact of temperature and rainfall on rice production in Punjab, Pakistan. *23*(2), 1706-1728.

Abd El-Hamid, H. T., & Alshehri, F. J. J. o. C. C. (2023). Integrated remote sensing data and machine learning for drought prediction in Eastern Saudi Arabia. *27*(5), 48.

Adnan, Ullah Abbas, S., Ullah, W., Waseem, M., Dou, X., Zhao, C., Karim, A., Zhu, J., Hagan, D. F. T., Bhatti, A. S., & Ali, G. (2022). Evaluation and projection of precipitation in Pakistan using the Coupled Model Intercomparison Project Phase 6 model simulations. *International Journal of Climatology*, *42*(13), 6665-6684. https://doi.org/10.1002/JOC.7602

Adnan Ullah, K., Gao, S., Khosa, A. H., & Ziqian, W. (2017). Shifting of agro-climatic zones, their drought vulnerability, and precipitation and temperature trends in Pakistan. *International Journal of Climatology*, *37*, 529-543.

Ahmad, S., Hussain, Z., Qureshi, A. S., Majeed, R., & Saleem, M. (2004). *Drought mitigation in Pakistan: current status and options for future strategies* (Vol. 85). IWMI.

Ahmad, S., Jia, H., Ashraf, A., Yin, D., Chen, Z., Xu, C., Chenyang, W., Jia, Q., Xiaoyue, Z., & Israr, M. J. W.-E. N. (2023). Water resources and their management in Pakistan: a critical analysis on challenges and implications.

Al-Faifi, A., Song, B., Hassan, M. M., Alamri, A., & Gumaei, A. (2019). A hybrid multi criteria decision method for cloud service selection from Smart data. *93*, 43-57.

Al Shoumik, B. A., Khan, M. Z., & Islam, M. S. J. E. C. (2023). Spatio-temporal characteristics of meteorological and agricultural drought indices and their dynamic relationships during the pre-monsoon season in drought-prone region of Bangladesh. *11*, 100695.

Alamdarloo, E. H., Manesh, M. B., & Khosravi, H. (2018). Probability assessment of vegetation vulnerability to drought based on remote sensing data. *Environmental Monitoring and Assessment*, *190*(12). https://doi.org/10.1007/S10661-018-7089-1

Ali, Z., Iqbal, M., Khan, I. U., Masood, M. U., Umer, M., Lodhi, M. U. K., & Tariq, M. A. U. R. (2023). Hydrological response under CMIP6 climate projection in Astore River Basin, Pakistan. *Journal of Mountain Science*, *20*(8), 2263-2281. https://doi.org/10.1007/S11629-022-7872-X/METRICS

Allafta, H., Opp, C. J. G., Natural Hazards, & Risk. (2021). GIS-based multi-criteria analysis for flood prone areas mapping in the trans-boundary Shatt Al-Arab basin, Iraq-Iran. *12*(1), 2087-2116.

An, S., Park, G., Jung, H., & Jang, D. (2022). Assessment of Future Drought Index Using SSP Scenario in Rep. of Korea. *Sustainability 2022, Vol. 14, Page 4252*, *14*(7), 4252-4252. https://doi.org/10.3390/SU14074252

Asuero, A. G., Sayago, A., & González, A. J. C. r. i. a. c. (2006). The correlation coefficient: An overview. *36*(1), 41-59.

Bachmair, S., Svensson, C., Prosdocimi, I., Hannaford, J., & Stahl, K. (1947). Developing drought impact functions for drought risk management. *Hazards Earth Syst. Sci*, *17*. https://doi.org/10.5194/nhess-17-1947-2017

Baig, M. H. A., Abid, M., Khan, M. R., Jiao, W., Amin, M., & Adnan, S. J. R. S. (2020). Assessing meteorological and agricultural drought in Chitral Kabul river basin using multiple drought indices. *12*(9), 1417.

Bakke, S. J., Ionita, M., & Tallaksen, L. M. (2023). Recent European drying and its link to prevailing large-scale atmospheric patterns. *Scientific Reports 2023 13:1*, *13*(1), 1-13. https://doi.org/10.1038/s41598-023-48861-4

Baral, U., Saha, U. D., Mukhopadhyay, U., & Singh, D. (2023). Drought risk assessment on the eastern part of Indian peninsula—a study on Purulia district, West Bengal. *Environmental Monitoring and Assessment*, *195*(11), 1-23. https://doi.org/10.1007/S10661-023-11920-4/FIGURES/8

Bayissa, Y., Tadesse, T., Demisse, G., & Shiferaw, A. J. R. S. (2017). Evaluation of satellite-based rainfall estimates and application to monitor meteorological drought for the Upper Blue Nile Basin, Ethiopia. *9*(7), 669.

Beguería, S., Vicente-Serrano, S. M., Reig, F., & Latorre, B. (2014). Standardized precipitation evapotranspiration index (SPEI) revisited: Parameter fitting, evapotranspiration models, tools, datasets and drought monitoring. *International Journal of Climatology*, *34*(10), 3001-3023. https://doi.org/10.1002/JOC.3887

Belayneh, A., Sintayehu, G., Gedam, K., Muluken, T. J. M. E. S., & Environment. (2020). Evaluation of satellite precipitation products using HEC-HMS model. *6*(4), 2015-2032.

Belgiu, M., Drăguţ, L. J. I. j. o. p., & sensing, r. (2016). Random forest in remote sensing: A review of applications and future directions. *114*, 24-31.

Bennett, A., & Nijssen, B. (2021). Deep Learned Process Parameterizations Provide Better Representations of Turbulent Heat Fluxes in Hydrologic Models. *Water Resources Research*, *57*(5), e2020WR029328-e022020WR029328. https://doi.org/10.1029/2020WR029328

Benzougagh, B., Meshram, S. G., El Fellah, B., Mastere, M., Dridri, A., Sadkaoui, D., Mimich, K., & Khedher, K. M. J. E. S. I. (2022). Combined use of Sentinel-2 and Landsat-8 to monitor water surface area and evaluated drought risk severity using Google Earth Engine. *15*(2), 929-940.

Bhushan, N., & Rai, K. (2004). Strategic decision-making. In *Strategic Decision Making: Applying the Analytic Hierarchy Process* (pp. 3-10). Springer.

Bilal, M., Muavia, A., Ali, Iqbal, M., Arshed, A. B., Ahmad, M. M. J. J. o. W., & Change, C. (2023). Spatio-temporal drought assessment and comparison of drought indices under climatic variations in drought-prone areas of Pakistan. *14*(10), 3726-3752.

Breiman, L. J. M. l. (2001). Random forests. *45*, 5-32.

Brown, C., Meeks, R., Hunu, K., & Yu, W. (2011). Hydroclimate risk to economic growth in sub-Saharan Africa. *Climatic Change*, *106*(4), 621-647. https://doi.org/10.1007/S10584-010-9956-9/METRICS

Chakraborty, S., Sahoo, S., Majumdar, D., Saha, S., & Roy, S. J. J. o. C. P. (2019). Future Mangrove Suitability Assessment of Andaman to strengthen sustainable development. *234*, 597-614.

Chattopadhyay, N., Malathi, K., Tidke, N., Attri, S., & Ray, K. J. J. o. E. S. S. (2020). Monitoring agricultural drought using combined drought index in India. *129*, 1-16.

Choi, S. G., Oh, M., Park, D. H., Lee, B., Lee, Y.-h., Jee, S. H., & Jeon, J. Y. J. S. r. (2023). Comparisons of the prediction models for undiagnosed diabetes between machine learning versus traditional statistical methods. *13*(1), 13101.

Convention | UNCCD. Retrieved 18 dec, 2023 from https://www.unccd.int/convention/overview

Cook, B. I., Mankin, J. S., Marvel, K., Williams, A. P., Smerdon, J. E., & Anchukaitis, K. J. (2020). Twenty-First Century Drought Projections in the CMIP6 Forcing Scenarios. *Earth's Future*, *8*(6), e2019EF001461-e002019EF001461. https://doi.org/10.1029/2019EF001461

Cunha, A. P. M. A., Zeri, M., Leal, K. D., Costa, L., Cuartas, L. A., Marengo, J. A., Tomasella, J., Vieira, R. M., Barbosa, A. A., Cunningham, C., Cal Garcia, J. V., Broedel, E., Alvalá, R., & Ribeiro-Neto, G. (2019). Extreme drought events over Brazil from 2011 to 2019. *Atmosphere*, *10*(11). https://doi.org/10.3390/ATMOS10110642

Danandeh Mehr, A., & Vaheddoost, B. (2020). Identification of the trends associated with the SPI and SPEI indices across Ankara, Turkey. *Theoretical and Applied Climatology*, *139*(3-4), 1531-1542. https://doi.org/10.1007/S00704-019-03071-9

Domínguez-Castro, F., Vicente-Serrano, S. M., Tomás-Burguera, M., Peña-Gallardo, M., Beguería, S., El Kenawy, A., Luna, Y., Morata, A. J. N. H., & Sciences, E. S. (2019). High-spatial-resolution probability maps of drought duration and magnitude across Spain. *19*(3), 611-628.

Droughts: Things to Know | U.S. Geological Survey. (June 8, 2018). In.

Duan, Z., Tuo, Y., Liu, J., Gao, H., Song, X., Zhang, Z., Yang, L., & Mekonnen, D. F. J. J. o. h. (2019). Hydrological evaluation of open-access precipitation and air temperature datasets using SWAT in a poorly gauged basin in Ethiopia. *569*, 612-626.

Dunne, A., & Kuleshov, Y. J. N. H. (2023). Drought risk assessment and mapping for the Murray–Darling Basin, Australia. *115*(1), 839-863.

Edwards, B., Gray, M., & Hunter, B. (2019). The social and economic impacts of drought. *Australian Journal of Social Issues*, *54*(1), 22-31. https://doi.org/10.1002/AJS4.52

Ejaz, N., Bahrawi, J., Alghamdi, K. M., Rahman, K. U., & Shang, S. (2023). Drought monitoring using landsat derived indices and Google Earth engine platform: A case study from Al-Lith Watershed, Kingdom of Saudi Arabia. *Remote Sensing*, *15*(4), 984.

Elnashar, A., Zeng, H., Wu, B., Zhang, N., Tian, F., Zhang, M., Zhu, W., Yan, N., Chen, Z., Sun, Z., Wu, X., & Li, Y. (2020). Downscaling TRMM Monthly Precipitation Using Google Earth Engine and Google Cloud Computing. *Remote Sensing 2020, Vol. 12, Page 3860*, *12*(23), 3860-3860. https://doi.org/10.3390/RS12233860

Essa, Y. H., Hirschi, M., Thiery, W., El-Kenawy, A. M., Yang, C. J. n. C., & Science, A. (2023). Drought characteristics in Mediterranean under future climate change. *6*(1), 133.

European Climate Risk Assessment. (2024). [Report]. P. O. o. t. E. Union. eea.europa.eu

Eyring, V., Bony, S., Meehl, G. A., Senior, C. A., Stevens, B., Stouffer, R. J., & Taylor, K. E. (1937). Overview of the Coupled Model Intercomparison Project Phase 6 (CMIP6) experimental design and organization. *Geosci. Model Dev*, *9*. https://doi.org/10.5194/gmd-9-1937-2016

Eyring, V., Bony, S., Meehl, G. A., Senior, C. A., Stevens, B., Stouffer, R. J., & Taylor, K. E. (2016). Overview of the Coupled Model Intercomparison Project Phase 6 (CMIP6)

experimental design and organization. *Geoscientific Model Development*, *9*(5), 1937-1958. https://doi.org/10.5194/GMD-9-1937-2016

Fagua, J. C., & Ramsey, R. D. (2019). Comparing the accuracy of MODIS data products for vegetation detection between two environmentally dissimilar ecoregions: the Chocó-Darien of South America and the Great Basin of North America. *GIScience and Remote Sensing*, *56*(7), 1046-1064. https://doi.org/10.1080/15481603.2019.1611024

Farooq, A., Anwar, A., Ahad, M., Shabbir, G., Imran, Z. A. J. J. o. E., & Sciences, A. (2024). A validity of environmental Kuznets curve under the role of urbanization, financial development index and foreign direct investment in Pakistan. *40*(2), 288-307.

Funk, C., Peterson, P., Landsfeld, M., Pedreros, D., Verdin, J., Shukla, S., Husak, G., Rowland, J., Harrison, L., Hoell, A., & Michaelsen, J. (2015). The climate hazards infrared precipitation with stations—a new environmental record for monitoring extremes. *Scientific Data 2015 2:1*, *2*(1), 1-21. https://doi.org/10.1038/sdata.2015.66

Ghajarnia, N., Liaghat, A., & Daneshkar Arasteh, P. (2015). Comparison and evaluation of high resolution precipitation estimation products in Urmia Basin-Iran. *Atmospheric Research*, *158-159*, 50-65. https://doi.org/10.1016/J.ATMOSRES.2015.02.010

Ghaleb, F., Mario, M., & Sandra, A. N. (2015). Regional landsat-based drought monitoring from 1982 to 2014. *Climate*, *3*(3), 563-577.

Ghamghami, M., & Irannejad, P. (2019). An analysis of droughts in Iran during 1988–2017. *SN Applied Sciences*, *1*(10), 1-21. https://doi.org/10.1007/S42452-019-1258-X/TABLES/5

Gorelick, N., Hancher, M., Dixon, M., Ilyushchenko, S., Thau, D., & Moore, R. (2017). Google Earth Engine: Planetary-scale geospatial analysis for everyone. *Remote Sensing of Environment*, *202*, 18-27. https://doi.org/10.1016/J.RSE.2017.06.031

Greener, J. G., Kandathil, S. M., Moffat, L., & Jones, D. T. J. N. r. M. c. b. (2022). A guide to machine learning for biologists. *23*(1), 40-55.

Haider, S., & Adnan, S. J. I. j. o. e. (2014). Classification and assessment of aridity over Pakistan provinces (1960-2009). *3*(4), 24-35.

Han, Z., Zhao, J., Leung, H., Ma, K. F., & Wang, W. J. I. S. J. (2019). A review of deep learning models for time series prediction. *21*(6), 7833-7848.

Hersbach, H., Bell, B., Berrisford, P., Dahlgren, P., Horányi, A., Munoz-Sebater, J., Nicolas, J., Radu, R., Schepers, D., & Simmons, A. J. E. g. u. g. a. (2020). The ERA5 Global

Reanalysis: achieving a detailed record of the climate and weather for the past 70 years. 3-8.

Hersbach, H., Bell, B., Berrisford, P., Hirahara, S., Horányi, A., Muñoz-Sabater, J., Nicolas, J., Peubey, C., Radu, R., Schepers, D., Simmons, A., Soci, C., Abdalla, S., Abellan, X., Balsamo, G., Bechtold, P., Biavati, G., Bidlot, J., Bonavita, M., . . . Thépaut, J. N. (2020). The ERA5 global reanalysis. *Quarterly Journal of the Royal Meteorological Society*, *146*(730), 1999-2049. https://doi.org/10.1002/QJ.3803

Hongmei, Feng Li, L., & Zhou, T. (2011). Multi-model projection of July-August climate extreme changes over China under CO2 doubling. Part I: Precipitation. *Advances in Atmospheric Sciences*, *28*(2), 433-447. https://doi.org/10.1007/S00376-010-0013-4/METRICS

Huete, A., Didan, K., van Leeuwen, W., Miura, T., & Glenn, E. (2011). MODIS vegetation indices. *Remote Sensing and Digital Image Processing*, *11*, 579-602. https://doi.org/10.1007/978-1-4419-6749-7_26

Huffman, G. J., Bolvin, D. T., Braithwaite, D., Hsu, K. L., Joyce, R. J., Kidd, C., Nelkin, E. J., Sorooshian, S., Stocker, E. F., Tan, J., Wolff, D. B., & Xie, P. (2020). Integrated Multi-satellite Retrievals for the Global Precipitation Measurement (GPM) Mission (IMERG). *Advances in Global Change Research*, *67*, 343-353. https://doi.org/10.1007/978-3-030-24568-9_19

Huffman, G. J., & Bolvin, D. T. J. N., Greenbelt, USA. (2013). TRMM and other data precipitation data set documentation. *28*(2.3), 1.

Hussain, M. A., Shuai, Z., Moawwez, M. A., Umar, T., Iqbal, M. R., Kamran, M., & Muneer, M. J. W. (2023). A review of spatial variations of multiple natural hazards and risk management strategies in Pakistan. *15*(3), 407.

IPCC. (2013). *Climate Change 2013: The Physical Science Basis. Contribution of Working Group I to the Fifth Assessment Report of the Intergovernmental Panel on Climate Change* (T. F. Stocker, D. Qin, G.-K. Plattner, M. Tignor, S. K. Allen, J. Boschung, A. Nauels, Y. Xia, V. Bex, & P. M. Midgley, Eds.). Cambridge University Press. https://doi.org/10.1017/CBO9781107415324

Iqbal, Z., Shahid, S., Ahmed, K., Ismail, T., Ziarh, G. F., Chung, E. S., & Wang, X. (2021). Evaluation of CMIP6 GCM rainfall in mainland Southeast Asia. *Atmospheric Research*, *254*, 105525-105525. https://doi.org/10.1016/J.ATMOSRES.2021.105525

Ishaq, Ali, H., Muhammad, Z., Ullah, R., Iqbal, S., Nafidi, H. A., Bourhia, M., & Salamatullah, A. M. (2024). Evaluation of climate change impact on plants and hydrology. *Frontiers*

in *Environmental* *Science,* *12,* 1328808-1328808. https://doi.org/10.3389/FENVS.2024.1328808/BIBTEX

Jiang, L., & Bauer-Gottwein, P. (2019). How do GPM IMERG precipitation estimates perform as hydrological model forcing? Evaluation for 300 catchments across Mainland China. *Journal* *of* *Hydrology,* *572,* 486-500. https://doi.org/10.1016/J.JHYDROL.2019.03.042

Jianing, Chang, W., & Zhou, S. (2015). An improved MCDM model with cloud TOPSIS method. *Proceedings of the 2015 27th Chinese Control and Decision Conference, CCDC 2015*, 873-878. https://doi.org/10.1109/CCDC.2015.7162042

Jiao, W., Tian, C., Chang, Q., Novick, K. A., Wang, L. J. A., & meteorology, f. (2019). A new multi-sensor integrated index for drought monitoring. *268*, 74-85.

Jiao, W., Zhang, L., Chang, Q., Fu, D., Cen, Y., & Tong, Q. (2016). Evaluating an enhanced vegetation condition index (VCI) based on VIUPD for drought monitoring in the continental United States. *Remote Sensing, 8*(3). https://doi.org/10.3390/RS8030224

Jing, & Sun, W., Lin. (2017). Comparison and Evaluation of Different MODIS Aerosol Optical Depth Products over the Beijing-Tianjin-Hebei Region in China. *IEEE Journal of Selected Topics in Applied Earth Observations and Remote Sensing, 10*(3), 835-844. https://doi.org/10.1109/JSTARS.2016.2595624

Kalambukattu, J. G., Kumar, S., & Ghotekar, Y. S. J. E. J. o. S. S. (2018). Spatial variability analysis of soil quality parameters in a watershed of Sub-Himalayan Landscape-A case study. *7*(3), 238-250.

Karimi, M., Shahedi, K., Raziei, T., Miryaghoubzadeh, M. J. S. E. R., & Assessment, R. (2022). Meteorological and agricultural drought monitoring in Southwest of Iran using a remote sensing-based combined drought index. *36*(11), 3707-3724.

Kartal, V., & Nones, M. (2024). Assessment of meteorological, hydrological and groundwater drought in the Konya closed basin, Türkiye. *Environmental Earth Sciences 2024 83:9, 83*(9), 1-27. https://doi.org/10.1007/S12665-024-11587-1

Khalil, Shang, R., Songhao, Balkhair, K. S., Gabriel, H. F., Jadoon, K. Z., Zaman, K. J. N. H., & Discussions, E. S. S. (2023). Catchment scale assessment of drought impact on environmental flow in the Indus Basin, Pakistan. *2023*, 1-31.

Khan, R., & Gilani, H. (2021). Global drought monitoring with drought severity index (DSI) using Google Earth Engine. *Theoretical and Applied Climatology, 146*(1-2), 411-427. https://doi.org/10.1007/S00704-021-03715-9/FIGURES/2

Khan, R., Gilani, H. J. E. S., & Research, P. (2021). Global drought monitoring with big geospatial datasets using Google Earth Engine. *28*, 17244-17264.

Khorrami, B., Ali, S., & Gündüz, O. J. H. P. (2023). An appraisal of the local-scale spatio-temporal variations of drought based on the integrated GRACE/GRACE-FO observations and fine-resolution FLDAS model. *37*(11), e15034.

Kogan, & N, F. (1997). Global Drought Watch from Space. *BAMS*, *78*(4), 621-621. https://doi.org/10.1175/1520-0477(1997)078

Kumari, M., Kumar, D., Science, V. J. I. J. o. E., & Technology. (2023). Dynamic drought risk assessment and analysis with multi-source drought indices and analytical hierarchy process. *20*(3), 2839-2856.

Li, J., Li, Y., Yin, L., & Zhao, Q. (2024). A novel composite drought index combining precipitation, temperature and evapotranspiration used for drought monitoring in the Huang-Huai-Hai Plain. *Agricultural Water Management*, *291*, 108626-108626. https://doi.org/10.1016/J.AGWAT.2023.108626

Liu, H. C., Quan, M. Y., Shi, H., & Guo, C. (2019). An integrated MCDM method for robot selection under interval-valued Pythagorean uncertain linguistic environment. *International Journal of Intelligent Systems*, *34*(2), 188-214. https://doi.org/10.1002/INT.22047

López-Moreno, J. I., Vicente-Serrano, S. M., Zabalza, J., Beguería, S., Lorenzo-Lacruz, J., Azorin-Molina, C., & Morán-Tejeda, E. (2013). Hydrological response to climate variability at different time scales: A study in the Ebro basin. *Journal of Hydrology*, *477*, 175-188. https://doi.org/10.1016/J.JHYDROL.2012.11.028

Mahan, J. R., & Lascano, R. J. (2016). Irrigation Analysis Based on Long-Term Weather Data. *6*(3), 42. https://www.mdpi.com/2077-0472/6/3/42

Malczewski, J. J. I. j. o. g. i. s. (2006). GIS-based multicriteria decision analysis: a survey of the literature. *20*(7), 703-726.

Mangi, M. Y., Chandio, I. A., Shaikh, F. A., Talpur, M. A. h. J. M. U. R. J. o. E., & Technology. (2018). Urban land use planning trend and sustainable challenges in socio-economic development. *37*(2), 397-404.

McNally, A., Arsenault, K., Kumar, S., Shukla, S., Peterson, P., Wang, S., Funk, C., Peters-Lidard, C. D., & Verdin, J. P. (2017). A land data assimilation system for sub-Saharan Africa food and water security applications. *Scientific Data 2017 4:1*, *4*(1), 1-19. https://doi.org/10.1038/sdata.2017.12

McNicholl, B., Lee, Y. H., Campbell, A. G., & Dev, S. (2022). Evaluating the Reliability of Air Temperature from ERA5 Reanalysis Data. *IEEE Geoscience and Remote Sensing Letters*, *19*. https://doi.org/10.1109/LGRS.2021.3137643

Mendoza, G. A., Prabhu, R. J. F. e., & management. (2000). Multiple criteria decision making approaches to assessing forest sustainability using criteria and indicators: a case study. *131*(1-3), 107-126.

Mercedes, M., Sánchez, S., Nilda, Piles, M., Ruscica, R. C., González-Zamora, Á., Roitberg, E., & Martínez-Fernández, J. (2021). The added-value of remotely-sensed soil moisture data for agricultural drought detection in Argentina. *IEEE journal of selected topics in applied earth observations*

remote sensing, *14*, 6487-6500.

Miao, C., Ni, J., Borthwick, A. G. L., & Yang, L. (2011). A preliminary estimate of human and natural contributions to the changes in water discharge and sediment load in the Yellow River. *Global and Planetary Change*, *76*(3-4), 196-205. https://doi.org/10.1016/J.GLOPLACHA.2011.01.008

Mishra, A. K., & Singh, V. P. J. J. o. h. (2010). A review of drought concepts. *391*(1-2), 202-216.

Mokarram, M., Pourghasemi, H. R., Hu, M., & Zhang, H. (2021). Determining and forecasting drought susceptibility in southwestern Iran using multi-criteria decision-making (MCDM) coupled with CA-Markov model. *Science of The Total Environment*, *781*, 146703-146703. https://doi.org/10.1016/J.SCITOTENV.2021.146703

Muhammad, S., & Thapa, A. (2021). Daily Terra-Aqua MODIS cloud-free snow and Randolph Glacier Inventory 6.0 combined product (M∗D10A1GL06) for high-mountain Asia between 2002 and 2019. *Earth System Science Data*, *13*(2), 767-776. https://doi.org/10.5194/ESSD-13-767-2021

Nashwan, M. S., Shahid, S., & Wang, X. J. R. S. (2019). Assessment of satellite-based precipitation measurement products over the hot desert climate of Egypt. *11*(5), 555.

Nath, S. K., Sengupta, A., & Srivastava, A. J. N. H. (2021). Remote sensing GIS-based landslide susceptibility & risk modeling in Darjeeling–Sikkim Himalaya together with FEM-based slope stability analysis of the terrain. *108*(3), 3271-3304.

O'Brien, D. (2015, Apr 21, 2015). Technology to Help Us Deal with Drought. https://www.usda.gov/media/blog/2015/04/21/technology-help-us-deal-drought

O'Neill, B. C., Tebaldi, C., Van Vuuren, D. P., Eyring, V., Friedlingstein, P., Hurtt, G., Knutti, R., Kriegler, E., Lamarque, J.-F., & Lowe, J. J. G. M. D. (2016). The scenario model intercomparison project (ScenarioMIP) for CMIP6. *9*(9), 3461-3482.

Omar, M. S., & Kawamukai, H. (2020). Prediction of Drought based on NDVI – LST Relationship using Random Forest: Case Study of Garissa, Kenya.

Pakistan Bureau of Statistics. https://www.pbs.gov.pk/

Pakistan Meteorological Department. https://www.pmd.gov.pk/Observatories/

Palchaudhuri, M., & Biswas, S. (2016). Application of AHP with GIS in drought risk assessment for Puruliya district, India. *Natural Hazards*, *84*(3), 1905-1920. https://doi.org/10.1007/S11069-016-2526-3

Pan, Y., Zhu, Y., Lü, H., Yagci, A. L., Fu, X., Liu, E., Xu, H., Ding, Z., & Liu, R. J. A. W. M. (2023). Accuracy of agricultural drought indices and analysis of agricultural drought characteristics in China between 2000 and 2019. *283*, 108305.

Pandey, V., Komal, & Dincer, H. J. S. C. (2023). A review on TOPSIS method and its extensions for different applications with recent development. *27*(23), 18011-18039.

Pandey, V., & Srivastava, P. K. J. R. S. (2019). Integration of microwave and optical/infrared derived datasets for a drought hazard inventory in a sub-tropical region of India. *11*(4), 439.

Park, H., Kim, K., & Lee, D. K. J. W. (2019). Prediction of severe drought area based on random forest: Using satellite image and topography data. *11*(4), 705.

Peng, He, Z., Zhibin, Ma, D., & Wang, W. (2023). Evaluation of ERA5-Land reanalysis datasets for extreme temperatures in the Qilian Mountains of China. *Frontiers in Ecology and Evolution*, *11*. https://doi.org/10.3389/FEVO.2023.1135895

Pengfei, Xiao Zhang, M., Zhang, Z., Dai, Y., Liu, G., & Senge, M. (2023). Hydrological characteristics of different organic materials mulches. *Scientific Reports 2023 13:1*, *13*(1), 1-9. https://doi.org/10.1038/s41598-023-28124-y

Pham-Duc, B., Nguyen, H., Phan, H., & Tran-Anh, Q. (2023). Trends and applications of google earth engine in remote sensing and earth science research: a bibliometric analysis using scopus database. *Earth Science Informatics*, *16*(3), 2355-2371.

Pradhan, A. M. S., Lee, S. R., & Kim, Y. T. (2019). A shallow slide prediction model combining rainfall threshold warnings and shallow slide susceptibility in Busan, Korea. *Landslides*, *16*(3), 647-659. https://doi.org/10.1007/S10346-018-1112-Z/METRICS

Prasad, A. M., Iverson, L. R., & Liaw, A. J. E. (2006). Newer classification and regression tree techniques: bagging and random forests for ecological prediction. *9*, 181-199.

Pulwarty, R. S., Sivakumar, M. V. J. W., & Extremes, C. (2014). Information systems in a changing climate: Early warnings and drought risk management. *3*, 14-21.

Quan, S. J., & Bansal, P. (2021). A systematic review of GIS-based local climate zone mapping studies. *Building and Environment*, *196*. https://doi.org/10.1016/J.BUILDENV.2021.107791

Rahimi, J., Ebrahimpour, M., & Khalili, A. (2013). Spatial changes of Extended De Martonne climatic zones affected by climate change in Iran. *Theoretical and Applied Climatology*, *112*(3-4), 409-418. https://doi.org/10.1007/S00704-012-0741-8

Rahman, R., & Saha, S. J. J. o. S. S. (2008). Remote sensing, spatial multi criteria evaluation (SMCE) and analytical hierarchy process (AHP) in optimal cropping pattern planning for a flood prone area. *53*(2), 161-177.

Rashid, M. M. (2023). Drought Assessments in the Nonstationary Domain. *Integrated Drought Management, Volume 2: Forecasting, Monitoring, and Managing Risk*, *1*, 71-84. https://doi.org/10.1201/9781003276548-6/DROUGHT-ASSESSMENTS-NONSTATIONARY-DOMAIN-MD-MAMUNUR-RASHID

Ratner, B. J. J. o. t., measurement, & marketing, a. f. (2009). The correlation coefficient: Its values range between+ 1/− 1, or do they? , *17*(2), 139-142.

Rawat, K. S., Mishra, A. K., Kumar, R., Singh, J. J. J. o. A., & Science, N. (2012). Vegetation condition index pattern (2002-2007) over Indian agro-climate regions, using of GIS and SPOT sensor NDVI data. *4*(2), 214-219.

Raza, S. A., Ali, Y., & Mehboob, F. (2012). Role of agriculture in economic growth of Pakistan.

Rodriguez-Galiano, V. F., Ghimire, B., Rogan, J., Chica-Olmo, M., Rigol-Sanchez, J. P. J. I. j. o. p., & sensing, r. (2012). An assessment of the effectiveness of a random forest classifier for land-cover classification. *67*, 93-104.

Saaty, T. L. (1977). A scaling method for priorities in hierarchical structures. *15*(3), 234-281.

Saaty, T. L. (2004). Decision making—the analytic hierarchy and network processes (AHP/ANP). *Journal of systems science and systems engineering*, *13*, 1-35.

Saddique, N., Jehanzaib, M., Sarwar, A., Ahmed, E., Muzammil, M., Khan, M. I., Faheem, M., Buttar, N. A., Ali, S., & Bernhofer, C. J. A. (2022). A systematic review on farmers' adaptation strategies in Pakistan toward climate change. *13*(8), 1280.

Sadiq, A., Ibrahim, M. S., Usman, M., Zubair, M., & Khan, S. (2018). Chaotic time series prediction using spatio-temporal rbf neural networks. 2018 3rd International Conference on Emerging Trends in Engineering, Sciences and Technology (ICEEST),

Sahoo, P. P., Shukla, S. K., & Ganesh, R. (2020). Taylor's slope stability chart for combined effects of horizontal and vertical seismic coefficients. *Geotechnique*, *70*(9), 835-838. https://doi.org/10.1680/JGEOT.18.D.013/ASSET/IMAGES/SMALL/JGEOT.18.D.013-F12.GIF

Salvia, M., Sanchez, N., Piles, M., Gonzalez-Zamora, A., & Martínez-Fernández, J. (2020). Evaluation of the soil moisture agricultural drought index (SMADI) and precipitation-based drought indices in Argentina. 2020 IEEE Latin American GRSS & ISPRS Remote Sensing Conference (LAGIRS),

Sánchez, N., González-Zamora, Á., Piles, M., & Martínez-Fernández, J. J. R. S. (2016). A new Soil Moisture Agricultural Drought Index (SMADI) integrating MODIS and SMOS products: A case of study over the Iberian Peninsula. *8*(4), 287.

Scaini, A., Sánchez, N., Vicente-Serrano, S. M., & Martínez-Fernández, J. J. H. P. (2015). SMOS-derived soil moisture anomalies and drought indices: A comparative analysis using in situ measurements. *29*(3), 373-383.

Shah, H., Rane, V., Nainani, J., Jeyakumar, B., & Giri, N. (2017). Drought Prediction and Management using Big Data Analytics. *International Journal of Computer Applications*, *162*(4), 27-30. https://doi.org/10.5120/IJCA2017913276

Shahabfar, A., & Eitzinger, J. J. T. J. o. A. S. (2011). Agricultural drought monitoring in semi-arid and arid areas using MODIS data. *149*(4), 403-414.

Shahzada, Ullah, A., Kalim, & Shouting, G. J. J. o. C. (2016). Investigations into precipitation and drought climatologies in South Central Asia with special focus on Pakistan over the period 1951–2010. *29*(16), 6019-6035.

Shahzada, Ullah, A., Kalim, Shuanglin, L., Gao, S., Khan, A. H., & Mahmood, R. J. C. D. (2018). Comparison of various drought indices to monitor drought status in Pakistan. *51*, 1885-1899.

Shahzaman, M., Zhu, W., Bilal, M., Habtemicheal, B. A., Mustafa, F., Arshad, M., Ullah, I., Ishfaq, S., & Iqbal, R. J. R. S. (2021). Remote sensing indices for spatial monitoring of agricultural drought in South Asian countries. *13*(11), 2059.

Shengxue, Wang, H., & Qin, F. (2023). Genetic dissection of drought resistance for trait improvement in crops. *The Crop Journal*, *11*(4), 975-985. https://doi.org/10.1016/J.CJ.2023.05.002

Shrestha, A., Rahaman, M. M., Kalra, A., Jogineedi, R., & Maheshwari, P. J. F. (2020). Climatological drought forecasting using bias corrected CMIP6 climate data: A case study for India. *2*(2), 59-84.

Shukla, S., & Wood, A. W. (2008). Use of a standardized runoff index for characterizing hydrologic drought. *Geophysical Research Letters*, *35*(2). https://doi.org/10.1029/2007GL032487

Skofronick-Jackson, G., Petersen, W. A., Berg, W., Kidd, C., Stocker, E. F., Kirschbaum, D. B., Kakar, R., Braun, S. A., Huffman, G. J., & Iguchi, T. J. B. o. t. A. M. S. (2017). The Global Precipitation Measurement (GPM) mission for science and society. *98*(8), 1679-1695.

Son, N. T., Chen, C. F., Chen, C. R., Minh, V. Q., & Trung, N. H. (2014). A comparative analysis of multitemporal MODIS EVI and NDVI data for large-scale rice yield estimation. *Agricultural and Forest Meteorology*, *197*, 52-64. https://doi.org/10.1016/J.AGRFORMET.2014.06.007

Soyoung, & Kim, P., Jinsoo (2019). Landslide susceptibility mapping based on random forest and boosted regression tree models, and a comparison of their performance. *Applied Sciences*, *9*(5), 942.

Su, B., Huang, J., Mondal, S. K., Zhai, J., Wang, Y., Wen, S., Gao, M., Lv, Y., Jiang, S., Jiang, T., & Li, A. (2021). Insight from CMIP6 SSP-RCP scenarios for future drought characteristics in China. *Atmospheric Research*, *250*, 105375-105375. https://doi.org/10.1016/J.ATMOSRES.2020.105375

Sun, Z., Liu, Y., Chen, H., Zhang, J., Jin, J., Bao, Z., Wang, G., & Tang, L. (2024). Evaluation of future climatology and its uncertainty under SSP scenarios based on a bias processing procedure: A case study of the Lancang-Mekong River Basin. *Atmospheric Research*, *298*, 107134-107134. https://doi.org/10.1016/J.ATMOSRES.2023.107134

Supharatid, S., Aribarg, T., & Nafung, J. (2022). Bias-corrected CMIP6 climate model projection over Southeast Asia. *Theoretical and Applied Climatology*, *147*(1-2), 669-690. https://doi.org/10.1007/S00704-021-03844-1/FIGURES/10

Syed, A., Raza, T., Bhatti, T. T., & Eash, N. S. J. E. C. (2022). Climate Impacts on the agricultural sector of Pakistan: Risks and solutions. *6*, 100433.

Taherdoost, H., & Madanchian, M. J. E. (2023). Multi-criteria decision making (MCDM) methods and concepts. *3*(1), 77-87.

Taheri Qazvini, A., & Carrion, D. J. R. S. (2023). A Spatiotemporal Drought Analysis Application Implemented in the Google Earth Engine and Applied to Iran as a Case Study. *15*(9), 2218.

Tan, M. L., Armanuos, A. M., Ahmadianfar, I., Demir, V., Heddam, S., Al-Areeq, A. M., Abba, S. I., Halder, B., Cagan Kilinc, H., & Yaseen, Z. M. (2023). Evaluation of NASA POWER and ERA5-Land for estimating tropical precipitation and temperature extremes. *Journal of Hydrology*, *624*, 129940-129940. https://doi.org/10.1016/J.JHYDROL.2023.129940

Tang, B., Hu, W., & Duan, A. J. J. o. C. (2021). Future projection of extreme precipitation indices over the Indochina Peninsula and South China in CMIP6 models. *34*(21), 8793-8811.

Tariq, A., Shu, H., Siddiqui, S., Imran, M., & Farhan, M. (2021). Monitoring land use and land cover changes using geospatial techniques, a case study of Fateh Jang, Attock, Pakistan. *Geography, Environment, Sustainability*, *14*(1), 41-52.

Tladi, T., Ndambuki, J., & Salim, R. (2022). Meteorological drought monitoring in the Upper Olifants sub-basin, South Africa. *Physics*

Chemistry of the Earth, *128*, 103273.

TOPÇU, E., & GÜVEL, Ş. P. (2021). Drought Assessment by Using Geographic Information Systems and Remote Sensing. International Conference on Engineering Technologies (ICENTE'21),

Torabinezhad, N., Zarrin, A., & Dadashi-Roudbari, A. (2023). Analysis of different types of droughts and their characteristics in Iran using the Standardized Precipitation Evapotranspiration Index (SPEI). *Water and Soil*, *37*(3), 473-486.

Trenberth, K. E., Dai, A., Van Der Schrier, G., Jones, P. D., Barichivich, J., Briffa, K. R., & Sheffield, J. (2014). Global warming and changes in drought. *Nature Climate Change*, *4*(1), 17-22. https://doi.org/10.1038/NCLIMATE2067

Tsiros, E., Domenikiotis, C., Spiliotopoulos, M., & Dalezios, N. (2004). Use of NOAA/AVHRR-based vegetation condition index (VCI) and temperature condition

index (TCI) for drought monitoring in Thessaly, Greece. EWRA Symposium on water resources management: risks and challenges for the 21st century, Izmir, Turkey,

Ullah, W., Nihei, T., Nafees, M., Zaman, R., Ali, M. J. I. J. o. C. C. S., & Management. (2018). Understanding climate change vulnerability, adaptation and risk perceptions at household level in Khyber Pakhtunkhwa, Pakistan. *10*(3), 359-378.

Verma, A., Vishwakarma, A., Bist, S., Kumar, S., & Bhatla, R. M. (2023). A long-term drought assessment over India using CMIP6 framework: present and future perspectives. *74*(4), 963-972.

Vicente-Serrano, S. M., Beguería, S., & López-Moreno, J. I. (2010). A Multiscalar Drought Index Sensitive to Global Warming: The Standardized Precipitation Evapotranspiration Index. *Journal of Climate*, *23*(7), 1696-1718. https://doi.org/10.1175/2009JCLI2909.1

Vicente-Serrano, S. M., Quiring, S. M., Peña-Gallardo, M., Yuan, S., & Domínguez-Castro, F. (2020). A review of environmental droughts: Increased risk under global warming? *Earth-Science Reviews*, *201*, 102953-102953. https://doi.org/10.1016/J.EARSCIREV.2019.102953

Vilanova, R. S., Delgado, R. C., da Silva Abel, E. L., Teodoro, P. E., Junior, C. A. S., Wanderley, H. S., Capristo-Silva, G. F. J. R. S. A. S., & Environment. (2020). Past and future assessment of vegetation activity for the state of Amazonas-Brazil. *17*, 100278.

Wang, Y., Yuan, Q., Shen, H., Zheng, L., & Zhang, L. (2020). Investigating multiple aerosol optical depth products from MODIS and VIIRS over Asia: Evaluation, comparison, and merging. *Atmospheric Environment*, *230*, 117548-117548. https://doi.org/10.1016/J.ATMOSENV.2020.117548

Wei, Zhang Wei, J., Zhou, L., Xie, B., Zhou, J., & Li, C. (2021). Comparative evaluation of drought indices for monitoring drought based on remote sensing data. *Environmental Science and Pollution Research*, *28*(16), 20408-20425. https://doi.org/10.1007/S11356-020-12120-0/METRICS

Weigel, A. P., Liniger, M. A., & Appenzeller, C. (2008). Can multi-model combination really enhance the prediction skill of probabilistic ensemble forecasts? *Quarterly Journal of the Royal Meteorological Society*, *134*(630), 241-260. https://doi.org/10.1002/QJ.210

Weltzin, J. F., Loik, M. E., Schwinning, S., Williams, D. G., Fay, P. A., Haddad, B. M., Harte, J., Huxman, T. E., Knapp, A. K., & Lin, G. J. B. (2003). Assessing the response of terrestrial ecosystems to potential changes in precipitation. *53*(10), 941-952.

Wilhite, D. (2006). Drought monitoring and early warning: Concepts, progress and future challenges. *World Meteorological Organization, Geneva, Switzerland. WMO*, *1006*.

Wolteji, B. N., Bedhadha, S. T., Gebre, S. L., Alemayehu, E., & Gemeda, D. O. J. E. C. (2022). Multiple indices based agricultural drought assessment in the Rift Valley region of Ethiopia. *7*, 100488.

Xinmeng, Zhang, W., Jihong, Zhong, Y., Liu, Y., & Wu, W. (2023). GIS-based spatial suitability assessment for pacific oyster Crassostrea gigas reef restoration: A case study of Laizhou Bay, China. *Marine Pollution Bulletin*, *186*, 114416-114416. https://doi.org/10.1016/J.MARPOLBUL.2022.114416

Yang, H., Wang, Q., Liu, W. J. I. J. o. A. E. O., & Geoinformation. (2024). A stepwise method for downscaling SMAP soil moisture dataset in the CONUS during 2015–2019. *130*, 103912.

Yangyang, Zhang, Z., Jiahua, Bai, Y., Zhang, S., Yang, S., Henchiri, M., Seka, A. M., & Nanzad, L. (2022). Drought monitoring and performance evaluation based on machine learning fusion of multi-source remote sensing drought factors. *Remote Sensing*, *14*(24), 6398.

Yu, C., Hu, D., Di, Y., & Wang, Y. (2021). Performance evaluation of IMERG precipitation products during typhoon Lekima (2019). *Journal of Hydrology*, *597*, 126307-126307. https://doi.org/10.1016/J.JHYDROL.2021.126307

Zagade, N. D., & Umrikar, B. N. J. N. H. (2021). Drought severity modeling of upper Bhima river basin, western India, using GIS–AHP tools for effective mitigation and resource management. *105*, 1165-1188.

Zahid, M., & Rasul, G. J. C. c. (2012). Changing trends of thermal extremes in Pakistan. *113*(3), 883-896.

Zaman, M., Shahid, M. A., Ahmad, I., Shen, Y. J., Usman, M., Khan, M. I., & Saifullah, M. (2023). Spatiotemporal variability of precipitation concentration in Pakistan. *International Journal of Climatology*, *43*(16), 7646-7666. https://doi.org/10.1002/JOC.8285

Zarei, A. R., Mahmoudi, M. R., & Moghimi, M. M. (2023). Determining the most appropriate drought index using the random forest algorithm with an emphasis on agricultural drought. *Natural Hazards: Journal of the International Society for the Prevention and Mitigation of Natural Hazards*, *115*(1), 923-946. https://doi.org/10.1007/S11069-022-05579-2

Zeng, J., Zhang, R., Qu, Y., Bento, V. A., Zhou, T., Lin, Y., Wu, X., Qi, J., Shui, W., & Wang, Q. (2022). Improving the drought monitoring capability of VHI at the global scale via ensemble indices for various vegetation types from 2001 to 2018. *Weather and Climate Extremes*, *35*, 100412-100412. https://doi.org/10.1016/J.WACE.2022.100412

Zhang, X., Wei, C., Obringer, R., Li, D., Chen, N., & Niyogi, D. J. R. S. (2017). Gauging the severity of the 2012 Midwestern US drought for agriculture. *9*(8), 767.

Zhao, X., Xia, H., Liu, B., & Jiao, W. J. R. s. (2022). Spatiotemporal comparison of drought in Shaanxi–Gansu–Ningxia from 2003 to 2020 using various drought indices in google earth engine. *14*(7), 1570.